PX Beamline

Takashi Kumasaka

- Structural Biology Group, Japan Synchrotron Radiation Research Institute (JASRI) / SPring-8

- Graduate School of Science and Engineering, Kwansei Gakuin University

Contents

- 1: Recent trends in PX
- 2: Theoretical basics
  for considering PX beamlines
  (also as prep or review for the tomorrow practice)
  - 2.1: Diffraction data collection & processing
  - 2.2: Phasing / modeling & refinement
- 3: Recent advances in PX beamlines

1: Overview of recent trends in PX

Protein crystal structure and synchrotron

Number of determined structures

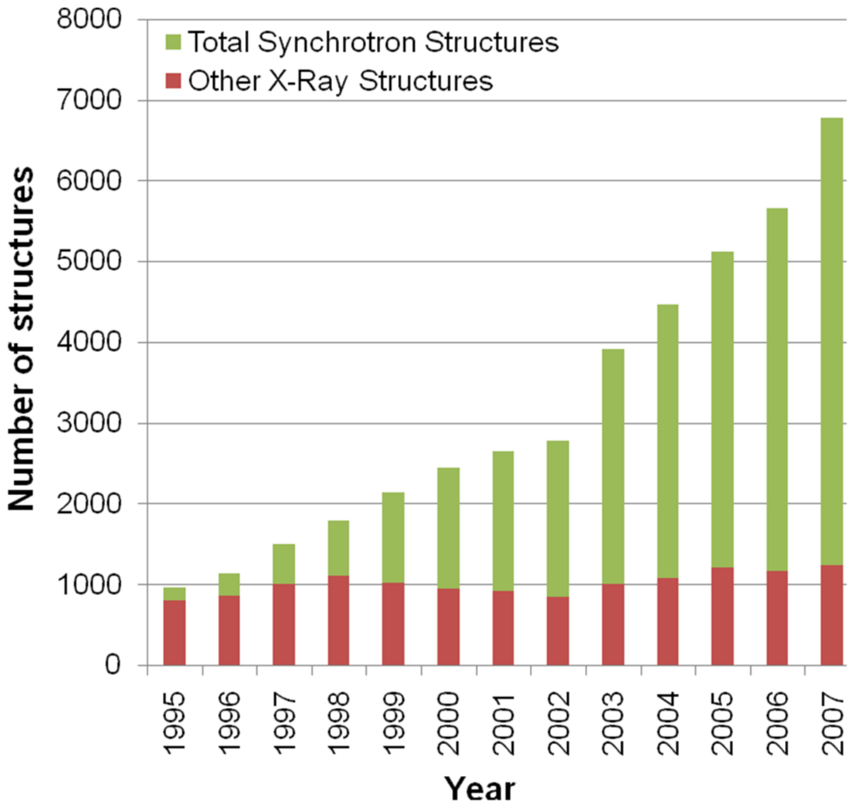

Asian contribution

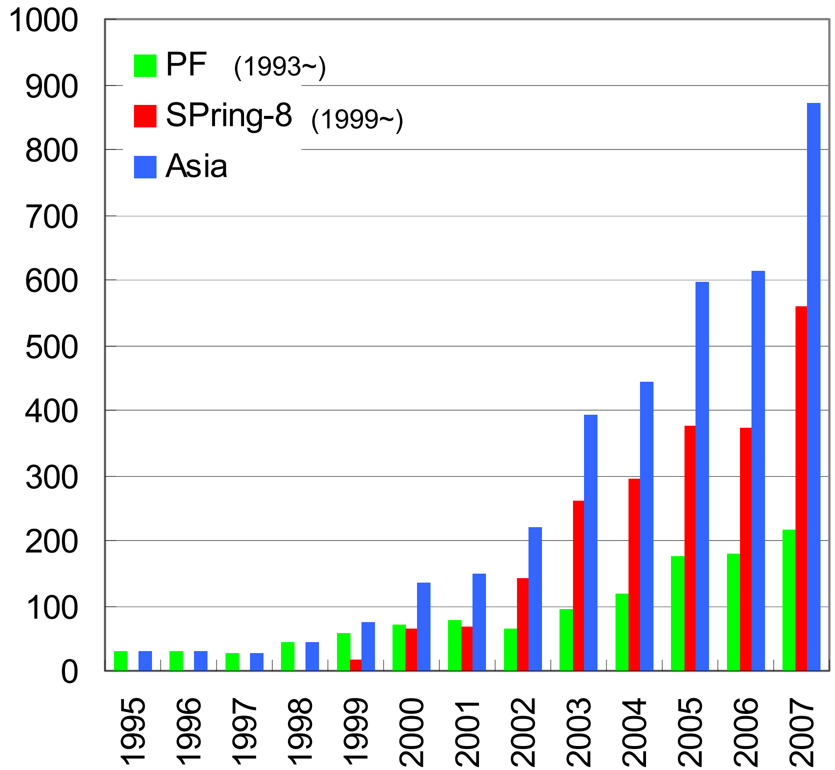

Nowadays, most structures are determined using SOR.

Determination of important and complex structures

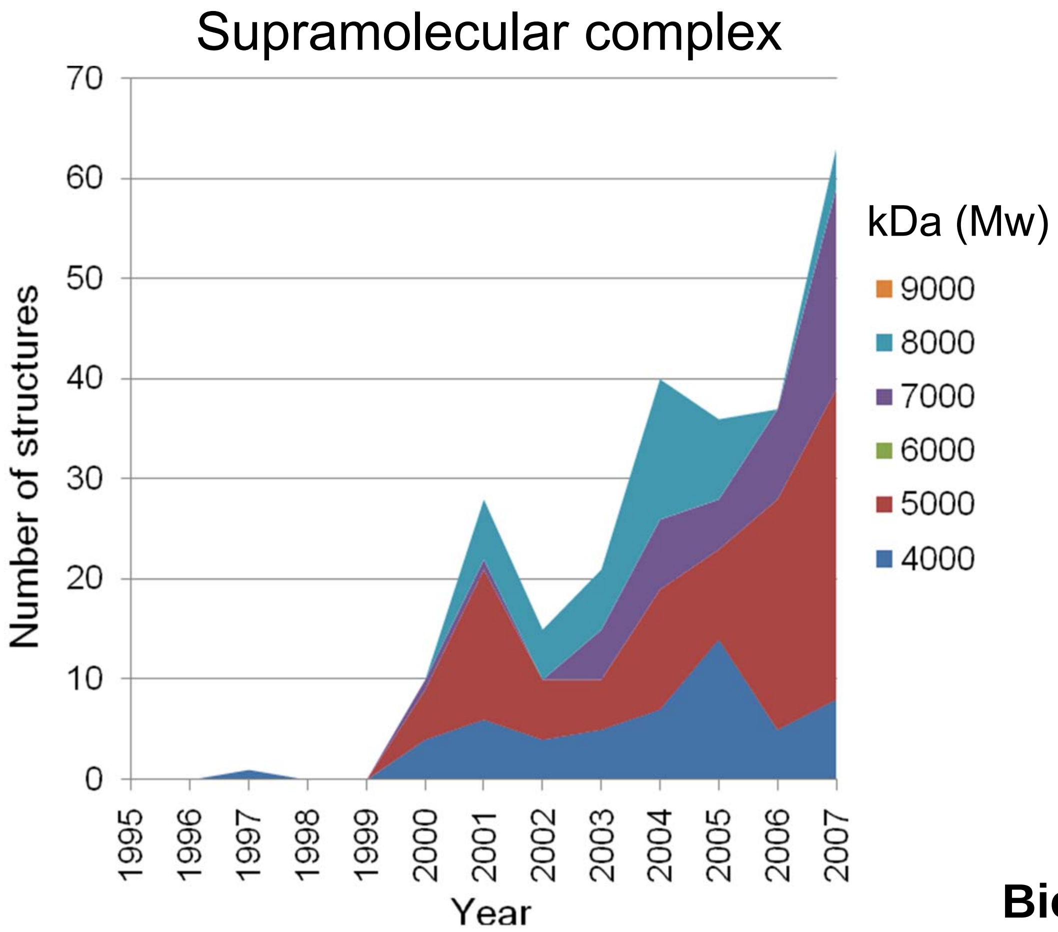

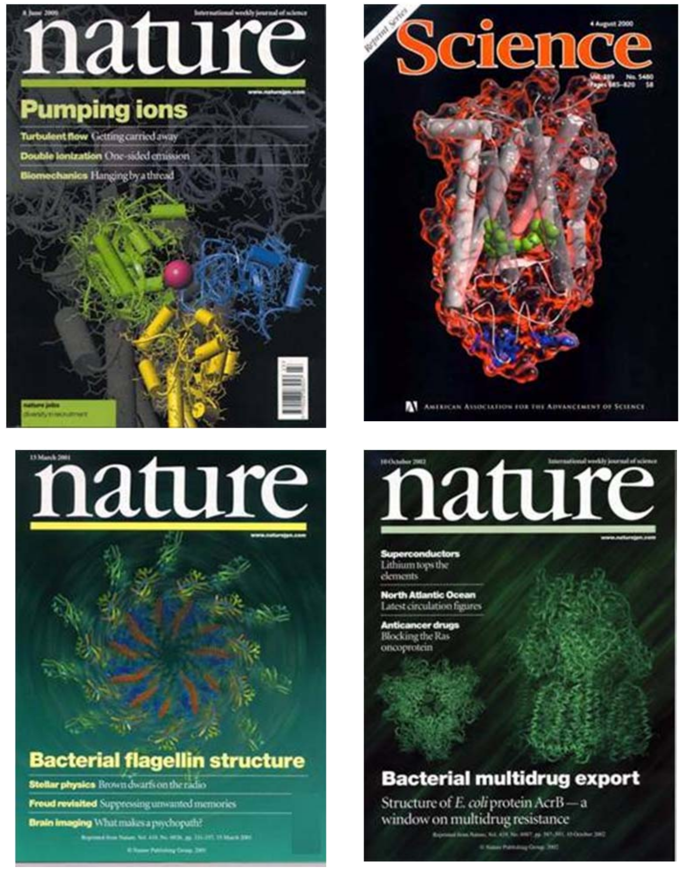

3G SOR came into this field from 2000, and accelerates large molecule analysis.

Biologically important proteins including membrane proteins:
Calcium pump, Rhodopsin, Bacterial flagella, Drug effilux protein and so forth.

History of development in MX

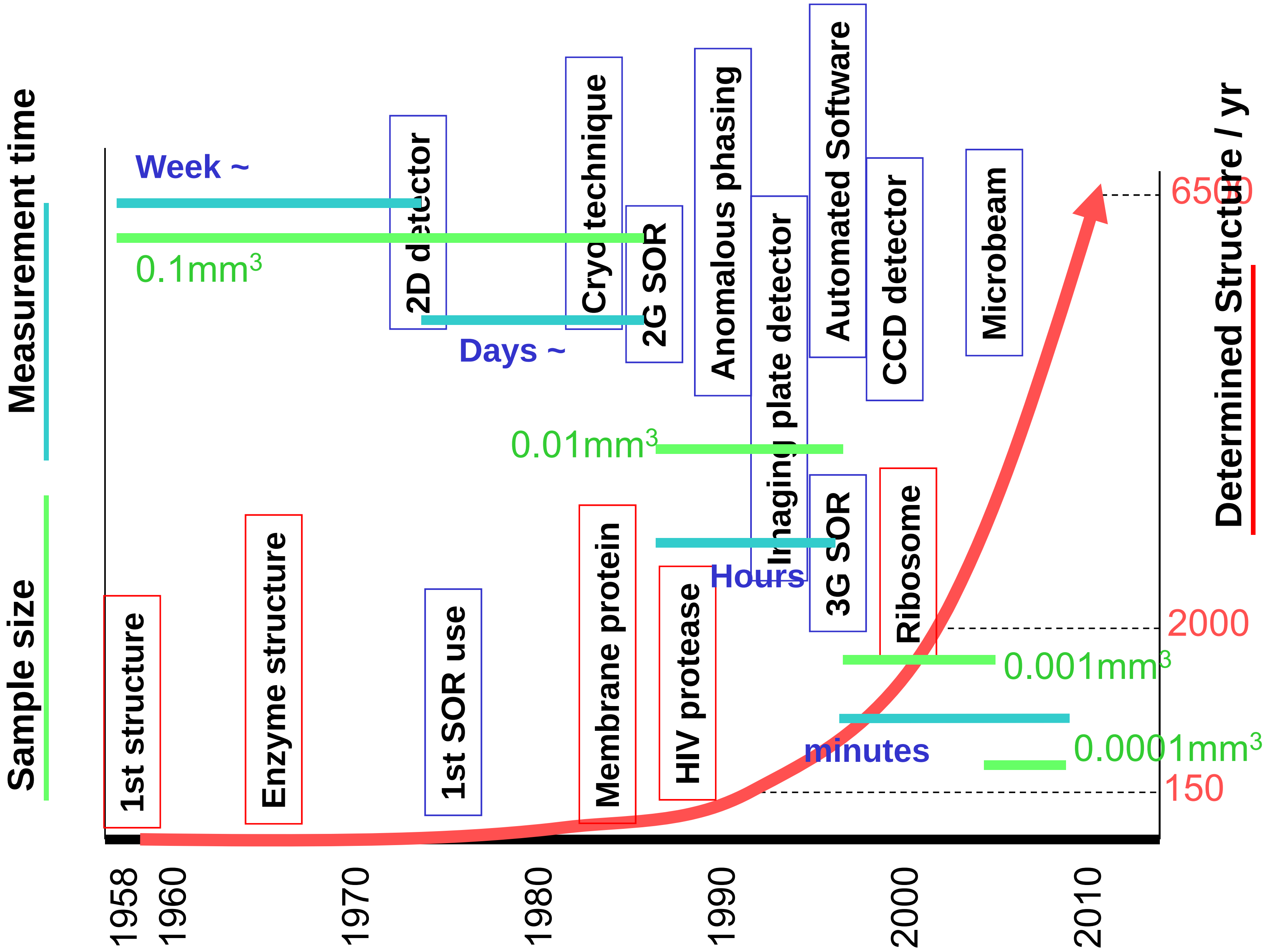

Advances in Protein Crystallography by Synchrotron Radiation

Steps in crystallographic analysis

Sample preparation

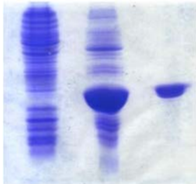

Crystallization

Diffraction Measurement

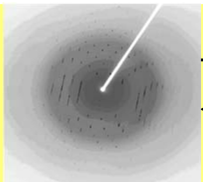

Phasing

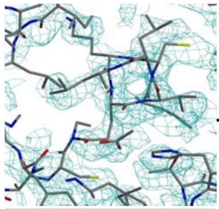

Structure Refinement

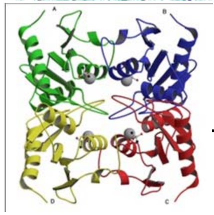

Before SOR	After SOR	3G SOR
Small amount of samples for		
10 mg~	0.1 mg~	
Small crystalline size		
0.1 mm^3~	0.01 mm^3~	0.001 mm^3~
High speed data collection		
day ~ week	**20 min ~**	**5 min ~**
New phasing method		
month ~ year	Day ~ a few months	
Automated refinement by high resolution data		
Month ~ year	Day ~ weeks	

Synchrotron data collection
> effective to not only X-ray measurement but also all other exp. steps in scale down / time reduction / high resolution.

2: Theoretical basics for considering PX beamlines

2.1: Diffraction data collection & processing

The Principle of X-ray Crystallography

Real Space

$f\,(x\ y\ z)$

Atomic Scattering Factor
(Real Number)

Crystal

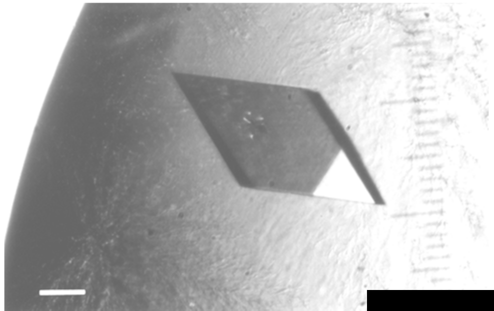

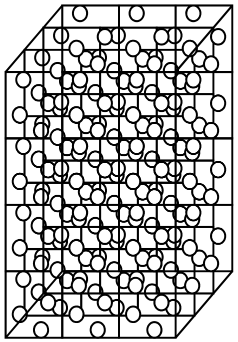

Atomic Coordinate

X-ray Diffraction →

Fourier Transform

$$\boldsymbol{F}(hkl) = \Sigma\, f_j \exp[2\pi i(hx+ky+lz)]$$

← Computation

Reciprocal Space

$\boldsymbol{F}\ (h\ k\ l)$

Structure Factor
(Complex Number)

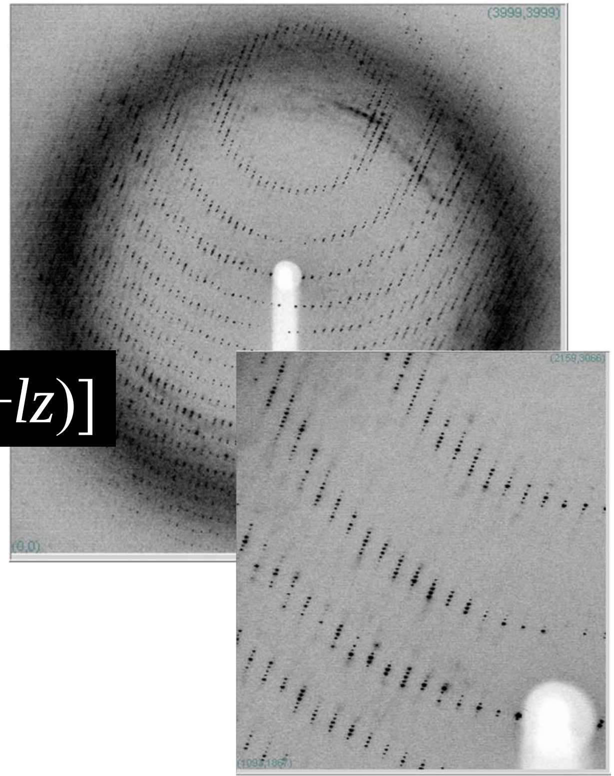

Diffraction Spot

Real space vs reciprocal space

$$\mathbf{F}(\mathbf{h}) = |\mathbf{F}(\mathbf{h})| \exp i\alpha$$
$$= \sum f_j \exp 2\pi i \mathbf{h} \cdot \mathbf{r}_j$$

Complex space

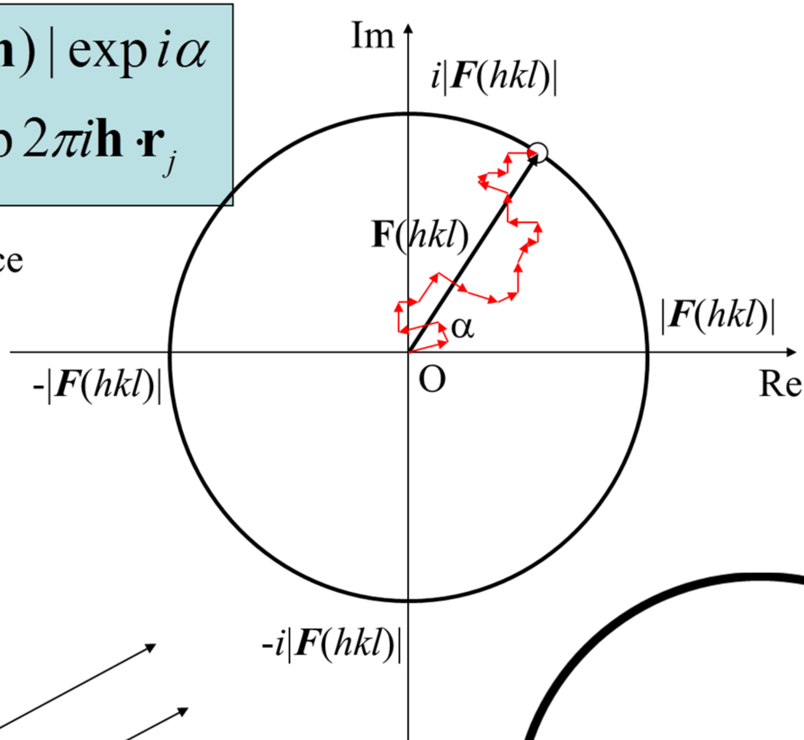

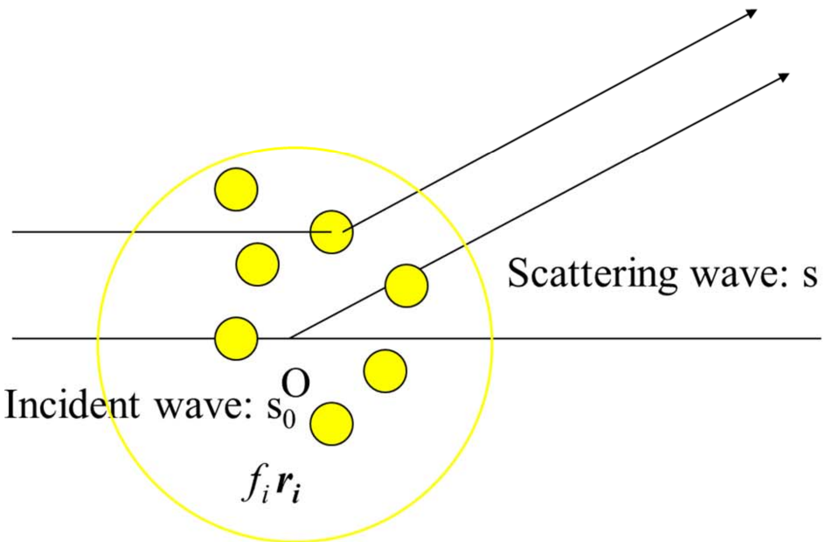

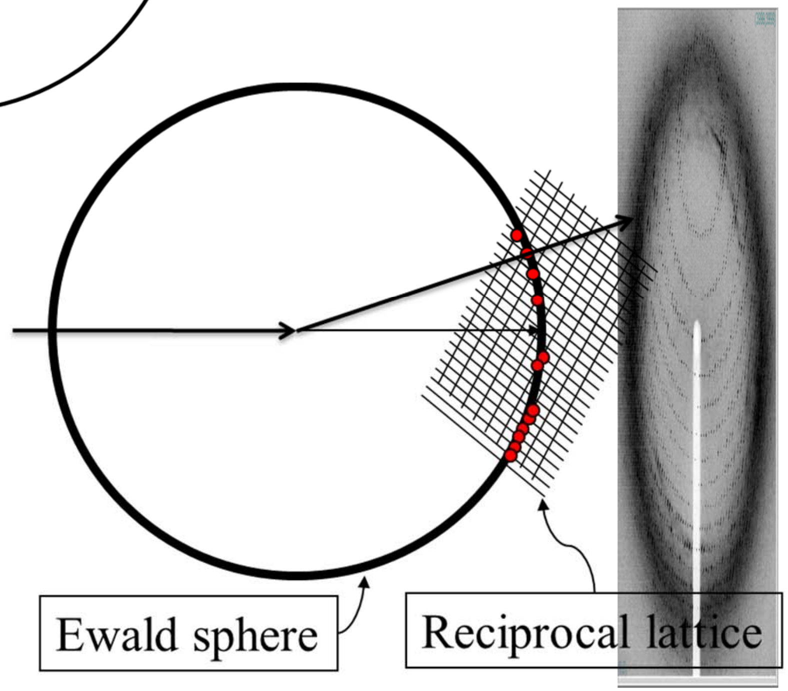

Crystallographic lattices between real and reciprocal space

In case of 2D lattice:

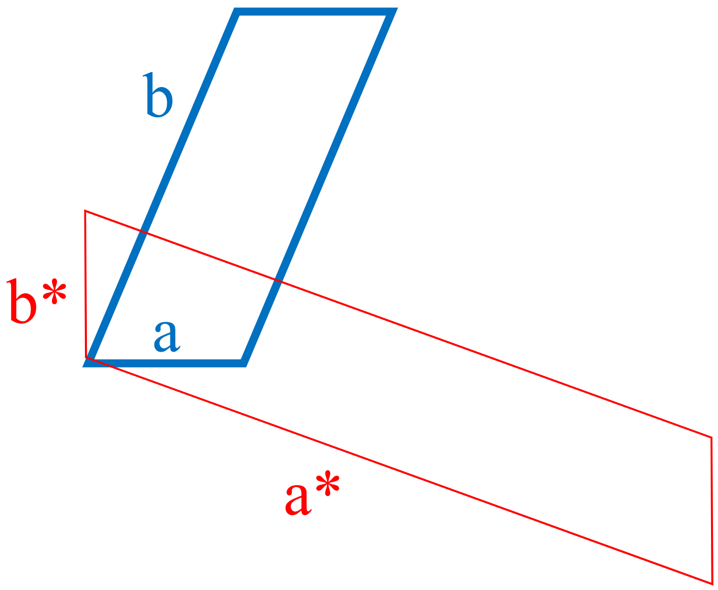

If a < b, then a* > b*

a* ⊥ b   a* ⊥ c

b* ⊥ a   b* ⊥ c

c* ⊥ a   c* ⊥ b

An example of reciprocal lattice

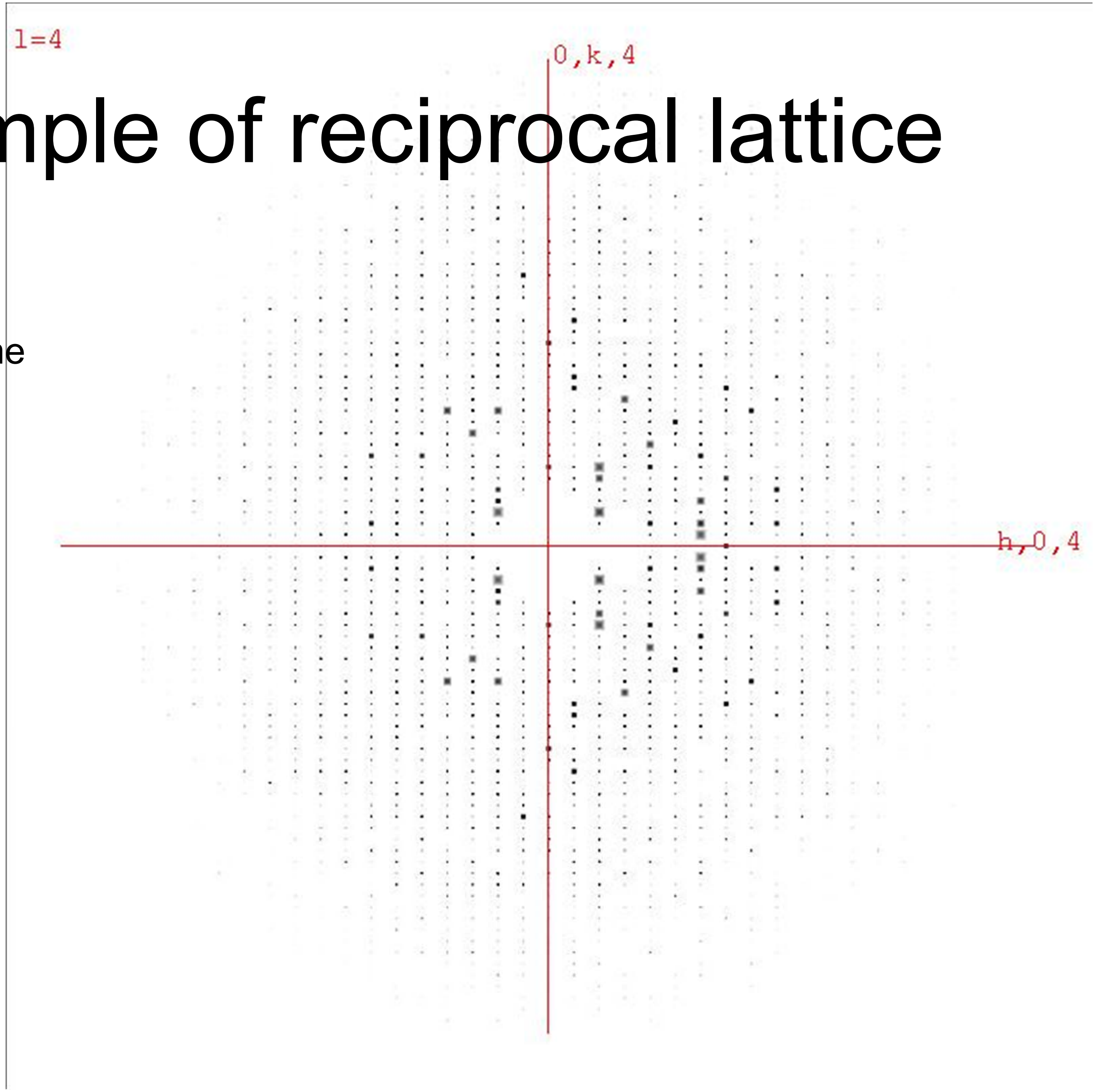

PDB ID: 1HF4
Egg white lysozyme
Space group: $P2_1$
Lattice constant:
$a = 27.94$
$b = 62.73$
$c = 60.25$
$\alpha = 90.0$
$\beta = 90.76$
$\gamma = 90.0$

X-ray diffraction data collection

Essentials in high quality data collection:

Incident X-ray: Intensity, Divergence, Wavelength

Detector: Detection accuracy, Speed, Image resolution

Crystal: Crystalline order, Size, Radiation resistance

Experimental setup

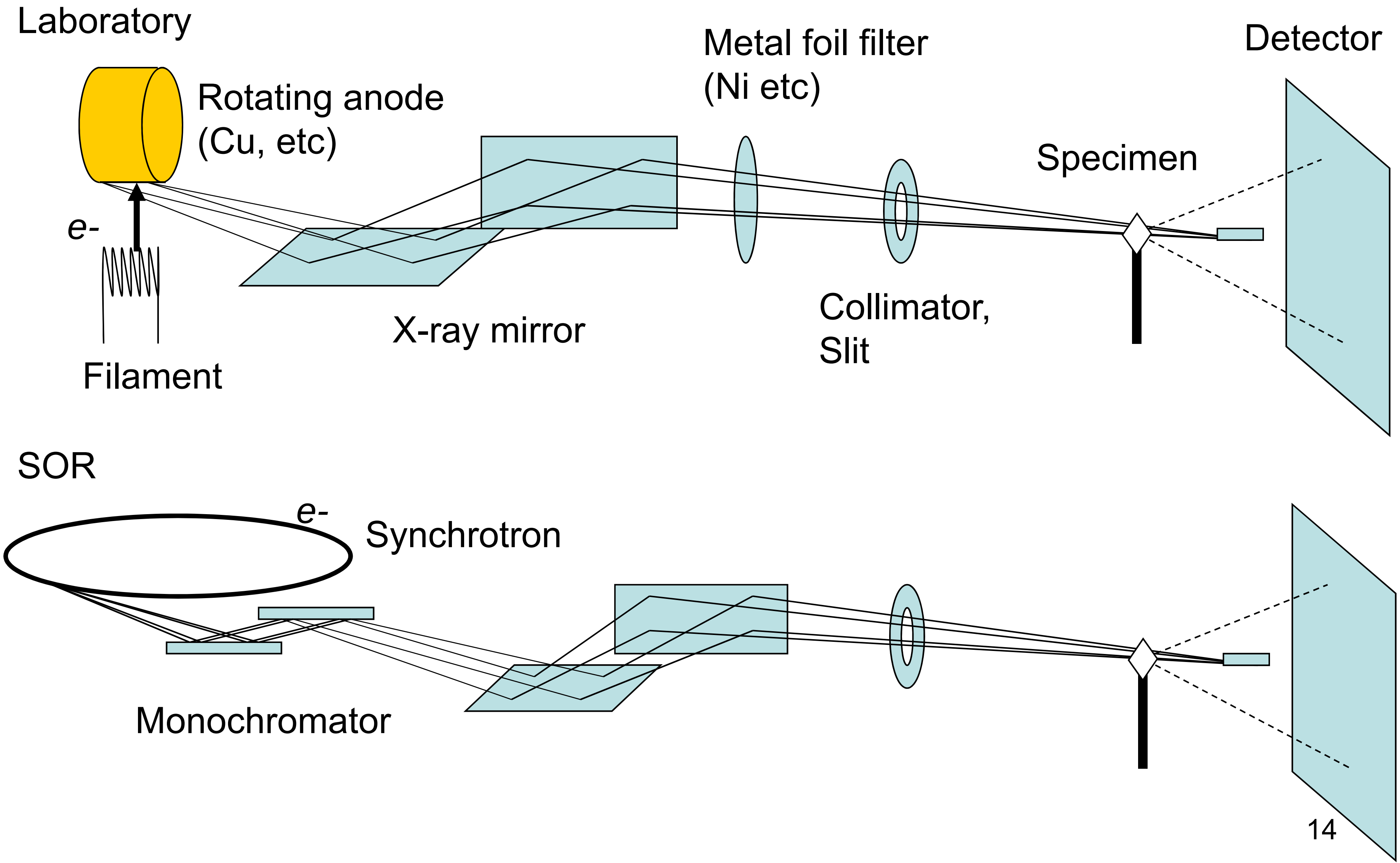

Oscillation method

To record all individual reciprocal spots, the crystal is rotated with a step-width around one axis. The step-width images are processed to obtain a data set.

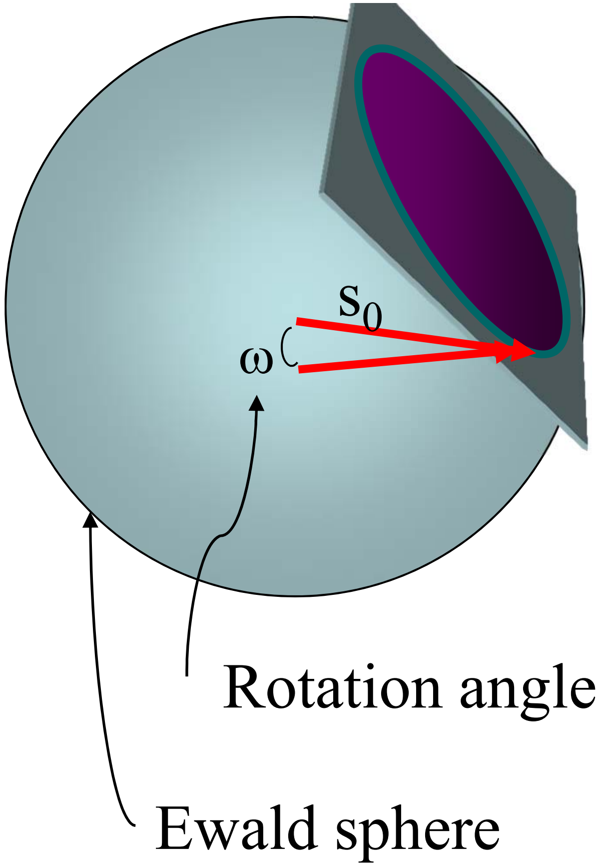

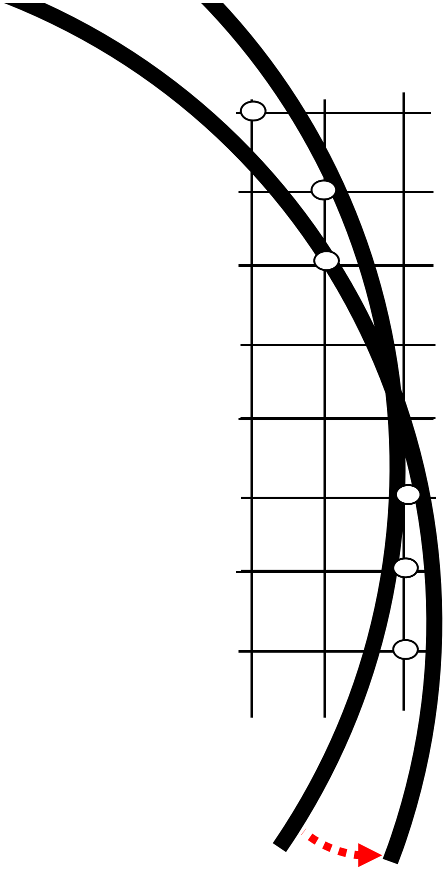

When a reciprocal points across the Ewald sphere, its intensity profile is recorded on detector.

A series of images

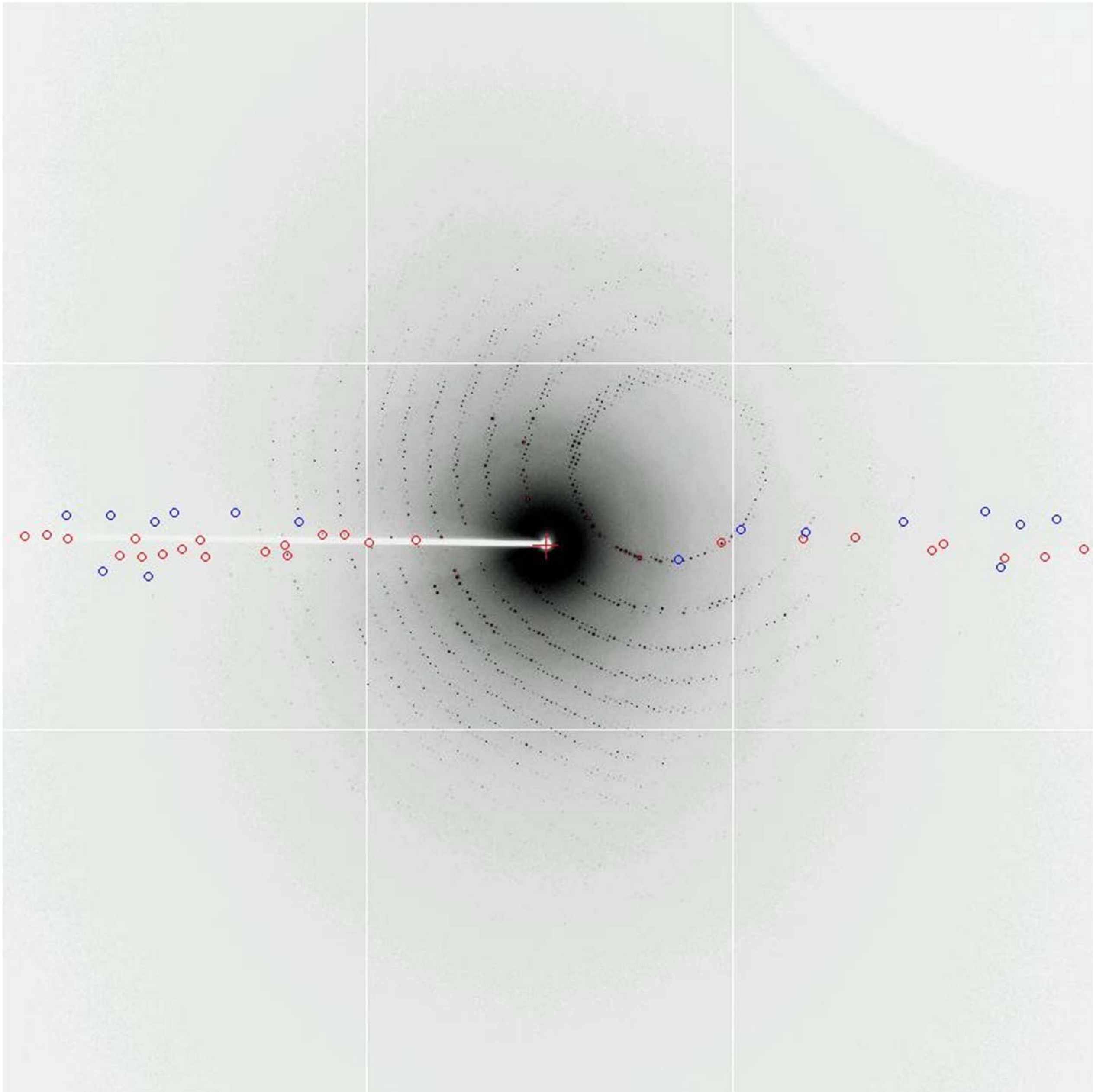

Parameters in oscillation method

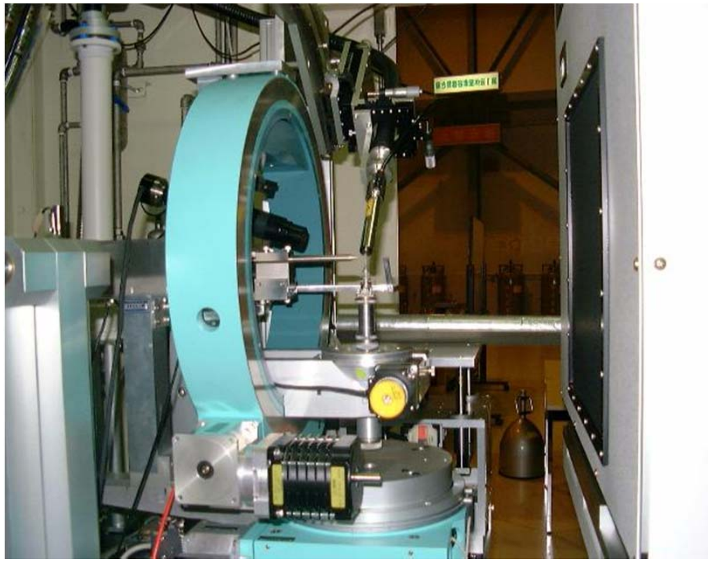

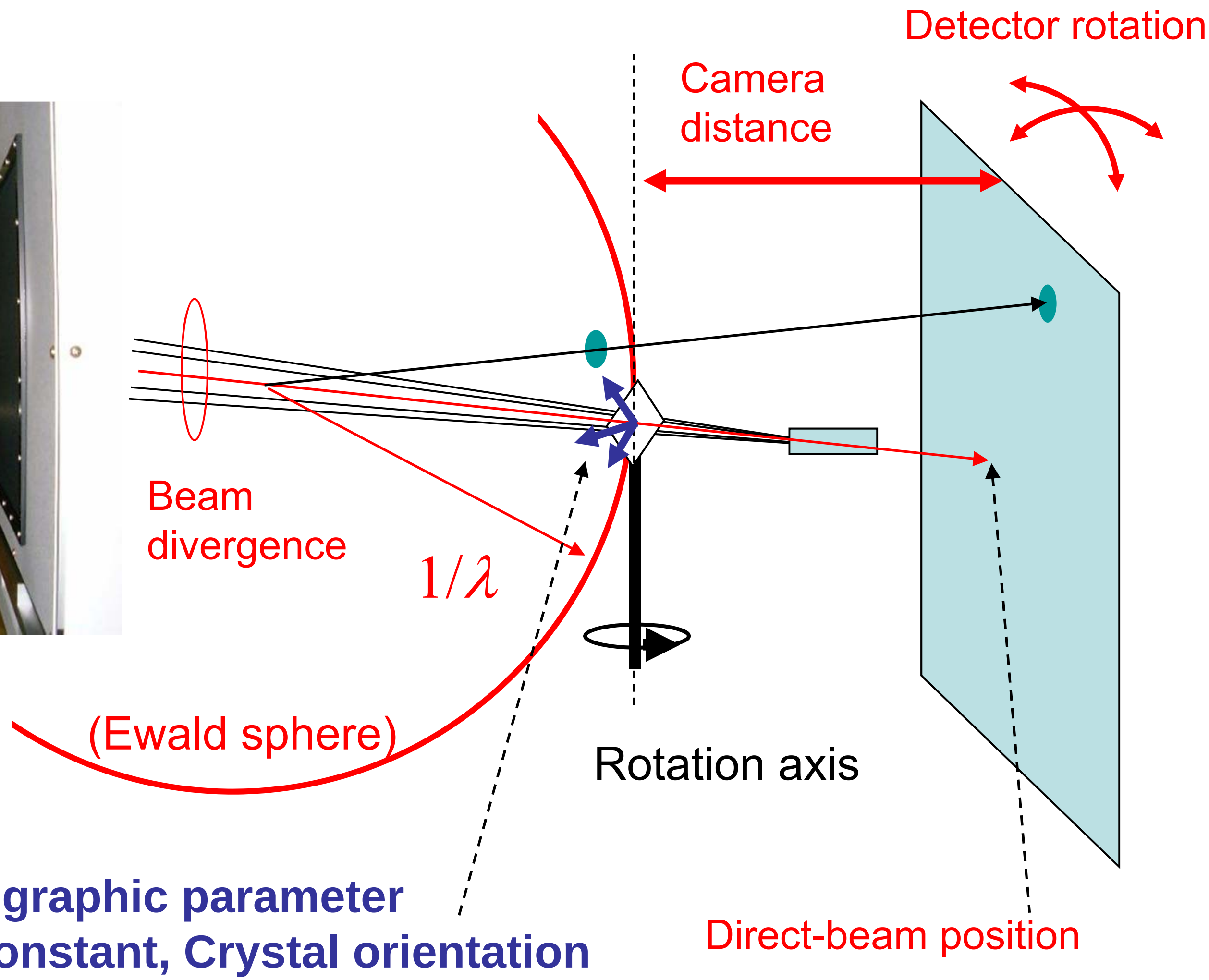

Diffraction image processing

Obtain index (hkl) and intensity (*I*) of each diffraction spot
In collected from single wavelength & single crystal

Software

MOSFLM, XDS (free software)
HKL2000, CrystalClear

Steps of image processing

Indexing:	Determine parameters incl. lattice const.
Integration:	Calculating peak intensity
Scaling:	Merging & averaging equivalent reflections

Spot Finding

Find spots and calculate and record its coordinates on detector.

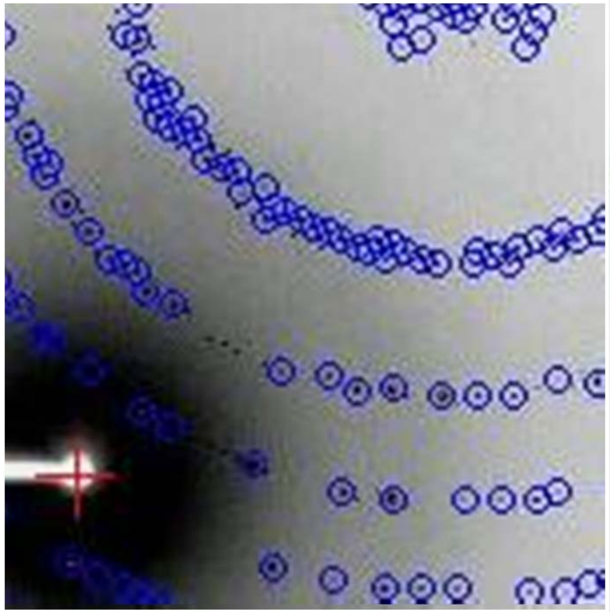

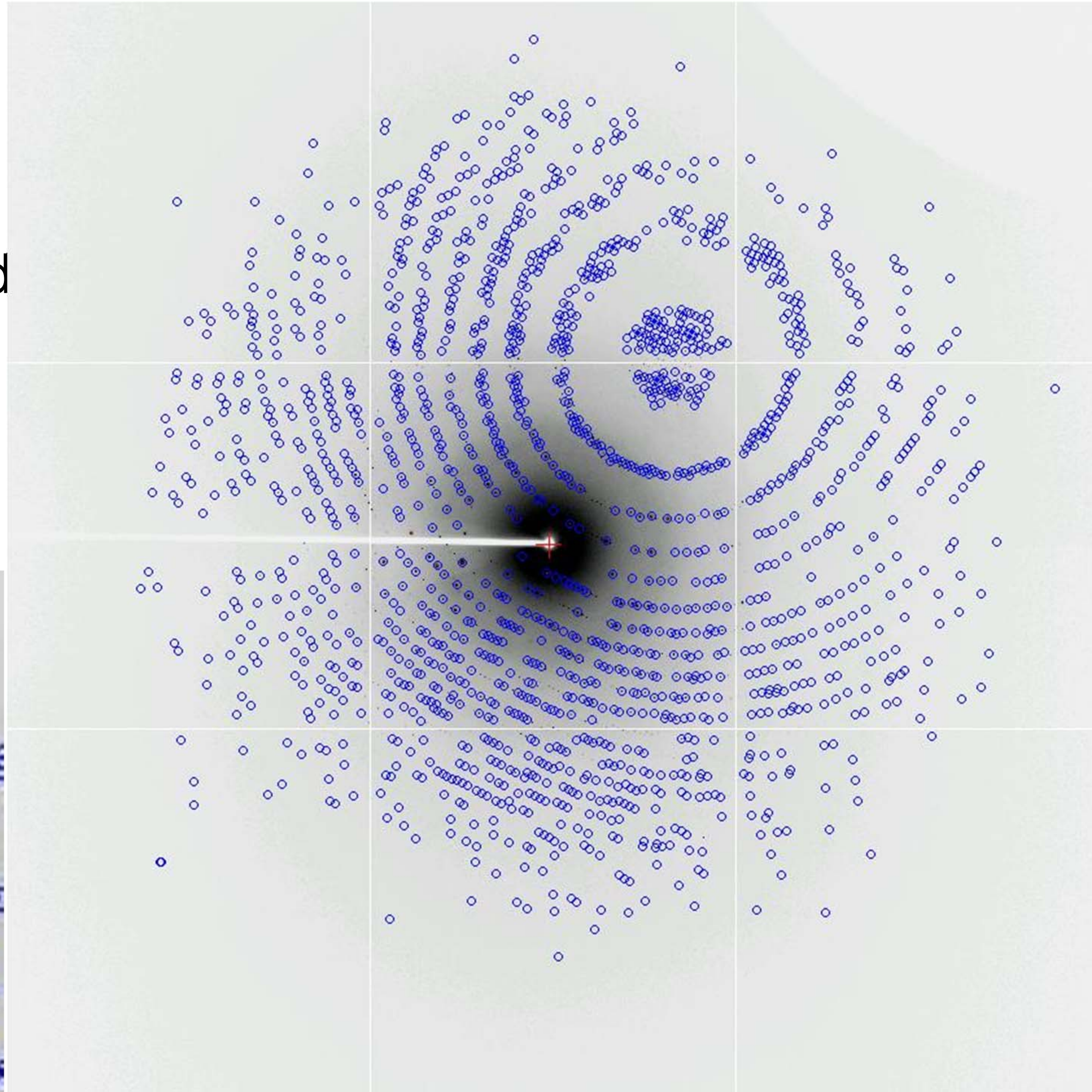

Autoindexing

Using spot positions, deduce possible crystal system and lattice parameters.

Choose a solution:

Soln	Least Sq	Spacegrp	Bravais	Lattice	a	b	c	Volume	α	β	γ
7	0.23	75	tetrago	P	77.02	77.02	37.44	222091	90.00	90.00	90.00
9	0.20	21	orthorh	C	108.87	108.97	37.44	444181	90.00	90.00	90.00
11	0.23	16	orthorh	P	37.44	77.01	77.03	222090	90.00	90.00	90.00
12	0.04	5	monocli	C	108.87	108.97	37.44	444181	90.00	90.00	90.00
13	0.12	3	monocli	P	37.44	77.01	77.03	222090	90.00	90.13	90.00
13b	0.17	3	monocli	P	37.44	77.01	77.03	222090	90.00	90.13	90.00
14	0.00	1	triclin	P	37.44	77.01	77.03	222090	89.95	89.87	89.90

Lattice type (Spacegrp, Bravais, Lattice)

Lattice constant (a, b, c, Volume, α, β, γ)

Agreement between observed and calculated spot position (Least Sq)

Refinement

Various parameters are optimized using spot positions

Crystal

All crystal · All cell · All lengths · Constrain unit cell according to symmetry · All angles · Goniometer orientation · All rotations

	a	b	c	α	β	γ	Rot1	Rot2	Rot3	Mosaicity
Start	77.02	77.02	37.44	90.00	90.00	90.00	-52.7353	-57.4633	-45.7115	0.11
Last	77.02	77.02	37.44	90.00	90.00	90.00	-52.7353	-57.4633	-45.7115	0.11
Δ	0.0000	0.0000	0.0000	0.0000	0.0000	0.0000	0.0000	0.0000	0.0000	0.0000
Result	77.0087	77.0087	37.4263	90.0000	90.0000	90.0000	-52.7466	-57.4508	-45.7226	0.1115
σ	0.0341	0.0341	0.0269	0.0000	0.0000	0.0000	0.0335	0.0203	0.0359	0.1000
Δ / σ	0.0000	0.0000	0.0000	0.0000	0.0000	0.0000	0.0000	0.0000	0.0000	0.0000

Detector

All detector · All translations · All rotations

	TransX	TransY	TransZ/ Dist	RotZ	RotX/ Swing	RotY
Start	0.5160	-0.0387	155.2467	0.0009	-0.0121	0.1902
Last	0.5160	-0.0387	155.2467	0.0009	-0.0121	0.1902
Δ	0.0000	0.0000	0.0000	0.0000	0.0000	0.0000
Result	0.5272	-0.0232	155.3774	-0.0284	-0.0075	0.1891
σ	0.0249	0.0253	0.0573	0.0174	0.0878	0.1002
Δ / σ	0.0000	0.0000	0.0000	0.0000	0.0000	0.0000

Source

All rotations

	Wavelength	Rot1	Rot2
Start	0.70850	-0.0001	0.0001
Last	0.70850	-0.0001	0.0001
Δ	fixed	-0.0000	0.0000
Result	0.7085	-0.0054	-0.0026
σ	fixed	0.0152	0.0112
Δ / σ	fixed	0.0000	0.0000

Refinement

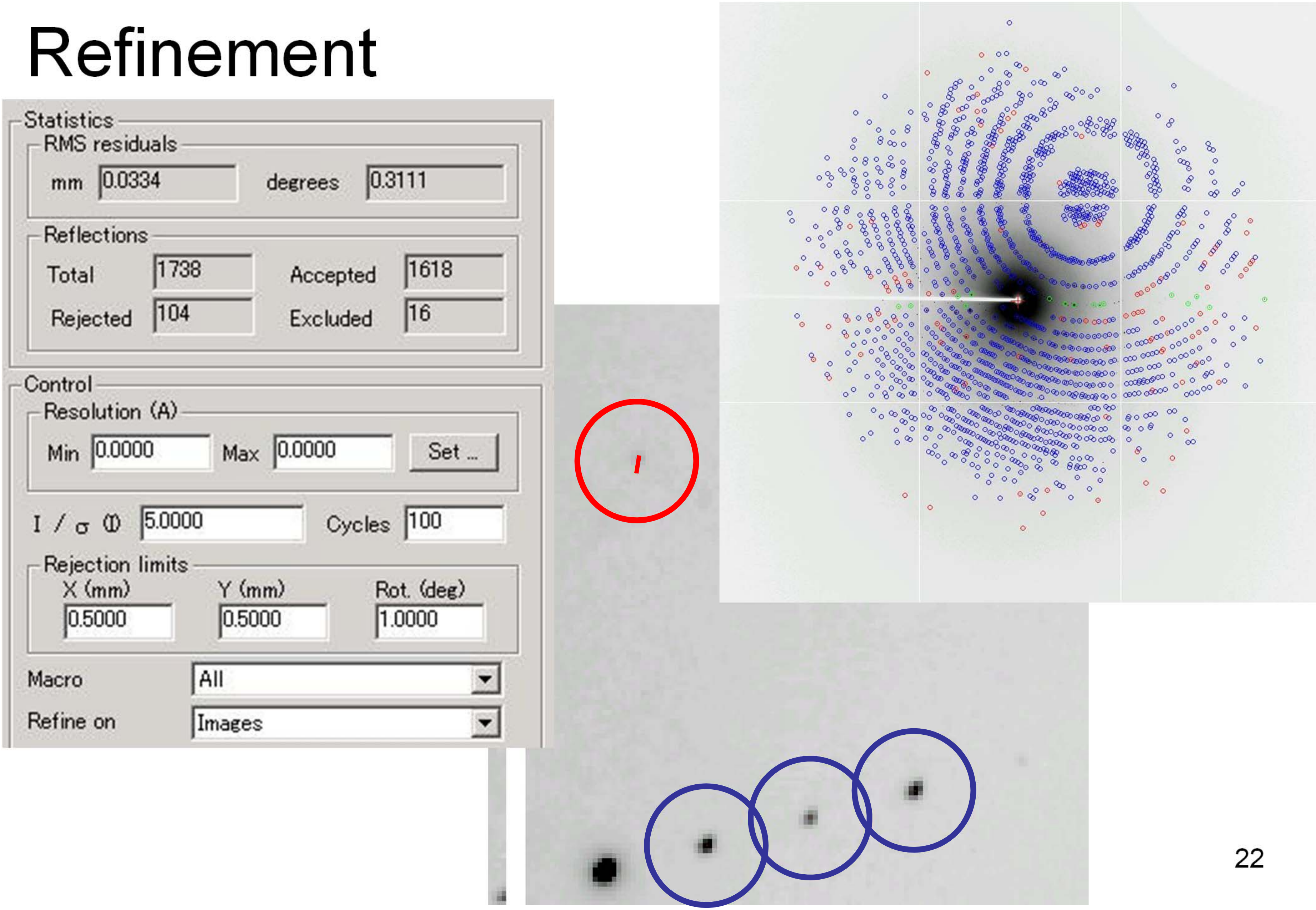
Statistics
RMS residuals
mm 0.0334
degrees 0.3111
Reflections
Total 1738
Accepted 1618
Rejected 104
Excluded 16
Control
Resolution (A)
Min 0.0000
Max 0.0000
Set ...
I / σ (I) 5.0000
Cycles 100
Rejection limits
X (mm) 0.5000
Y (mm) 0.5000
Rot. (deg) 1.0000
Macro All
Refine on Images

Integration

Integrate diffraction spot profile.

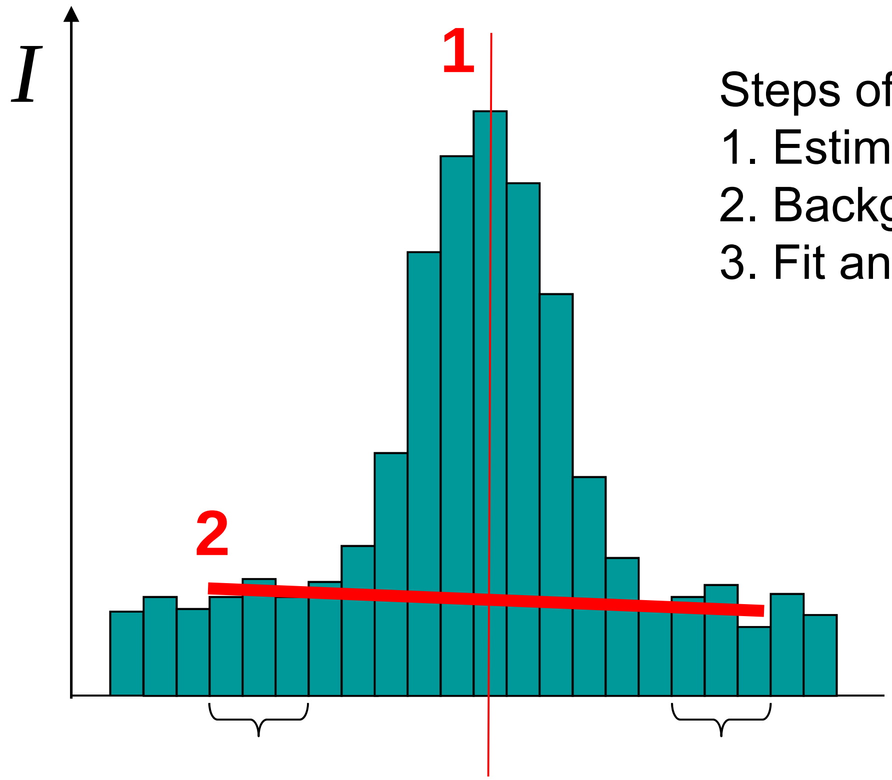

Steps of integration:
1. Estimate correct spot positions
2. Background estimation
3. Fit and integrate by averaged reflection profile

2D peak profile

Integration

Integrate diffraction spot profile.

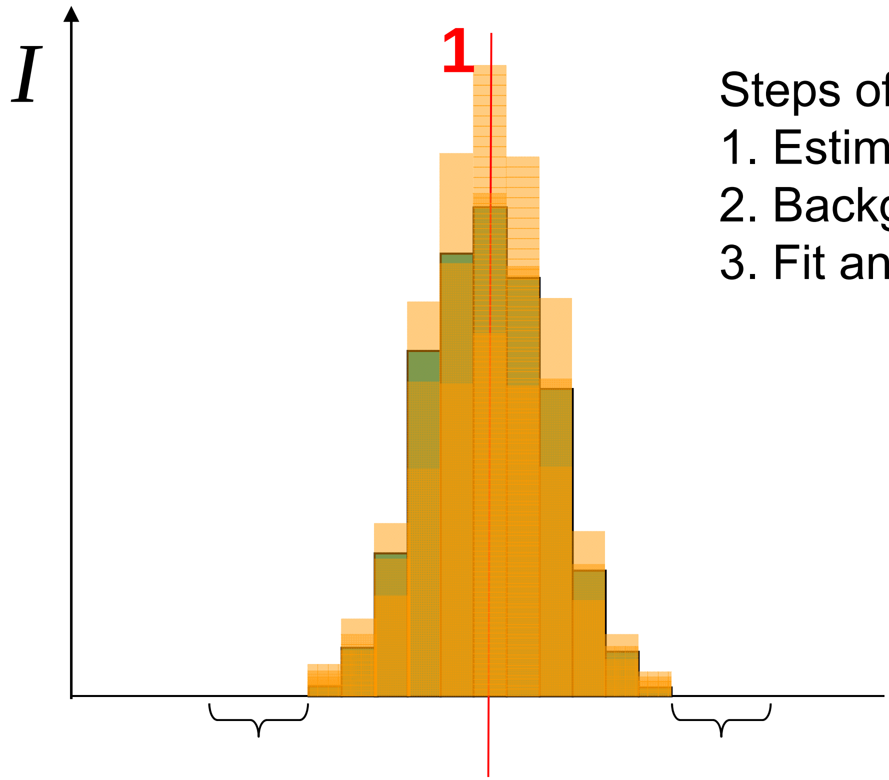

Steps of integration:

1. Estimate correct spot positions
2. Background estimation
3. Fit and integrate by averaged reflection profile

Scaling

Equivalent intensity among symmetrically equivalent reflections

ex. $P2_1$; $(x, y, z), (\bar{x}, y+1/2, \bar{z})$

$$I(h\ k\ l) = I(\bar{h}\ k\ \bar{l})$$

$$I(\bar{h}\ \bar{k}\ \bar{l}) = I(h\ \bar{k}\ l)$$

Estimate scale and falloff factor in each plate

Variation of incident intensity, absorption by crystal, etc.

during one data set

Rmerge overall:

Measures the agreement of symmetry related observations of a reflection.

Rmerge in the last shell:

Rmerge in the highest resolution shell.

I/sigma:

A measure of the signal to noise ratio.

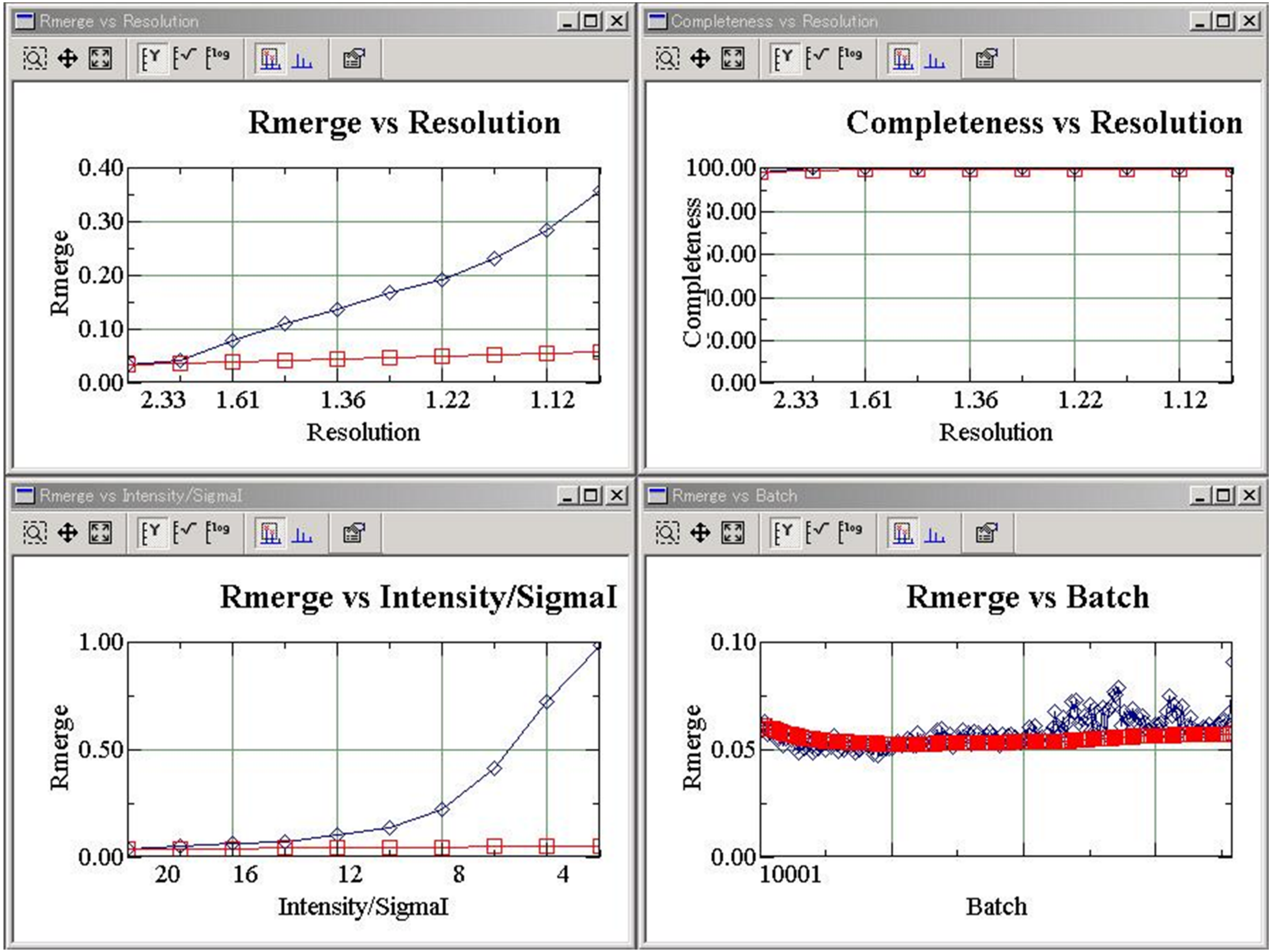

Rmerge vs Resolution
Rmerge vs Resolution
0.40
0.30
0.20
0.10
0.00
Rmerge
2.33
1.61
1.36
1.22
1.12
Resolution
Completeness vs Resolution
Completeness vs Resolution
100.00
0.00
Completeness
2.33
1.61
1.36
1.22
1.12
Resolution
Rmerge vs Intensity/SigmaI
Rmerge vs Intensity/SigmaI
1.00
0.50
0.00
Rmerge
20
16
12
8
4
Intensity/SigmaI
Rmerge vs Batch
Rmerge vs Batch
0.10
0.05
0.00
Rmerge
10001
Batch

Signal-Noise Ratio (S/N)

Signal: Diffraction intensity ~ Dose dependent

Noise: Radiation damage ~ Dose dependent

Scattering noise ~ Dose dependent

Detector dark noise ~ Time dependent

Detector readout noise ~ Image number dependent

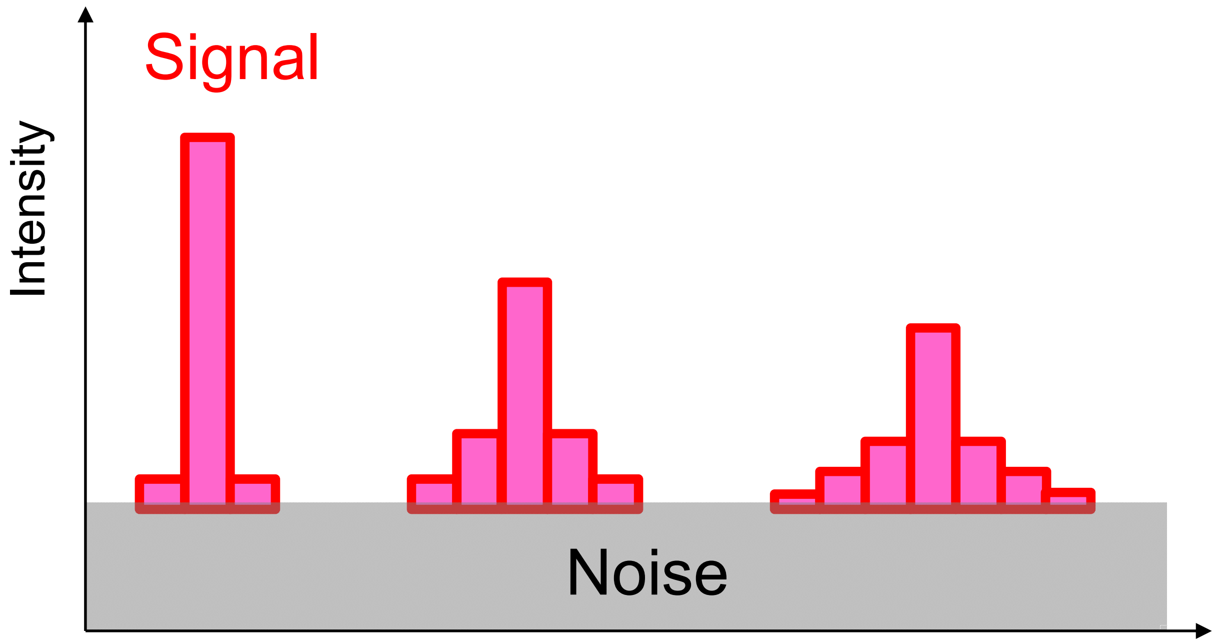

Signal: Diffraction power of crystal

Darwin's Formula

$$E(\mathbf{h}) = \frac{I_0}{\omega}\lambda^3 \frac{e^4}{m^2c^4}\frac{P\cdot L\cdot A\cdot V_x}{V^2}\cdot\left|F(\mathbf{h})\right|^2 \cdots$$

I_0: Incident intensity, ω: Angular velocity of crystal rotation, λ: Wavelength,
e: Charge of electron, P: Polarization factor (= $(1+\cos^2 2\theta)/2$),
L: Lotentz factor (= 1/sinθ when spindle x-ray),
A: Absorption coefficient, V_x: Crystal volume, V: Lattice volume

In case of protein crystal…

- High solvent contents (25 ~ 75%)
- Large unit cell

> Weak diffraction power ~ Low resolution

Temperature factor, B

Broader electron density (= higher thermal vibration) gives sharper scattering factor, this means it's contribution to higher resolution is smaller.

Debye-Waller factor to atomic scattering factor:

$$e^{-B\frac{\sin^2\theta}{\lambda^2}}$$

$$B = 8\pi^2 \times \overline{u^2}$$

Average square variation of atomic vibration

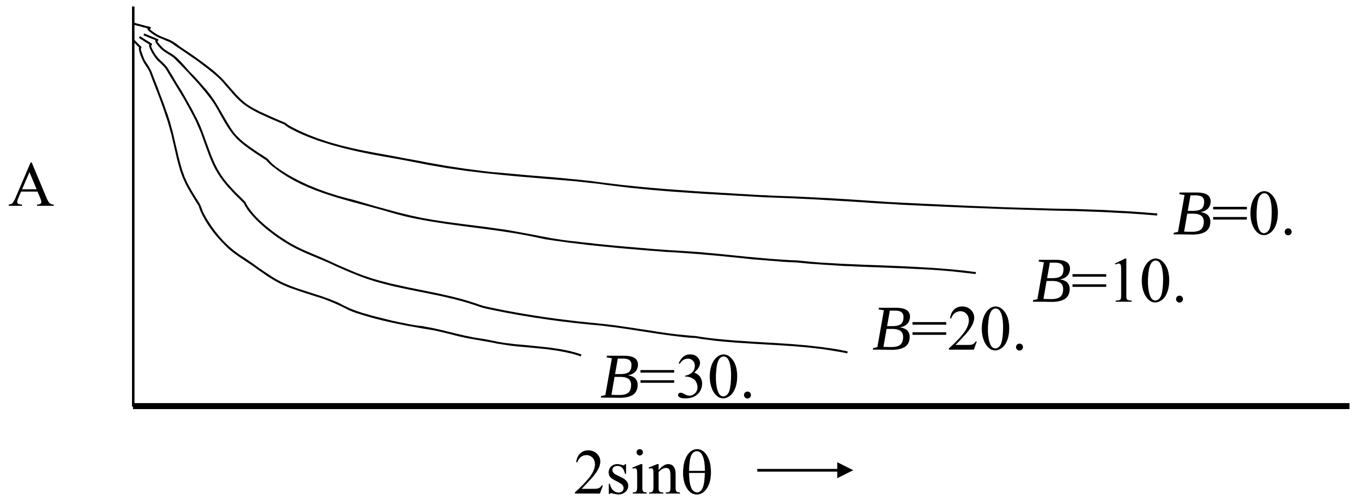

Electron density: Resolution and B-factor

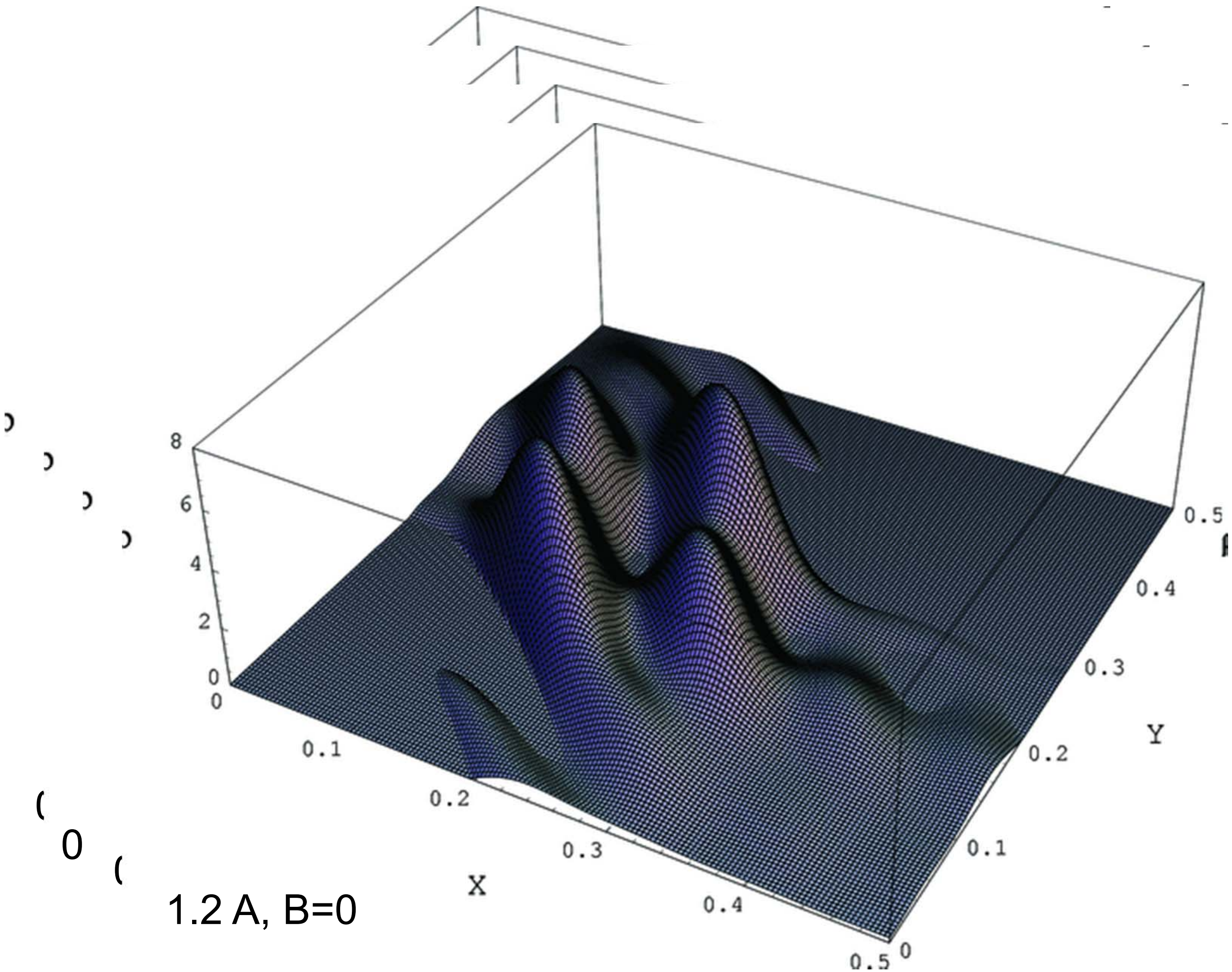

1.2 A, B=0

Crystal packing ~ molecular vibration ~ resolution

Relationship with B-factor (DWF)

Vibration in solution > Movie

Packing density V_M:

$V_M = V_{cell} / Mw_{cell}$

High density (small V_M) > High Rigidity

(Kantardjieff & Rupp, 2003)

Packing control by humidity control

FMS (Free Mounting System)

> lower humidity around crystal

> dehydration

> induce phase transition

(Kiefersauer et al., 2000)

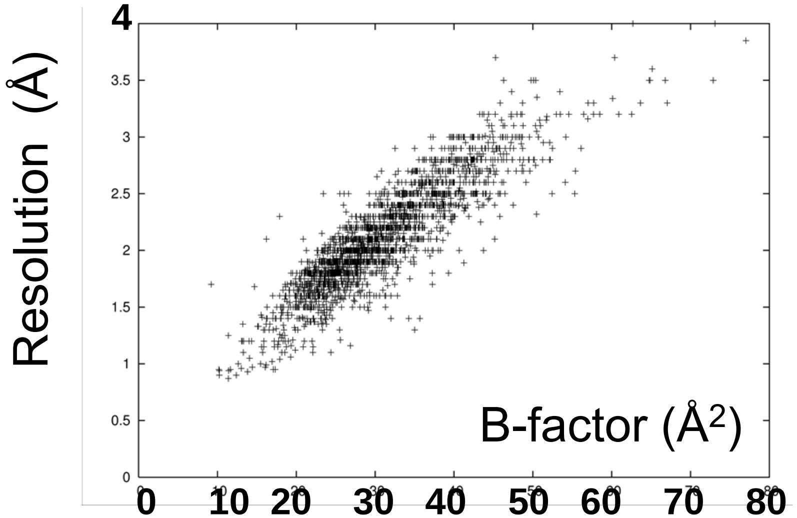

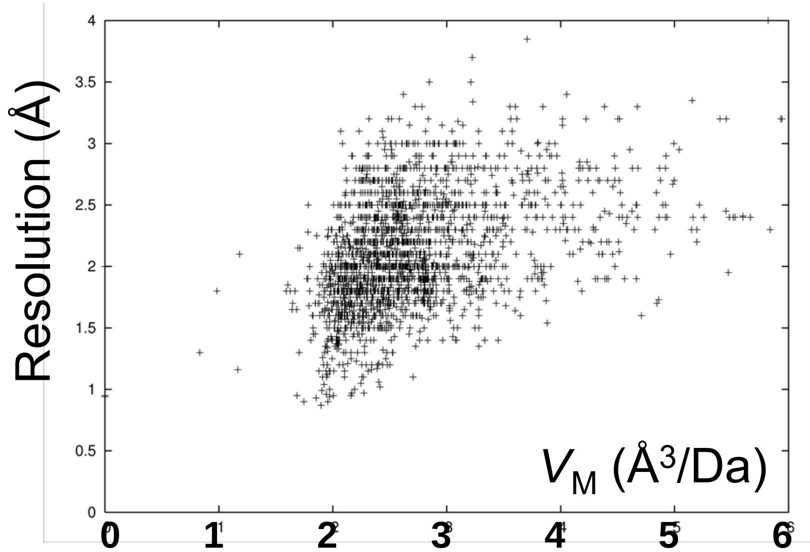

Freedom of rigid body motion

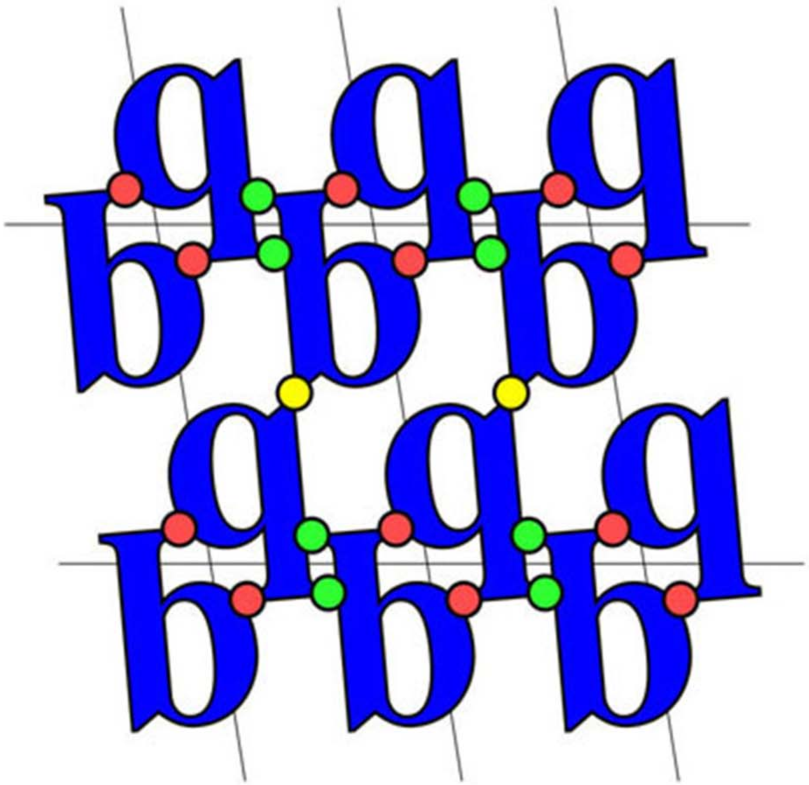

p2, C=3

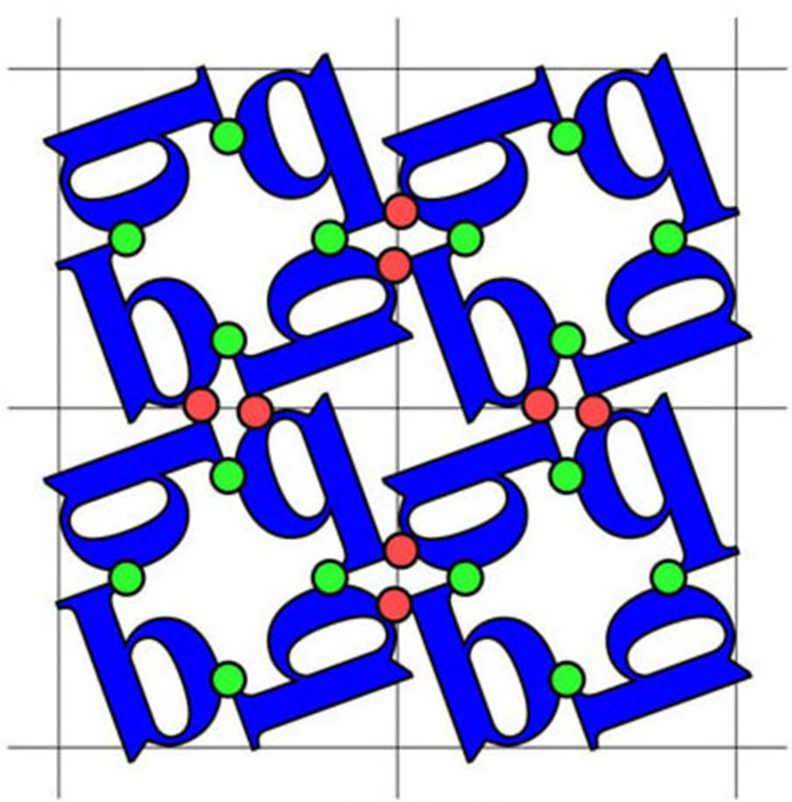

p4, C=2

This measure is also retated to space group occurrence.

- Wukovitz & Yeates. 1995. Nat. Struct. Biol. 2, 1062-7
- http://www.doe-mbi.ucla.edu/~yeates/old_space_group_freq.html
- Chruszcz, et al. 2008. Protein Science, 17, 623-632

Resolution and incident intensity

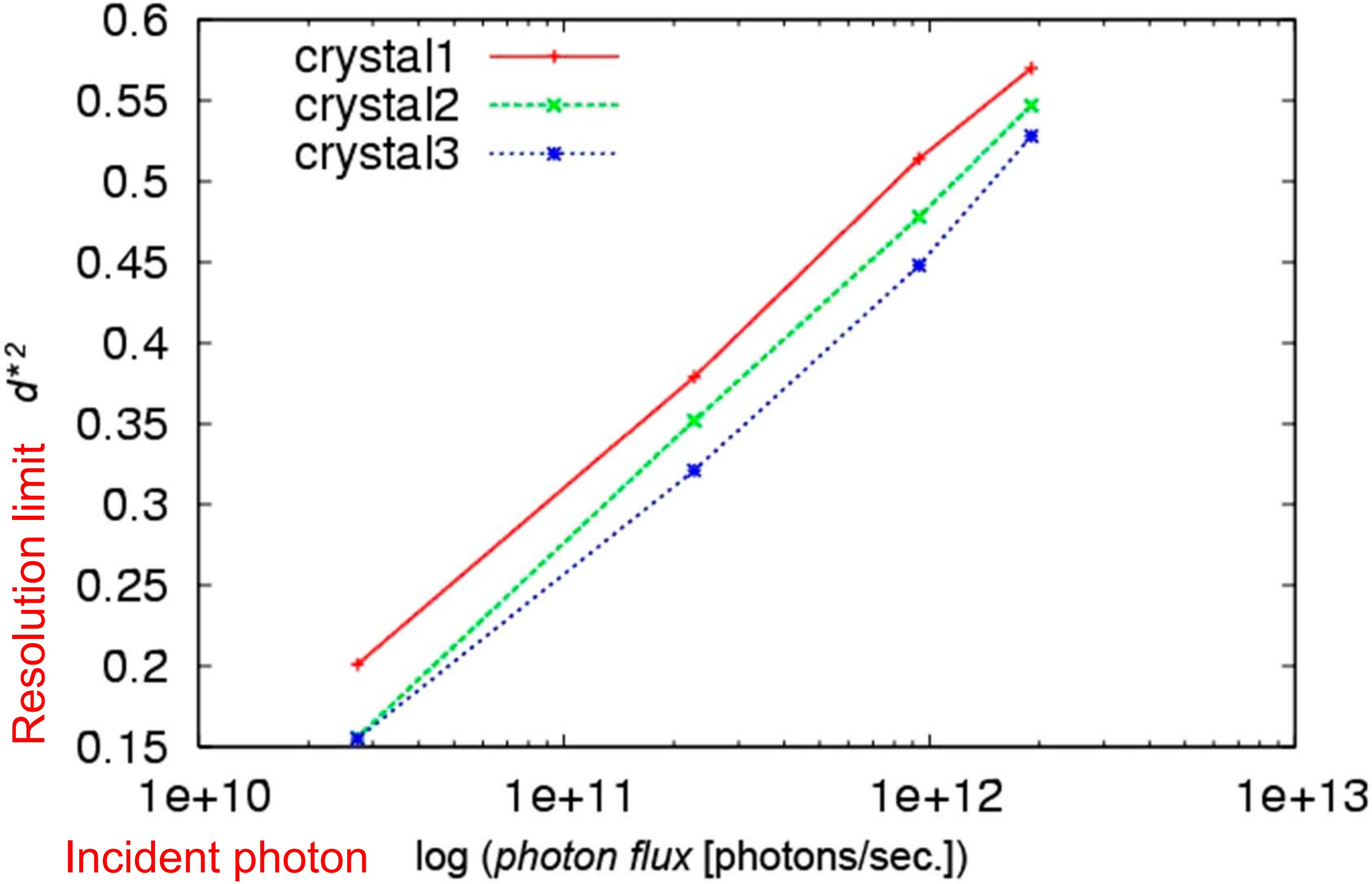

Reduction by radiation damage

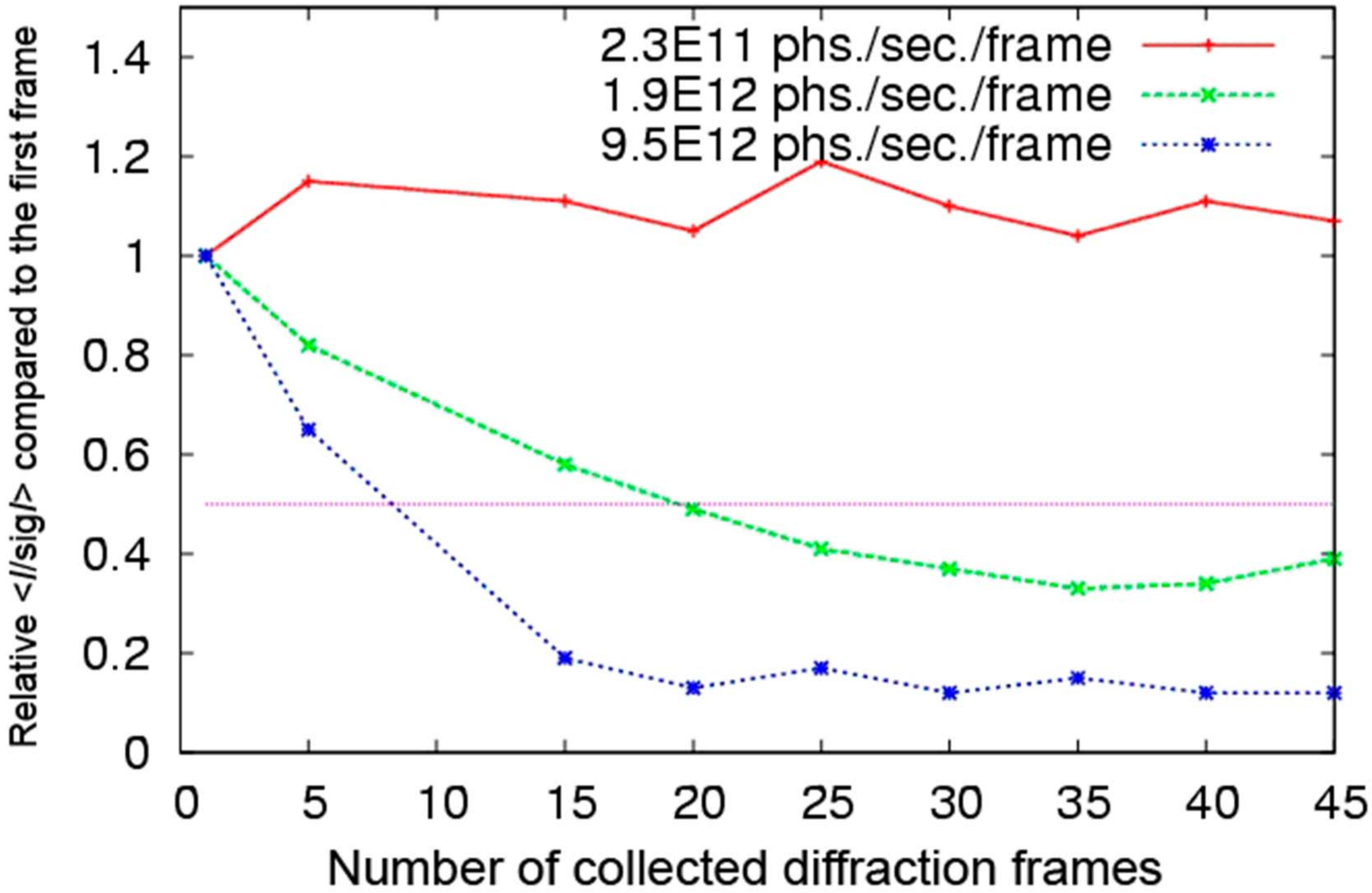

Mosaic spread

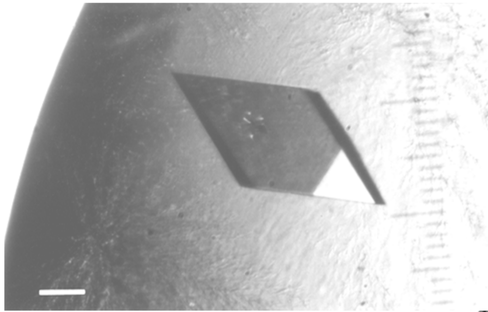

Protein crystals consist of mosaic pieces.

Any distribution of these orientation enlarging reciprocal lattice points and reduction of peak height.

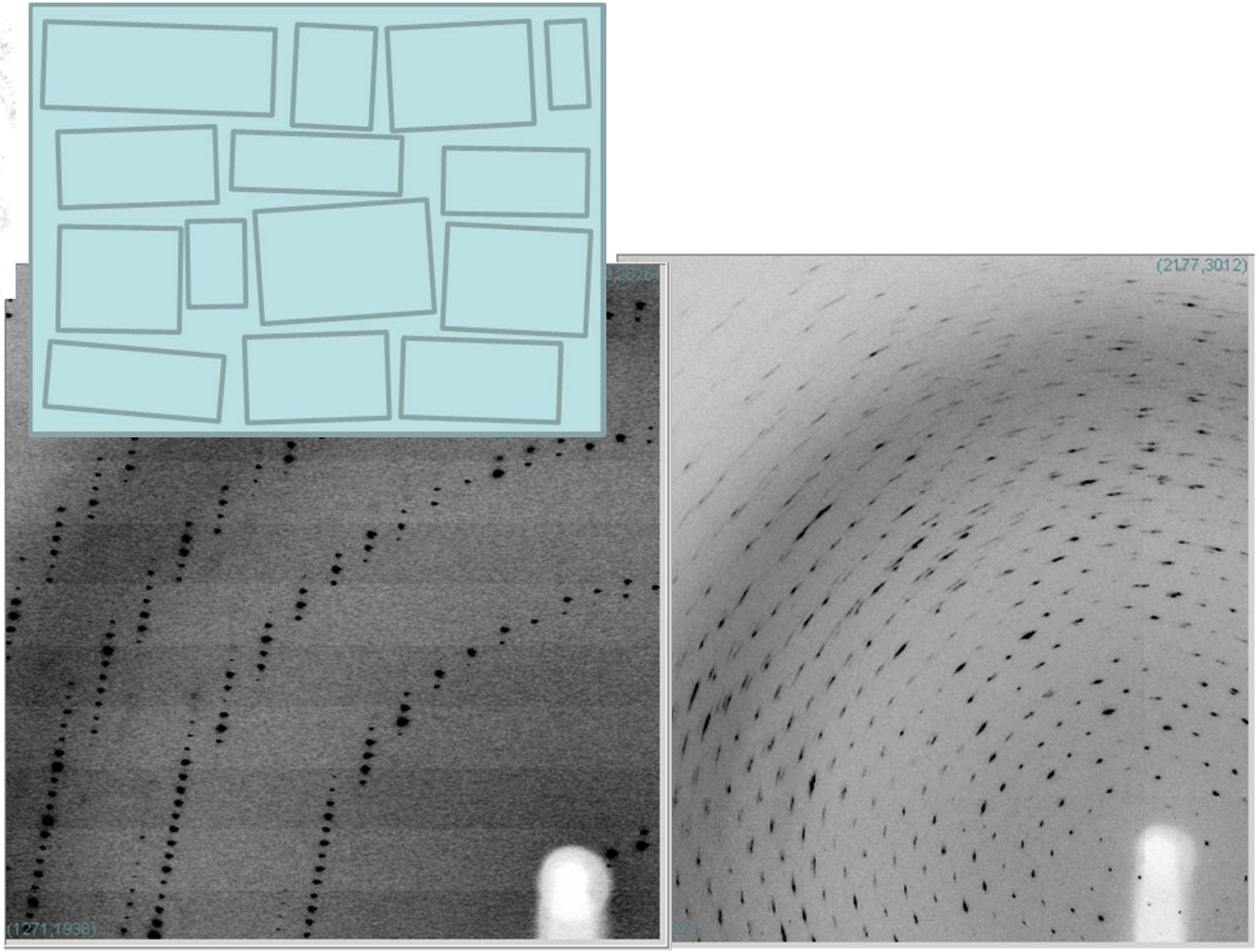

Spot sharpness depends on crystalline order.

Full reflection / Partial reflection

Full reflection:

Whole part of spot across the sphere.
> its whole intensity is recorded.

Partial reflection:

Only some part of spot across the sphere.
Its partiality can be estimated from crystal orientation and mosaic spread (spot width).

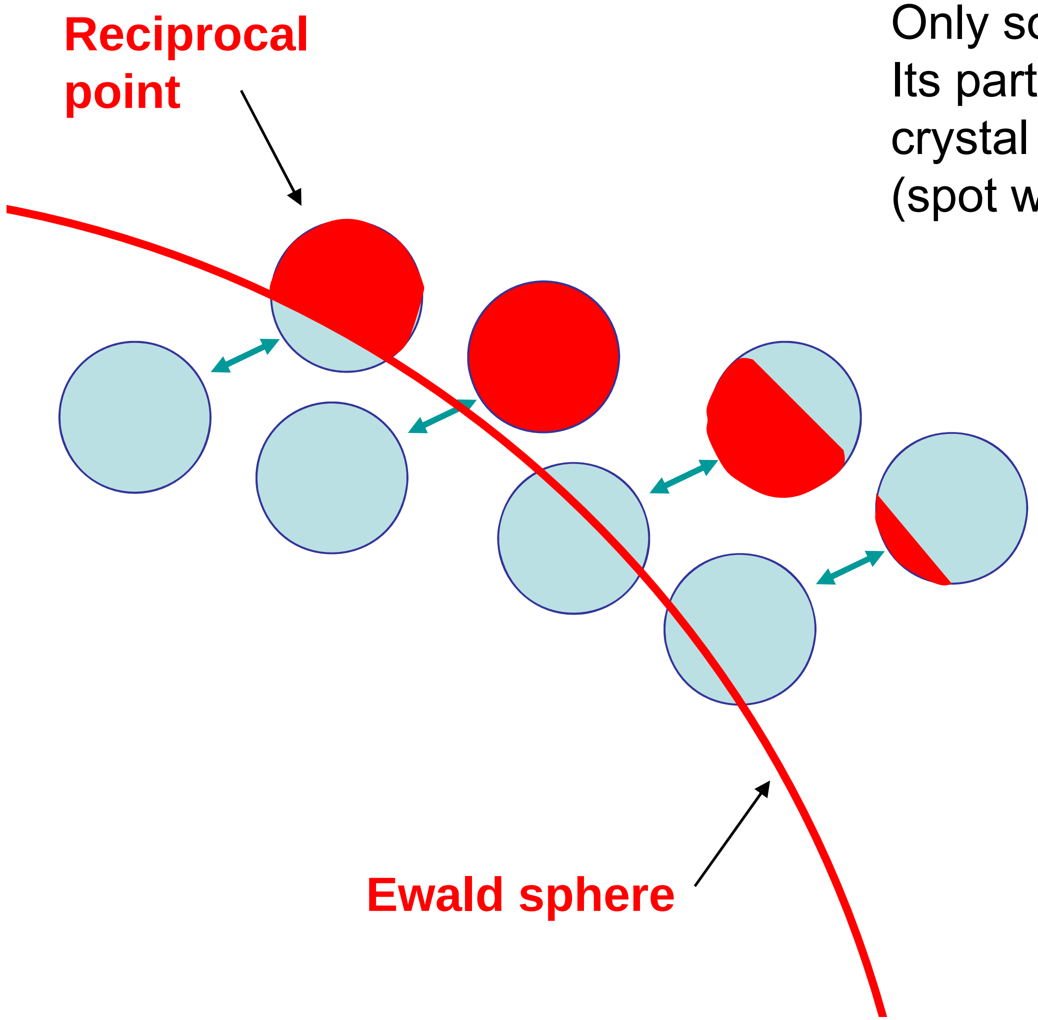

Reflection overlaps

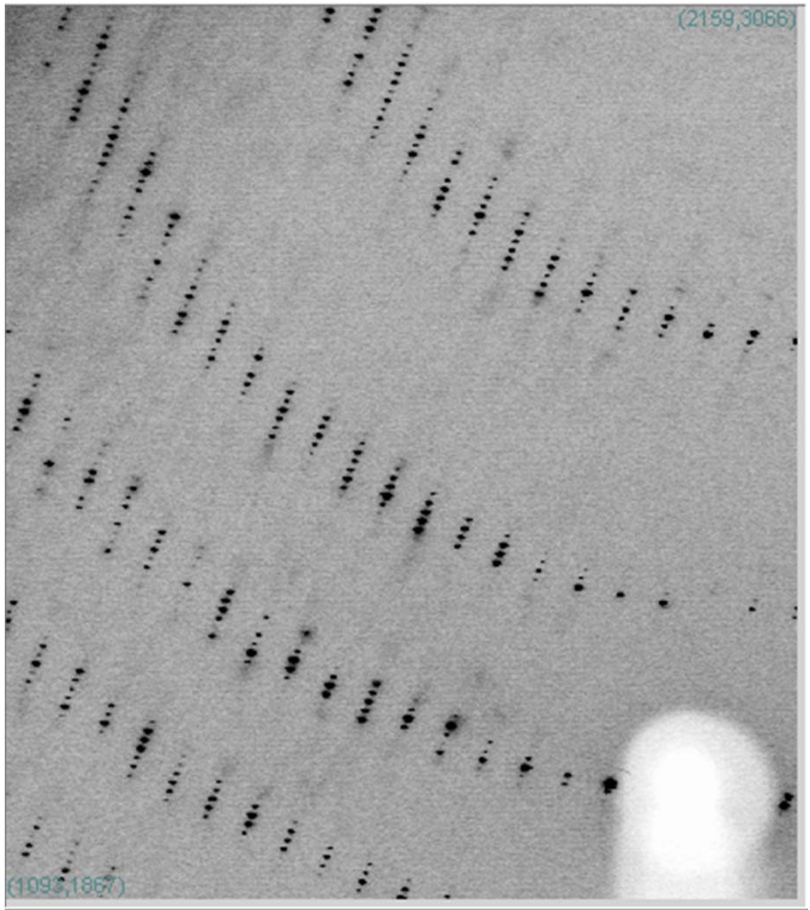

Longer lattice constant gives narrower spacing of adjacent reflections.

Long axis should be placed along rotation axis.

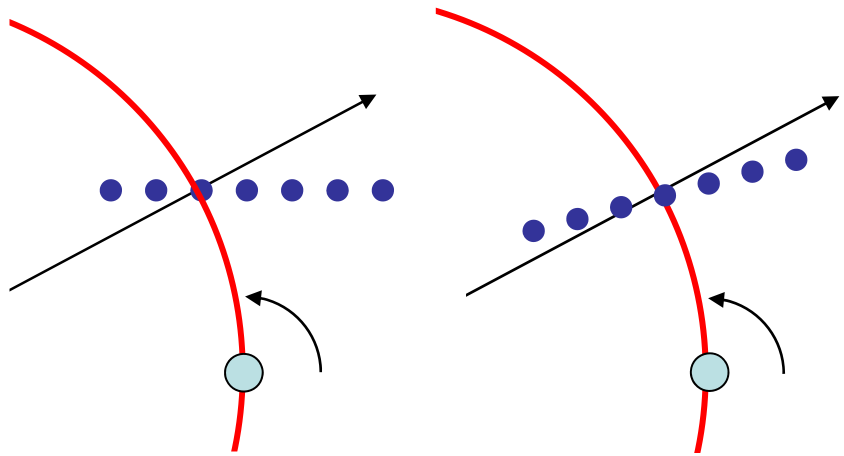

X-ray detector: 2D detectors for PX

	CMOS	CCD		Amorphous Selenium	Silicon Pixel	IP
		Indirect	Direct			
Area size (100-400mm)	○ Multi-element	○ ME+FOT	△ cm sq. order	◎ by processing tech.	○ ME	◎
Resolution (50-100μm)	◎ Few-200 μm Phosphor	○ 10 - 100 μm FOT&phosphor	◎ Few μm	○ 100~200 μm	△ ~200 μm	○ 50 μm~
Readout Speed	◎ Sub mSec Continuous readout	○ Sec		○ Sec	◎ Real time Counting	△ Min
Sensitivity	△～◎ Phosphor & Window	△～◎ Phosphor		△	△～◎ Low for high E photon	◎
Noise	△～○ Relatively high readout & dark noise	○ Successful Cooling Phosphor/FOT/Window		△ Higher noise by polycrystalline	◎ Counting (counting loss at high dose)	△ Stray light of laser / Loss of fluorescence Capture
Skew	◎	△ FOT	◎ Direct	◎ Direct	◎ Direct	○～◎ Geometry at readout
Dynamic range	△ ~12bit	○ ~16 bit		○ ~16 bit	◎ ∞ (Counting)	◎ ~20 bit
Cost	◎ Versatile Processing technology	△～○ Complex system	◎ Cheap but small	? Expecting Future development	△ Original tech. and monopolistic	◎ Simple and matured technology

Imaging plate

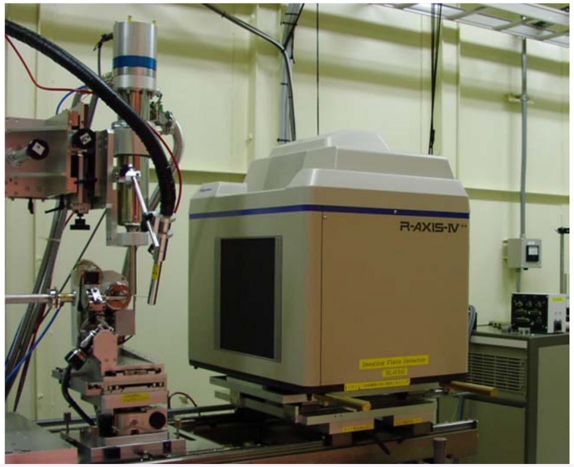

Plastic X-ray sensitive film
Photostimulated luminescence by $BaFBr:Eu^{2+}$

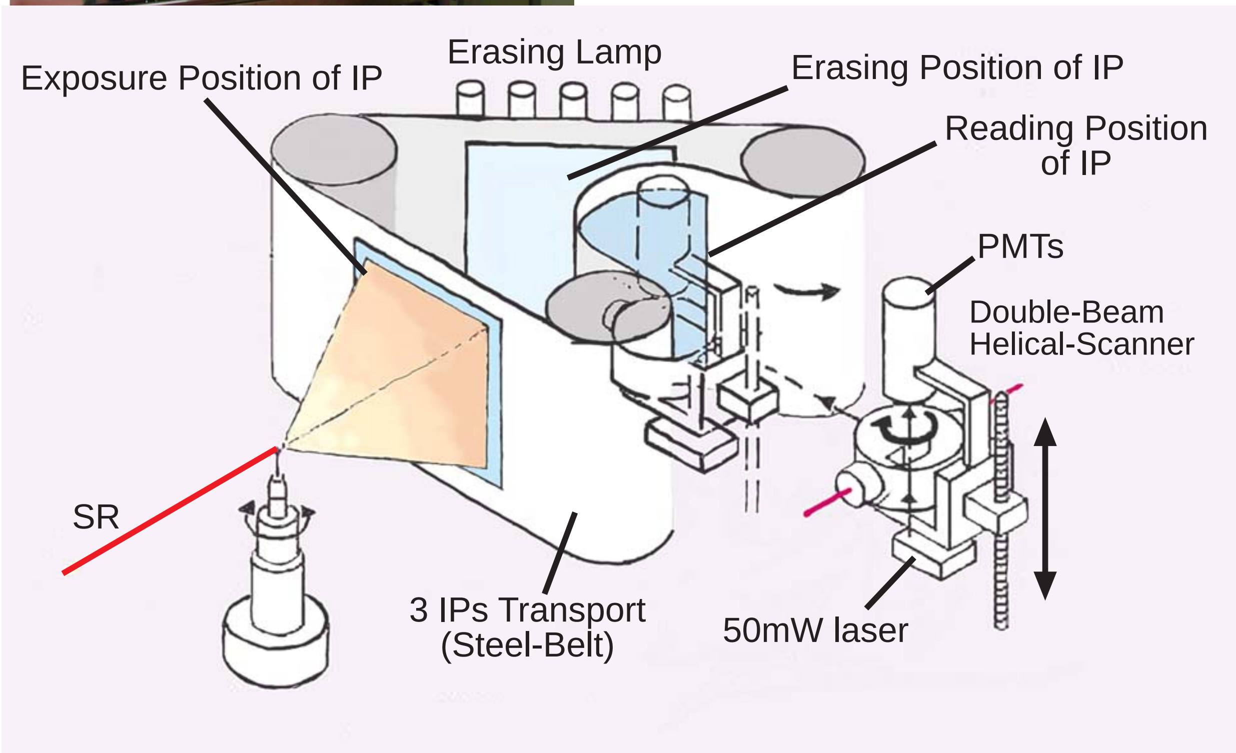

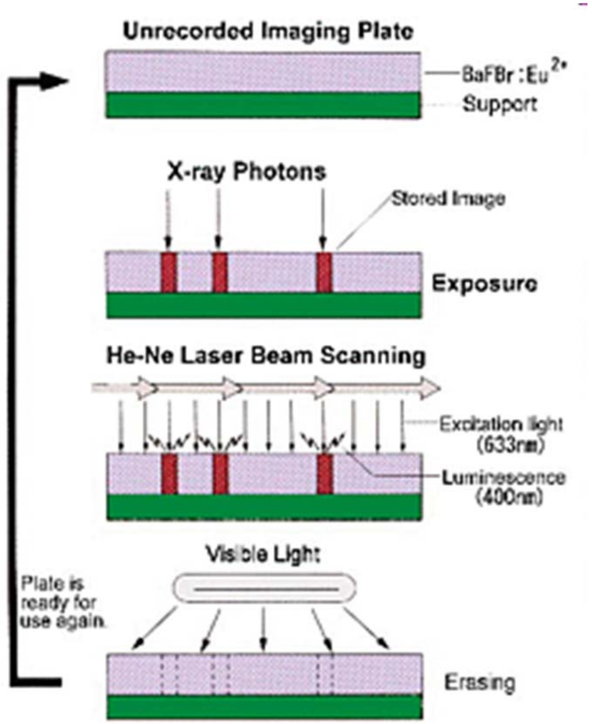

(Rigaku, Japan)

CCD Detector

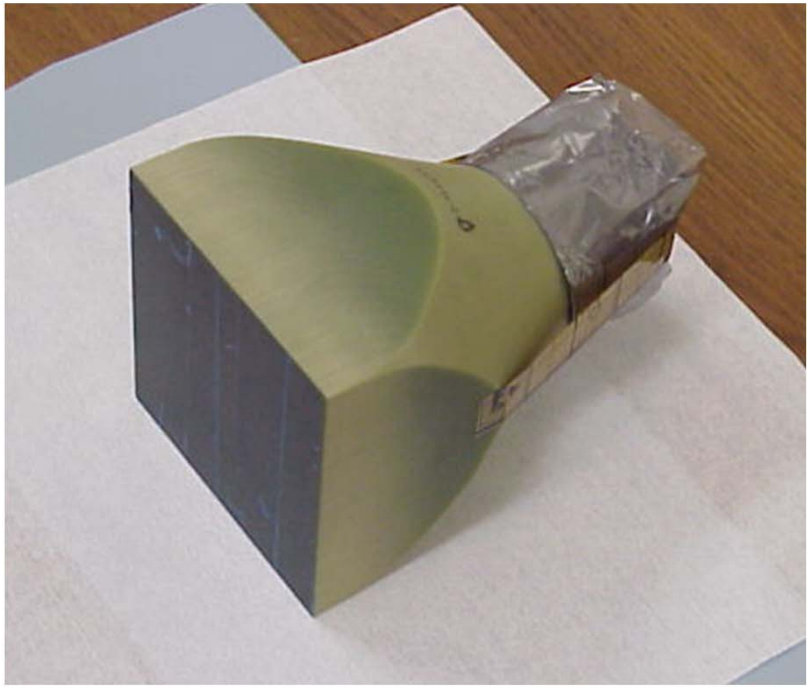

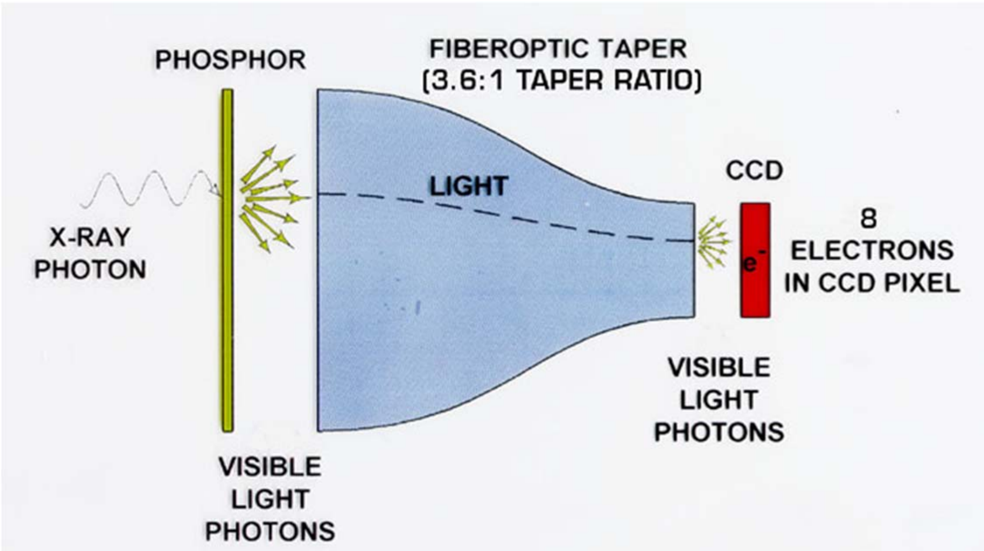

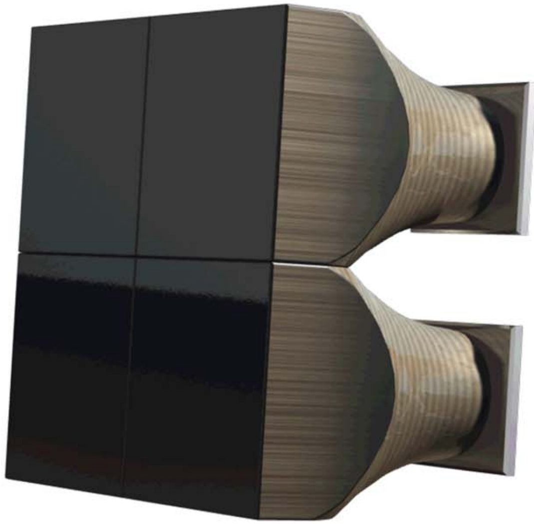

CCD detector system

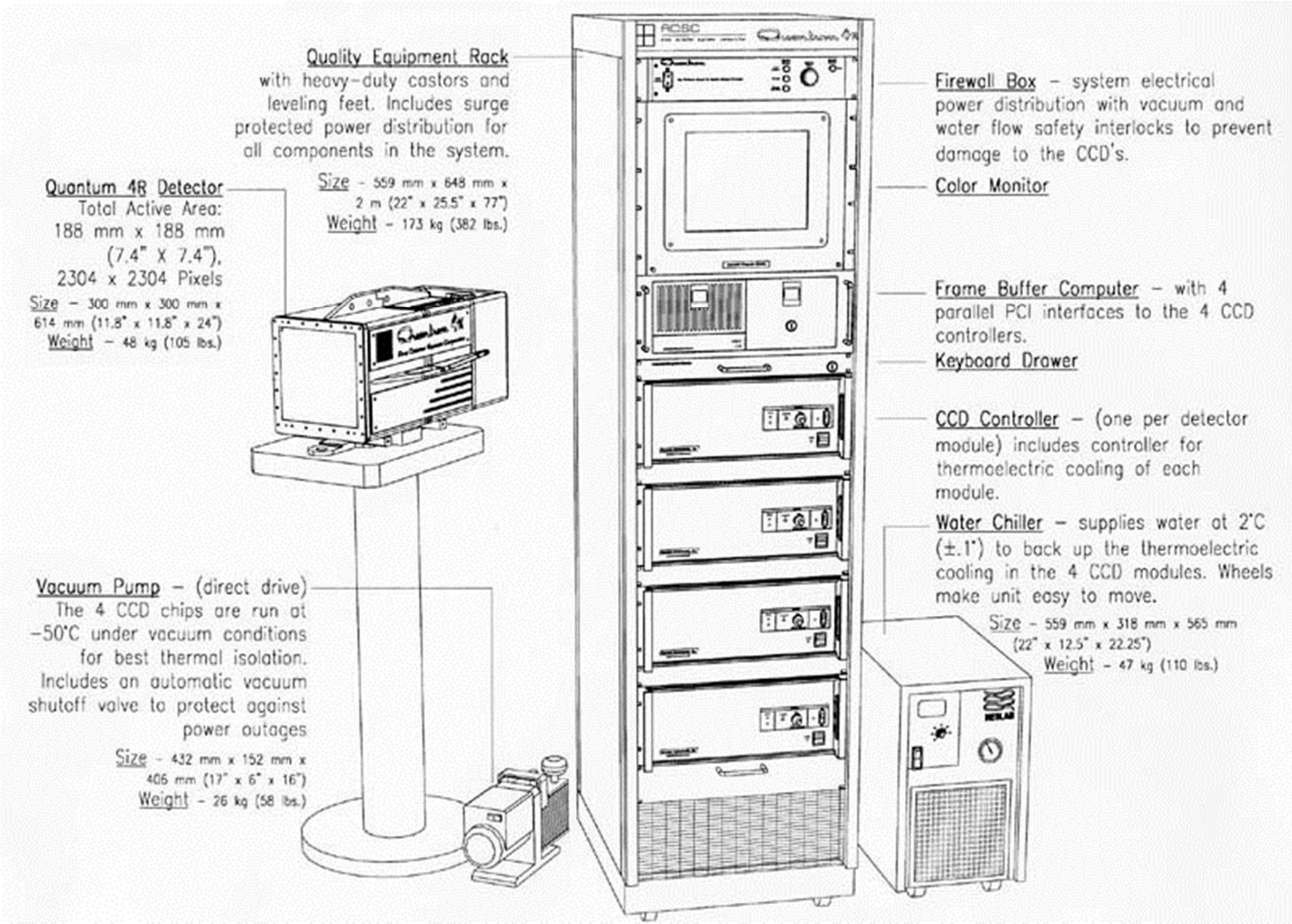

Area Detector Systems Co. http://www.adsc-xray.com

Continuous rotation data collection by CMOS Detector

Hasegawa (JASRI) &
Yamamoto (RIKEN)
Hamamatsu Photonics

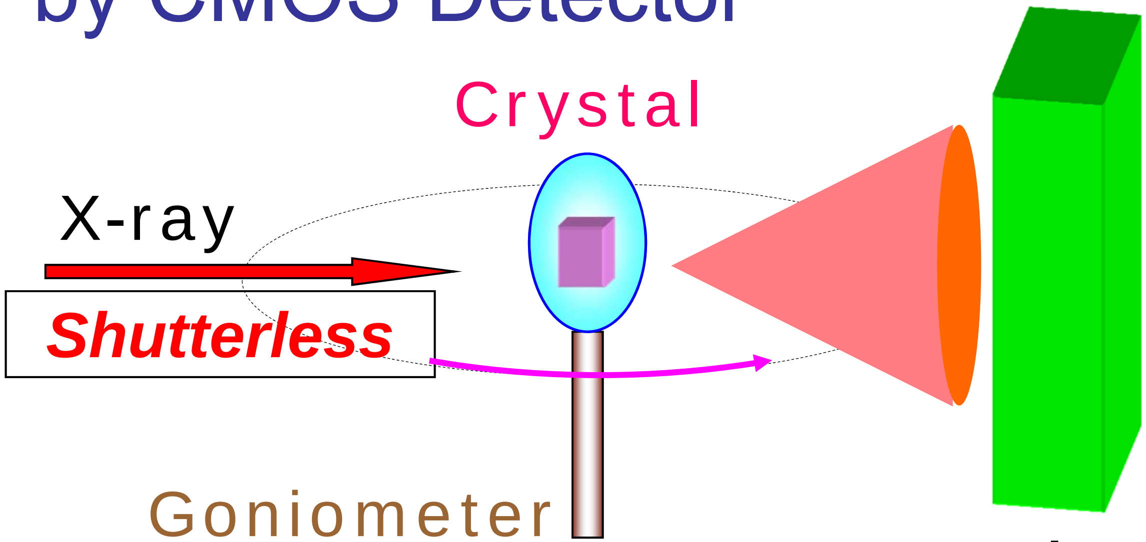

Rotate with a constant speed

Read out images with a constant frame rate

High throughput and/or Fine slice data collection

Specification	**Hamamatsu C10158DK**	**ADSC Q210**
Scintillator	**CsI:Tl**	**Gd_2O_2S:Tb**
Pixel size [mm²]	**50 x 50**	**51 x 51**
Detector area [mm²]	**118.8 x 118.8**	**210 x 210**
Output data [bits]	**14**	**16**
Dynamic range	**6,000**	**14,100**
Dead time due to readout	**14 msec / pixel**	**1.1 sec / frame**

Data inconsistency: Radiation damage

Bacterial flagelin F41 Crystal
@ SPring-8 BL41XU

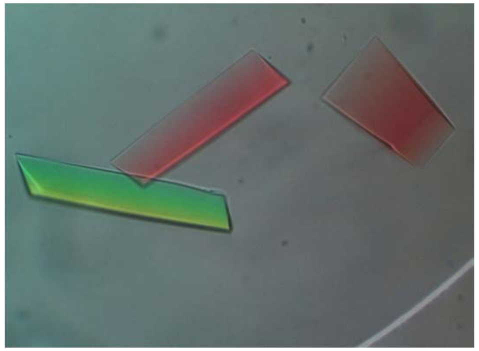

Very Thin Crystal (≒10μm)

1st frame	***15min.***	***25min.***

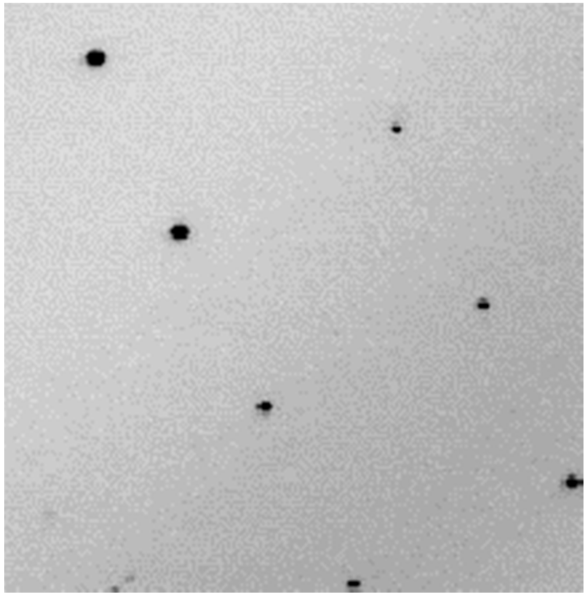

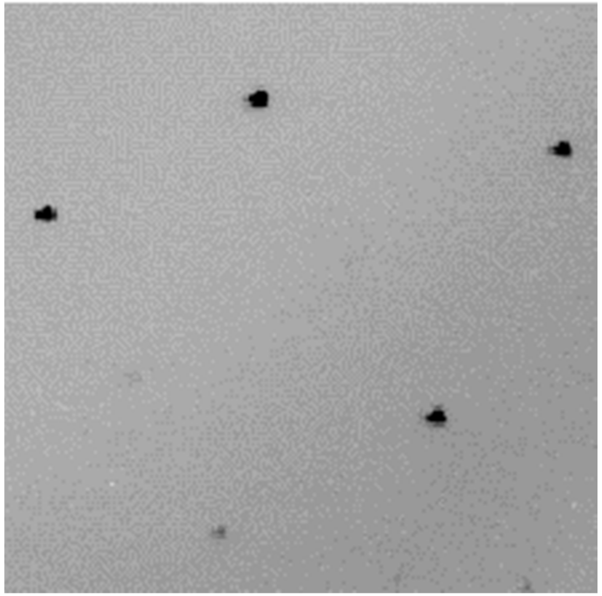

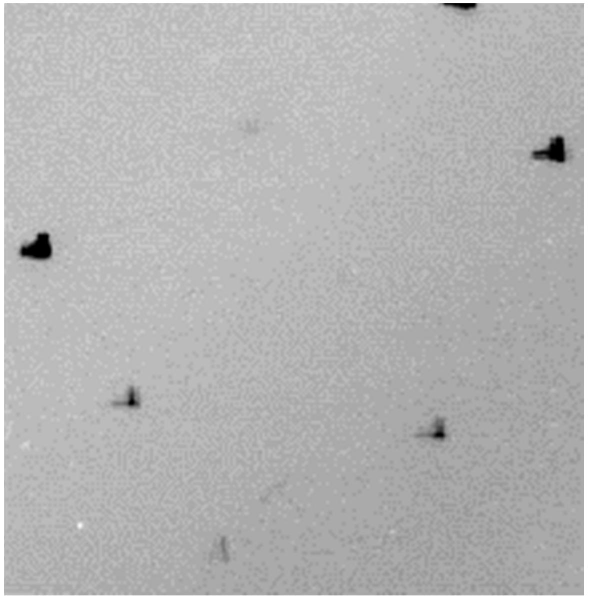

Total Flux at Sample **≒ 10^{13} photons/sec/mm^2**

F.A. Samatey, K.Imada, S.Nagashima, K.Namba (ERATO)

Radiation damage in real space

electron density at 1.6 Å resolution

Data set

1

R-factor 18.51 %
R_{free} 20.64 %

fo-fc	2.5σ
fo-fc	−2.5σ
2fo-fc	1.0σ

12

R-factor 18.50 %
R_{free} 20.68 %

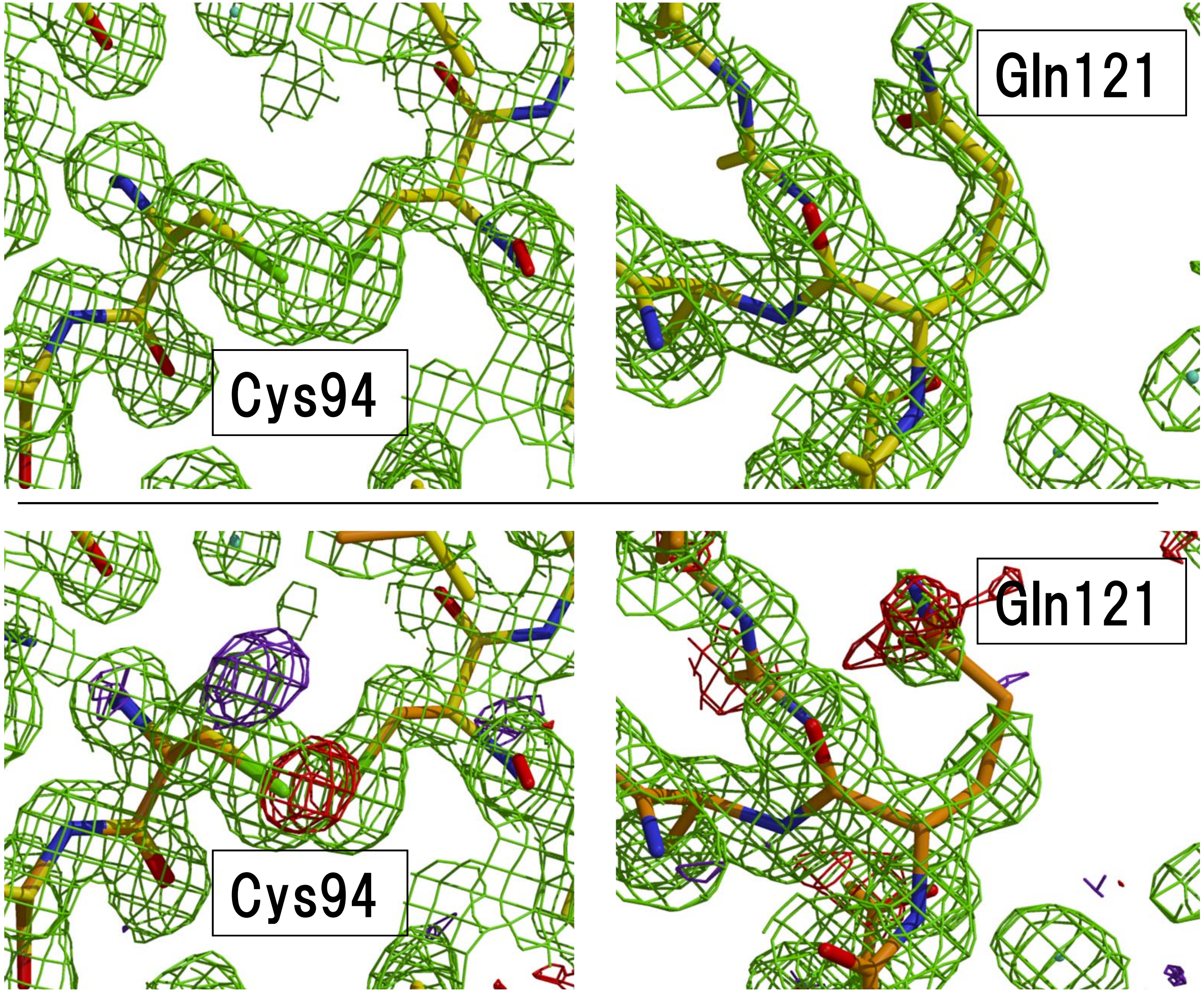

Cryocrystallographic technique

Prevent thermal degradation of sample
diffusion and reaction of free radicals
at cryogenic temperature (30 – 100 K)
using cold N_2/He gas stream

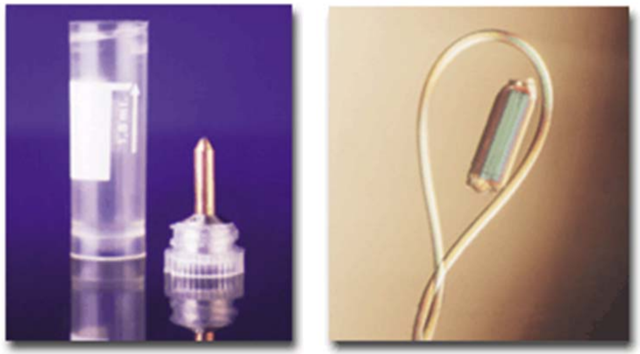

Sample Mount Pin & Cryoloop

Interaction between photon and protein

Primary Effect

▪Absorbed photon energy > **Temperature increment**

▪Photoelectron formation

> **Chemical reduction / Reactive radical formation**

X-ray dose	**dependent**
Temperature / Time	independent

Secondary Effect

▪Chemical reaction by free radicals

X-ray dose, temperature / time dependent

Photon-electron interaction

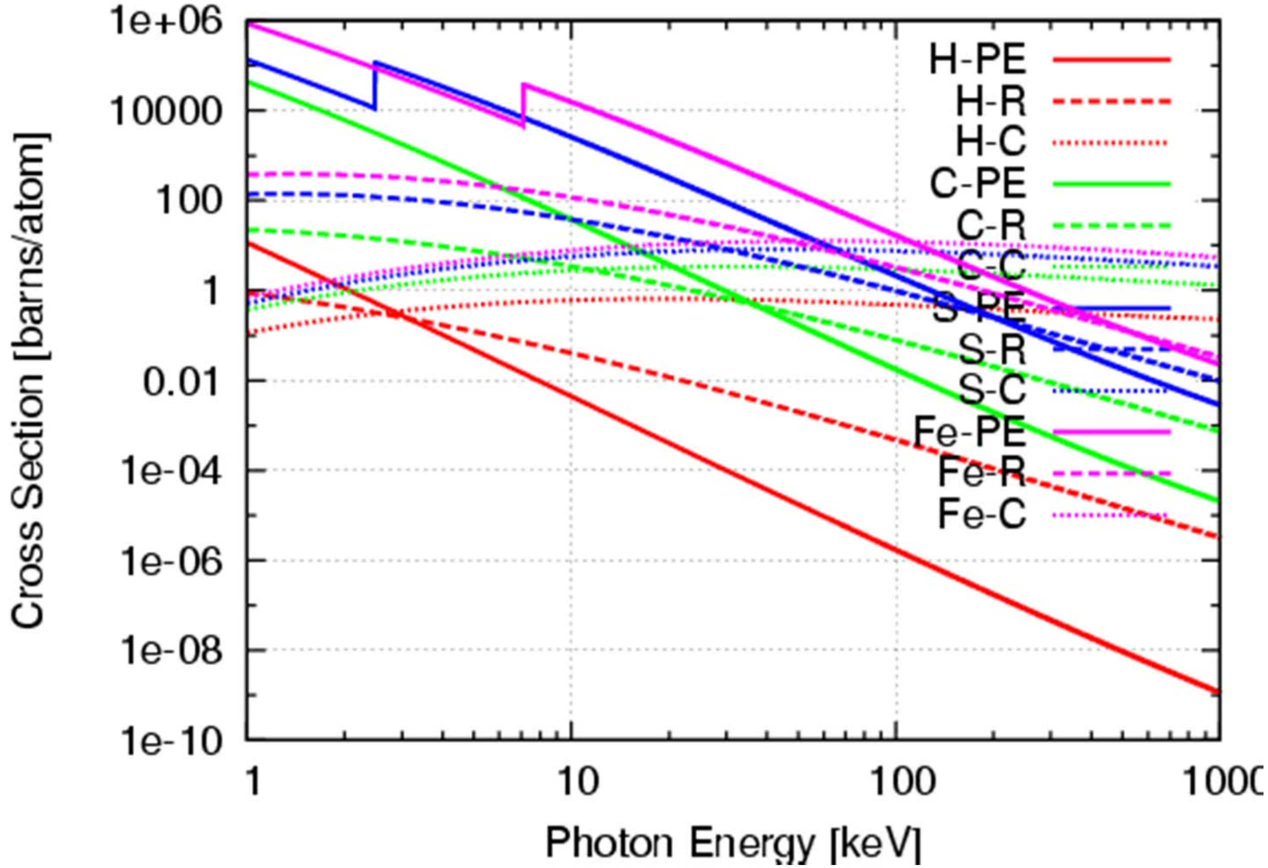

PE: Photoelectric absorption, R: Thomson (Reyleigh) scattering,
C: Compton scattering

Radiation induced temperature increment under cryogenic condition

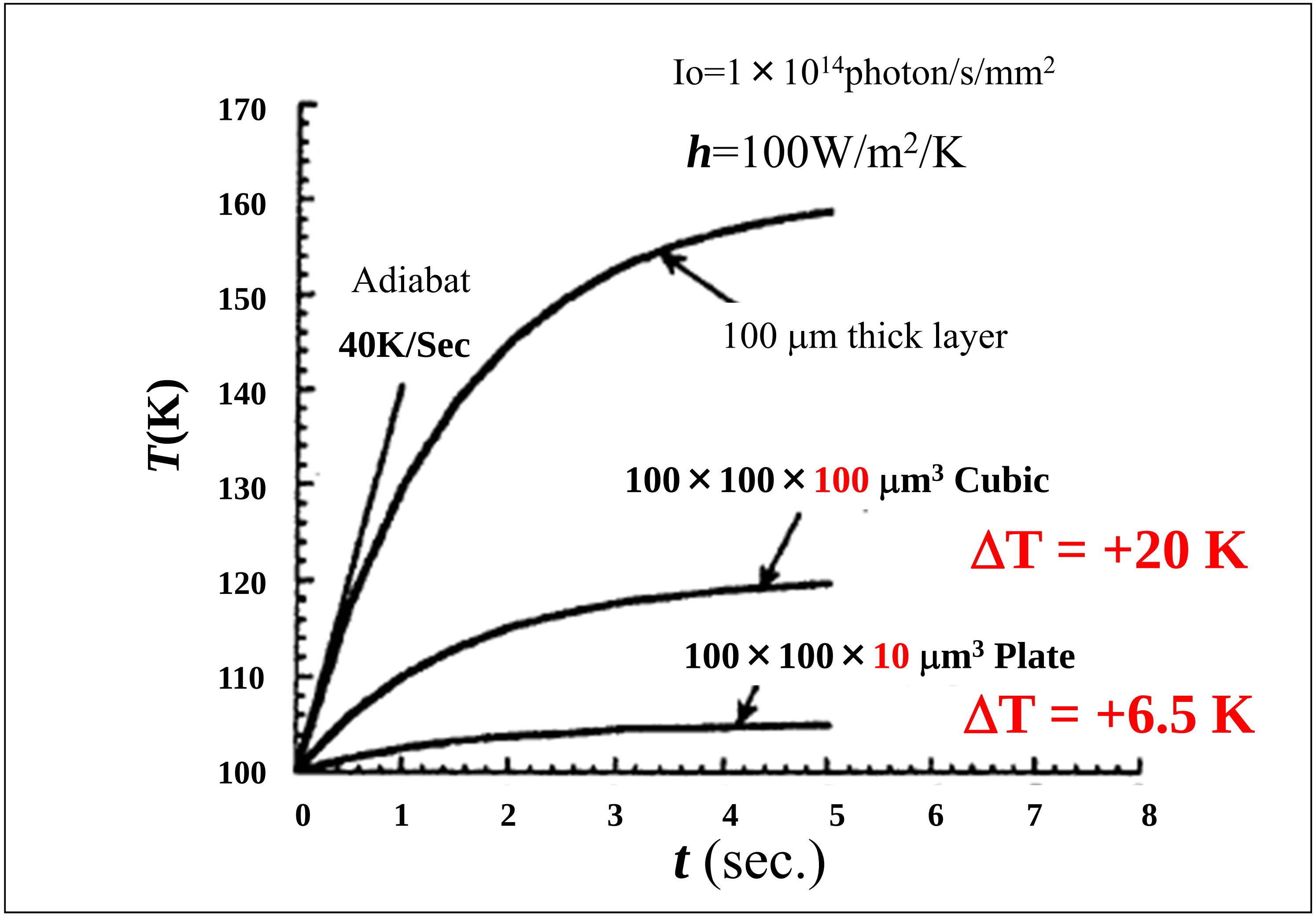

Kuzay *et al.* Acta Cryst. (2001). D57, 69-81

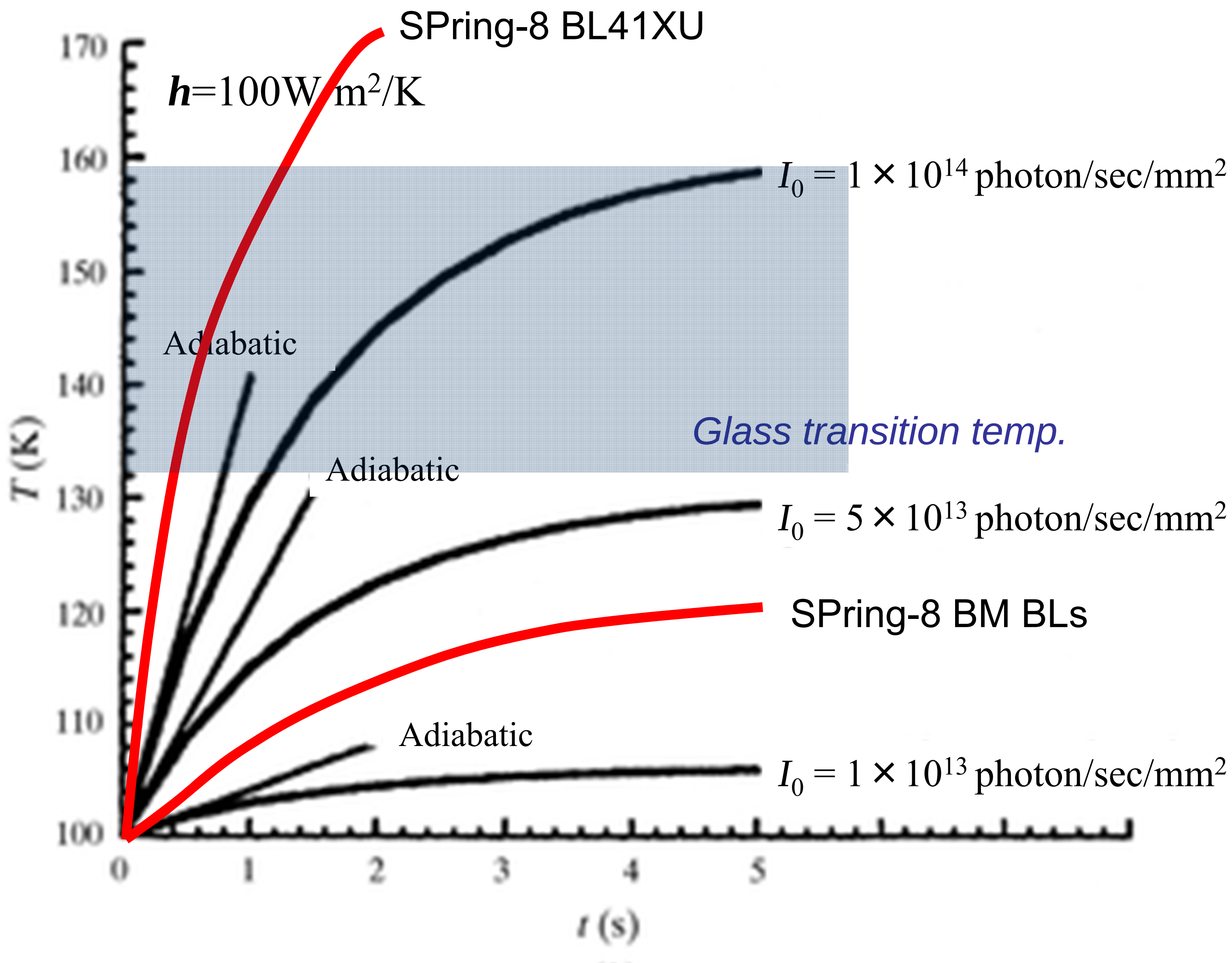
SPring-8 BL41XU
h=100W/m^2/K
$I_0 = 1 \times 10^{14}$ photon/sec/mm^2
Adiabatic
Glass transition temp.
Adiabatic
$I_0 = 5 \times 10^{13}$ photon/sec/mm^2
SPring-8 BM BLs
Adiabatic
$I_0 = 1 \times 10^{13}$ photon/sec/mm^2
T (K)
170
160
150
140
130
120
110
100
0
1
2
3
4
5
t (s)

Radiation induced formation of reactive radicals (1)

Water

$$H_2O \xrightarrow{h\nu} H_2O^{+} + e^{-}$$

$$H_2O^{+} + H_2O \longrightarrow H^{+} + OH^{\bullet}$$

$$e^{-} + H_2O \longrightarrow H_2O^{-}$$

$$H_2O^{-} + H_2O \longrightarrow H^{\bullet} + OH^{-}$$

$$H_2O \xrightarrow{h\nu} \underline{H}^{\bullet} + \underline{OH}^{\bullet}$$

Radiation induced formation of reactive radicals (2)

Disulfide bridge

$$(p)\text{-}CH_2SSCH_2\text{-}(p) \xrightarrow{h\nu} (p)\text{-}CH_2SS^{\bullet +}CH_2\text{-}(p) + e^-$$

$$(p)\text{-}CH_2SSCH_2\text{-}(p) + \underline{OH}^{\bullet} \longrightarrow (p)\text{-}CH_2SS^{\bullet +}CH_2\text{-}(p) + OH^-$$

$$(p)\text{-}CH_2SS^{\bullet +}CH_2\text{-}(p) + OH^- \longrightarrow (p)\text{-}CH_2SOH + (p)\text{-}CH_2S^{\bullet}$$

$$(p)\text{-}CH_2SSCH_2\text{-}(p) + \underline{OH}^{\bullet} \longrightarrow (p)\text{-}CH_2SOH + (p)\text{-}CH_2S^{\bullet}$$

Cysteine

$$(p)\text{-}CH_2SH + e^- \longrightarrow (p)\text{-}CH_2^{\bullet} + SH^-$$

$$(p)\text{-}CH_2SH + \underline{H}^{\bullet} \longrightarrow (p)\text{-}CH_2^{\bullet} + H_2S$$

Burmeister, Acta Cryst. (2000). D56, 328-341

Radiation induced formation of reactive radicals (3)

Aspartate & Glutamate

$$\text{(p)-CH}_2\text{CH}_2\text{COO}^- \xrightarrow{h\nu} \text{(p)-CH}_2\text{C}^{\bullet +}\text{H}_2\text{COO}^- + e^-$$

$$\text{(p)-CH}_2\text{C}^{\bullet +}\text{H}_2\text{COO}^- \longrightarrow \text{(p)-CH}_2\text{CH}_2^{\bullet} + \text{CO}_2$$

Tyrosine

$$\text{(p)-CH}_2\text{C}_6\text{H}_4\text{OH} \xrightarrow{h\nu} \text{(p)-CH}_2\text{C}_6\text{H}_4\text{OH}^{\bullet +} + e^-$$

$$\text{(p)-CH}_2\text{C}_6\text{H}_4\text{OH}^{\bullet +} \longrightarrow \text{(p) -CH}_2\text{C}_6\text{H}_4\text{O}^{\bullet} + \text{H}^+$$

Methionine

$$\text{(p)-CH}_2\text{CH}_2\text{SCH}_3 + 2\underline{\text{H}}^{\bullet} \longrightarrow \text{(p)-CH}_2\ \text{CH}_3 + \text{CH}_3\text{SH}$$

Burmeister, Acta Cryst. (2000). D56, 328-341

Dose limit

Estimated dose limit for ionizing radiation

1.3×10^{17} keV/mm^{-3}

1×10^{16} photon/mm^{2}@12.4keV

(Henderson, R. (1990). *Proc. R. Soc. London Ser. B*, **241**, 6–8.)

4×10^{17} keV/mm^{-3}

(Gonzalez, A., Nave, C. (1994). *Acta Cryst. D* **50**, 874–877.)

5×10^{16} photon/mm^{2}@12.4keV

(Sliz, P.,Harrison,S.C.Rosenbaum,G., (2002). *Structure*, **11**, 13–19.)

2.2: Phasing / Modeling & Refinement

Phasing: Crystallographic phase problem

Diffraction intensity is only measureable,
but its phase information is completely lost.

$$I(hkl) = \mathbf{F}(hkl)\,\mathbf{F}^*(hkl)$$

$$\mathbf{F}(hkl) = |\,\mathbf{F}(hkl)\,|\,\exp i\alpha$$

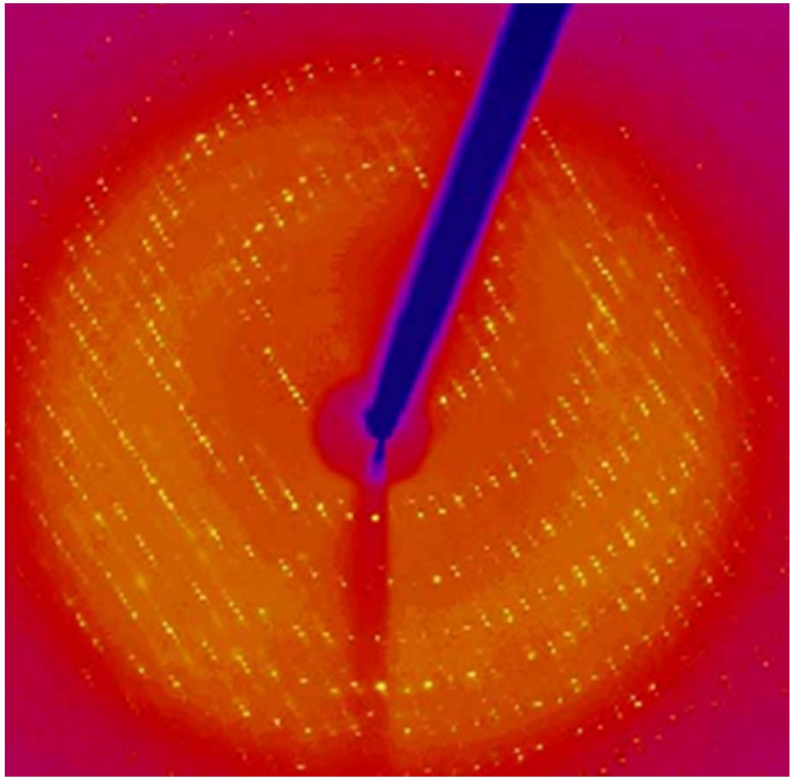

Solving methods
1. Direct method
2. Isomorphous replacement (IR)
3. Molecular replacement (MR)

|F| of (a)

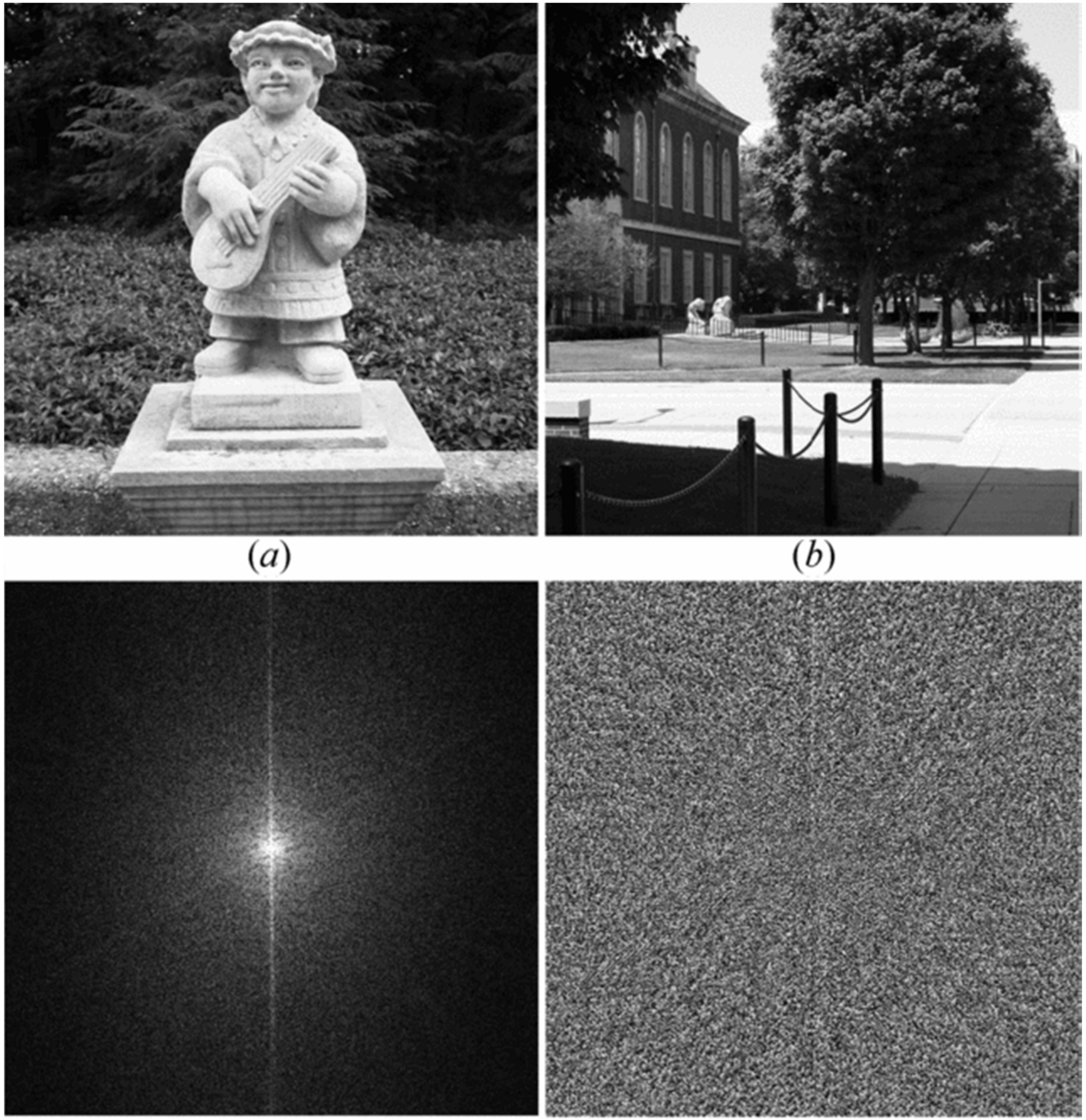

(a) (b)

(c) (d)

α of (a)

Albert & Lecomte, J. Appl. Cryst. 40, 1153 (2007)

|F| of (b)
α of (a)

(a)

(b)

|F| of (a)
α of (b)

random |F|
α of (a)

(a)

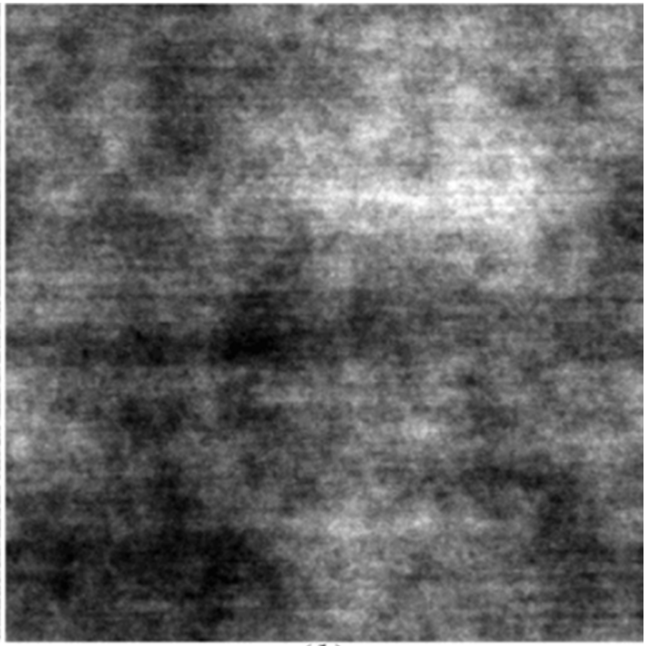

(b)

random |F
α of (b)

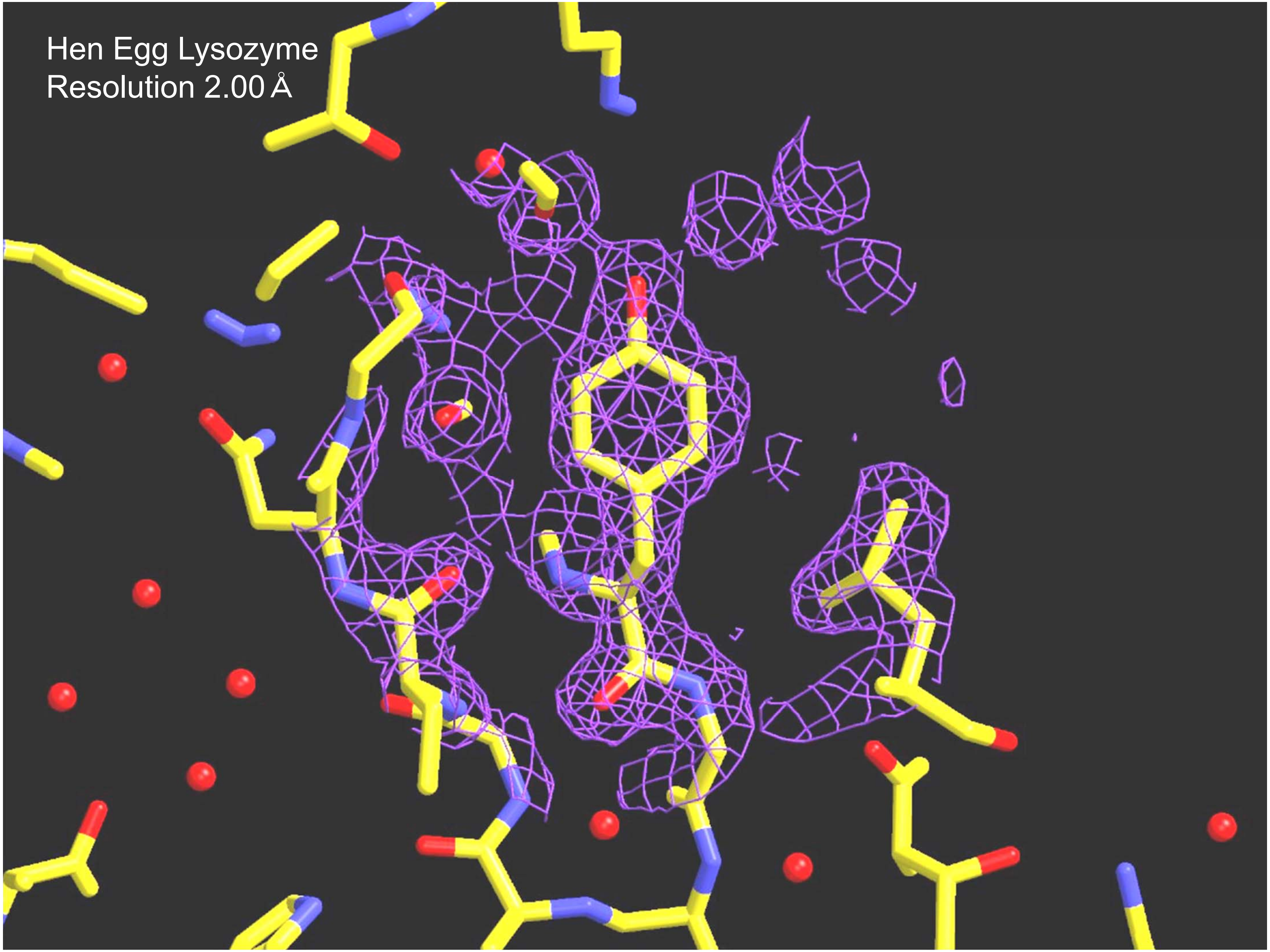
Hen Egg Lysozyme
Resolution 2.00 Å

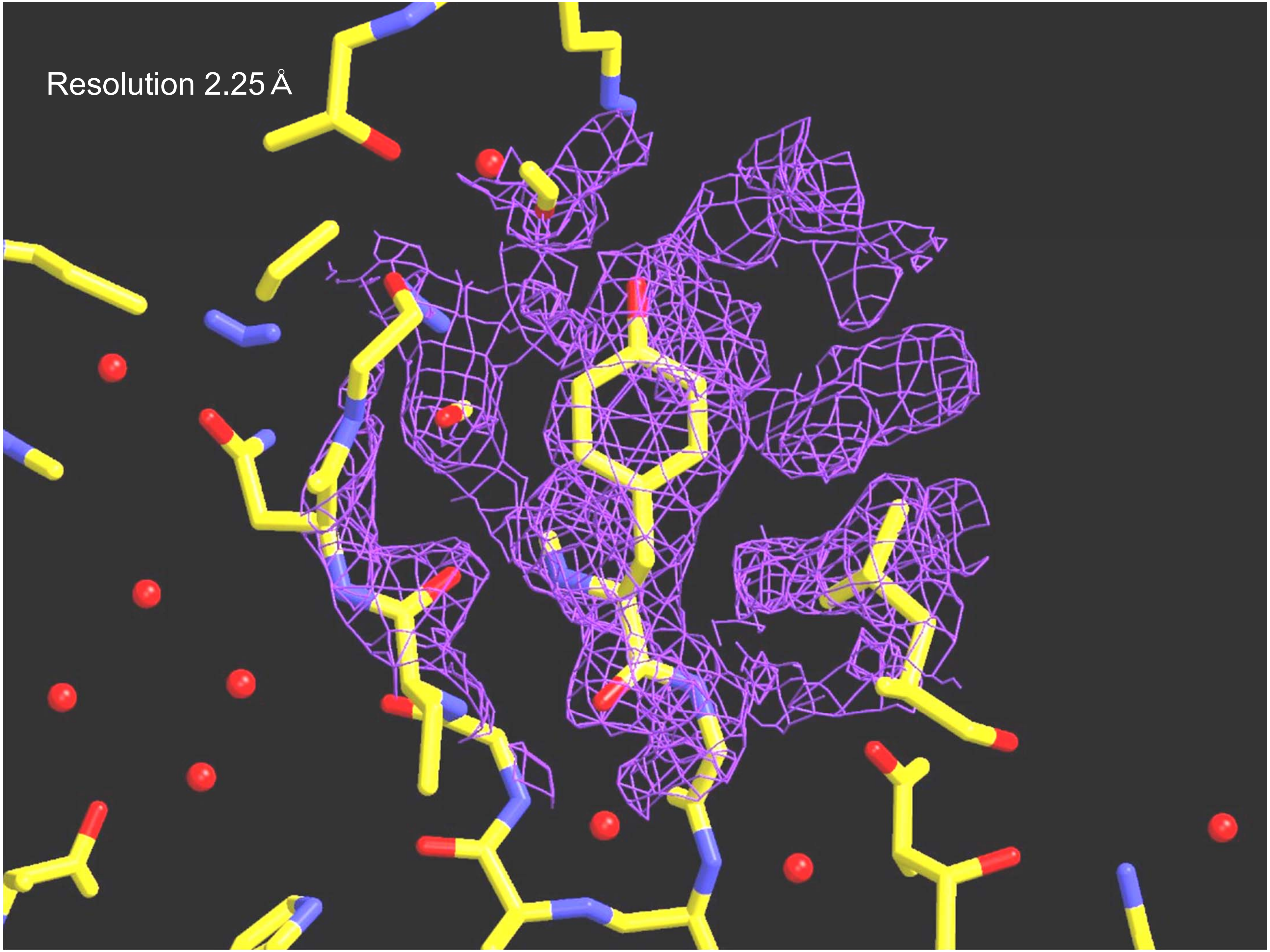
Resolution 2.25 Å

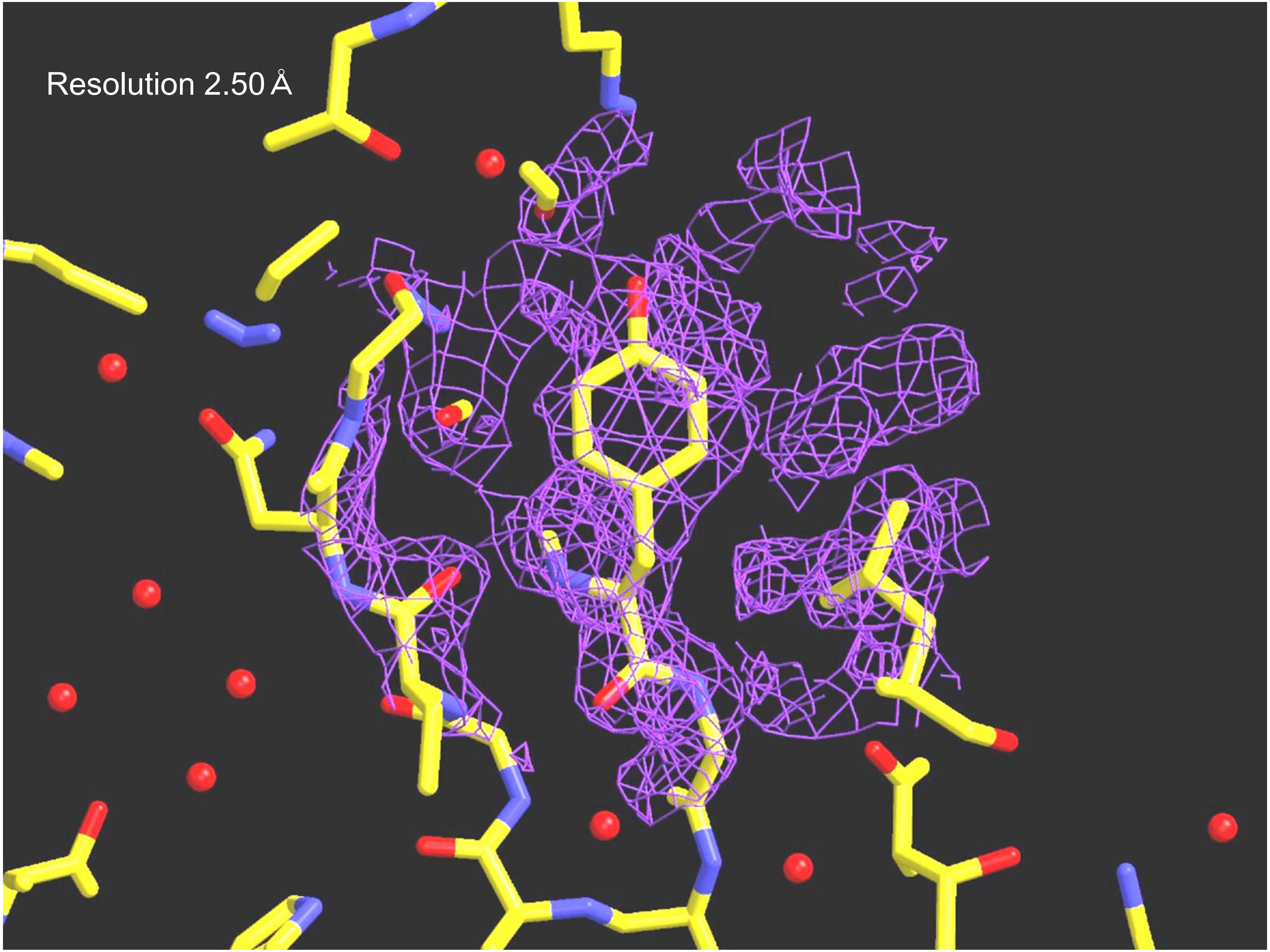
Resolution 2.50 Å

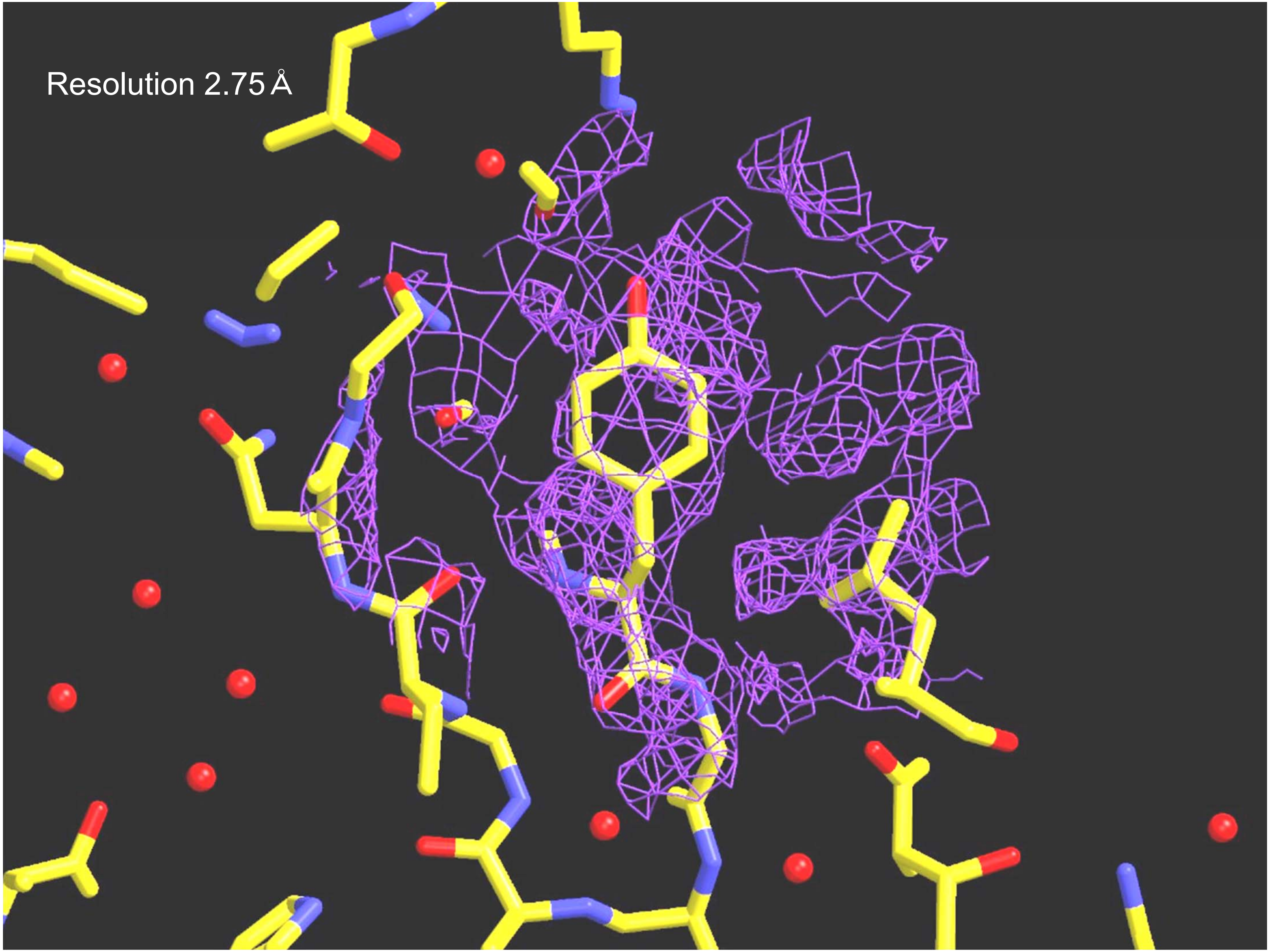
Resolution 2.75 Å

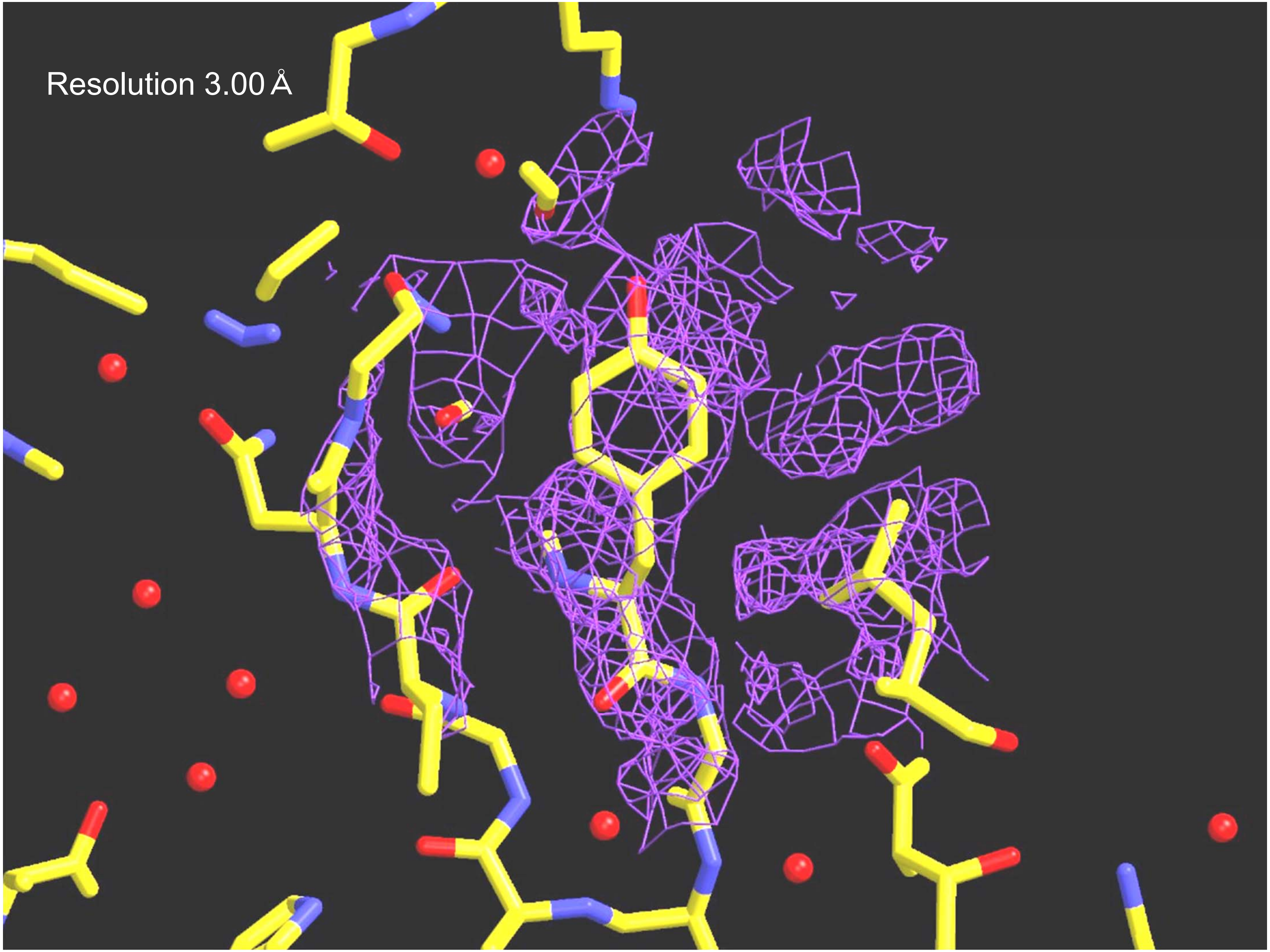
Resolution 3.00 Å

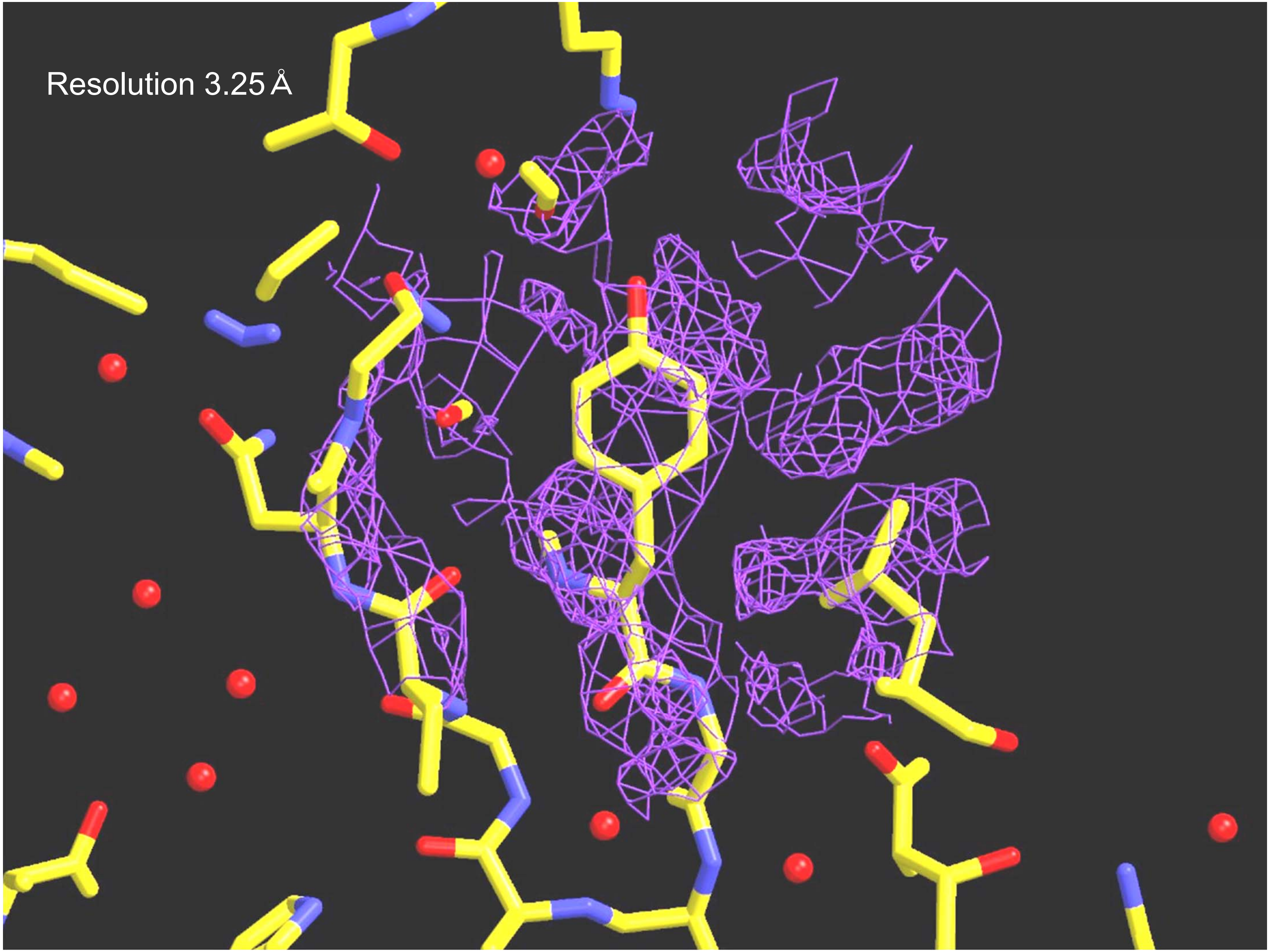
Resolution 3.25 Å

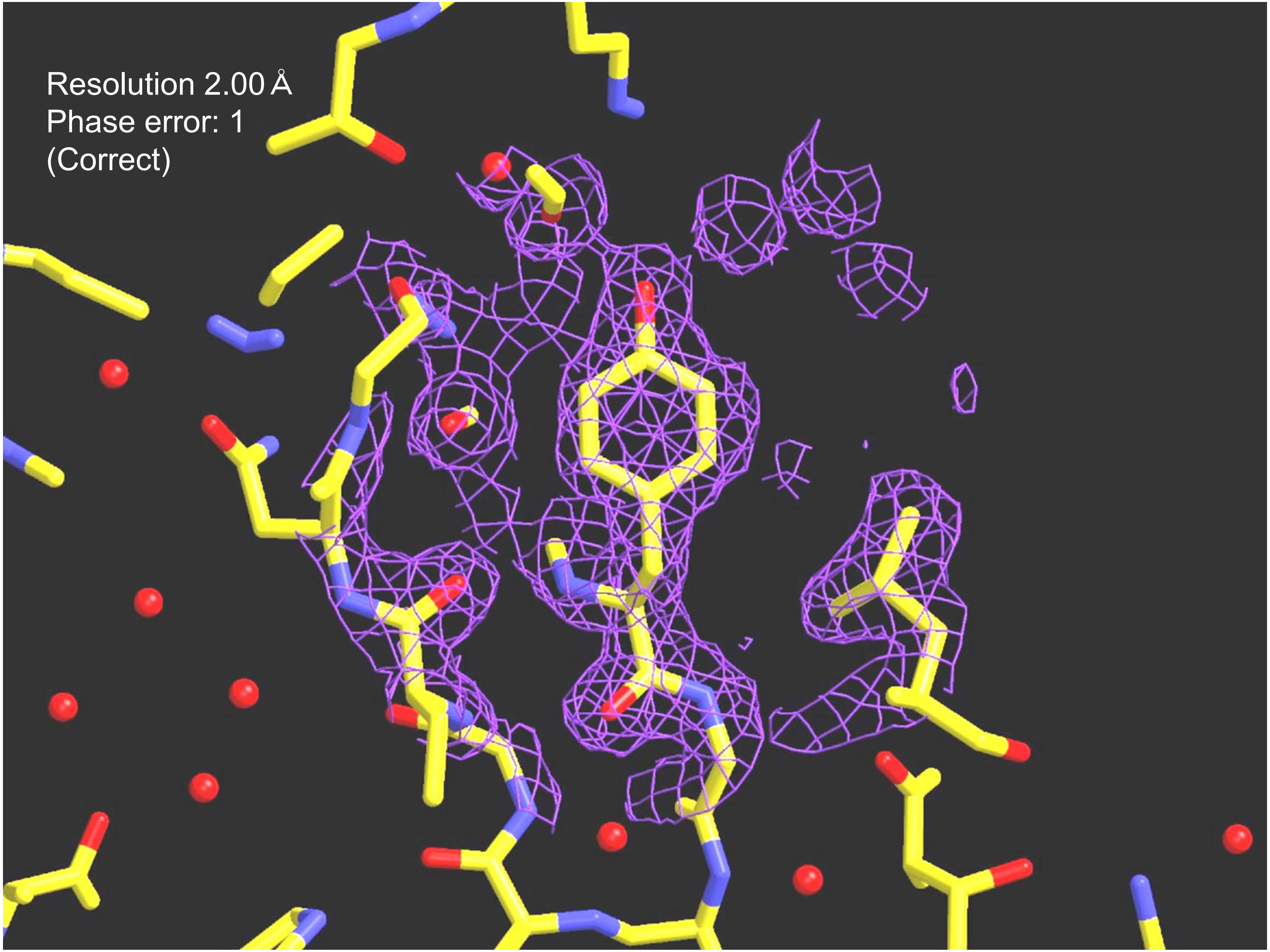
Resolution 2.00 Å
Phase error: 1
(Correct)

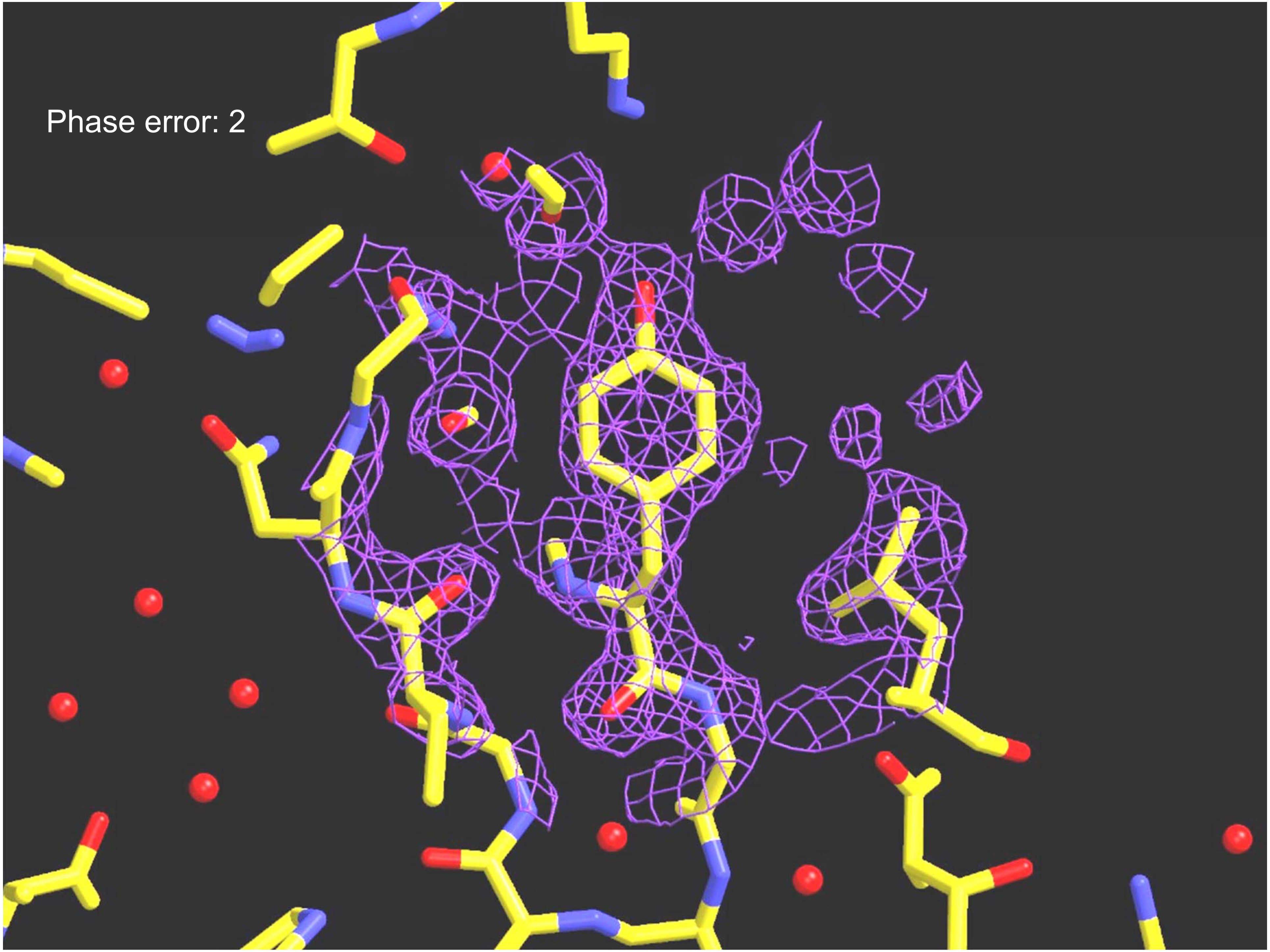
Phase error: 2

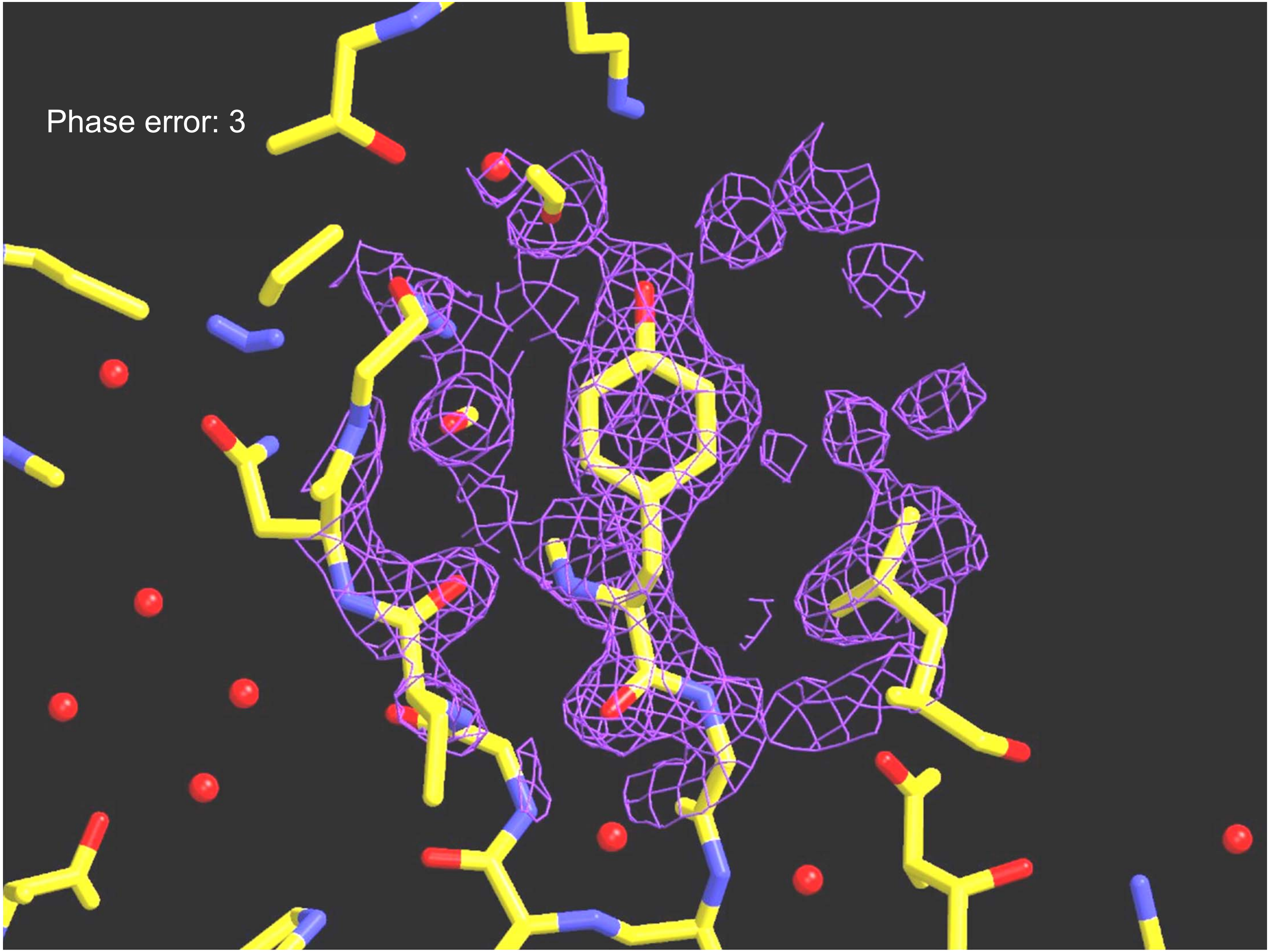
Phase error: 3

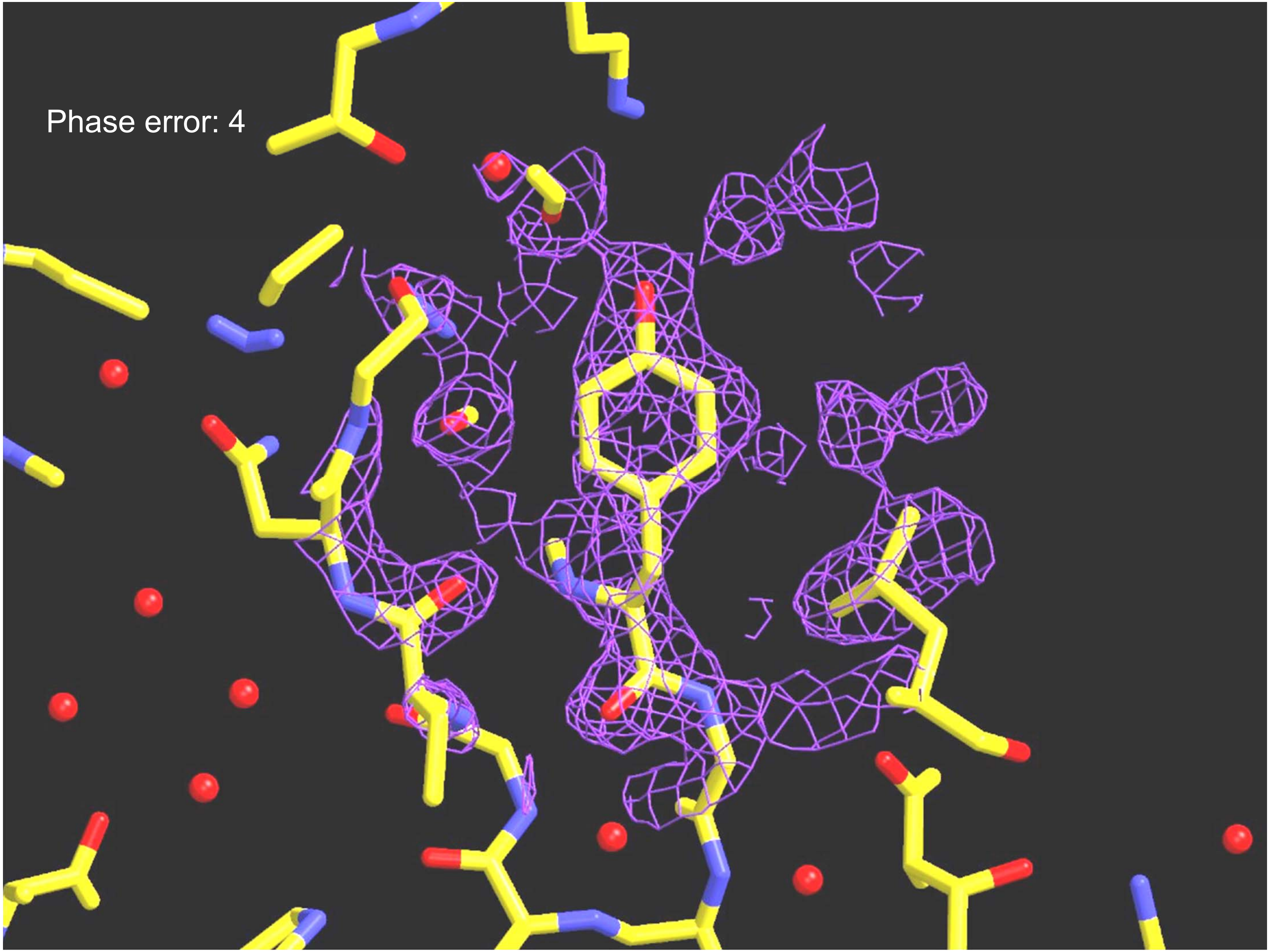
Phase error: 4

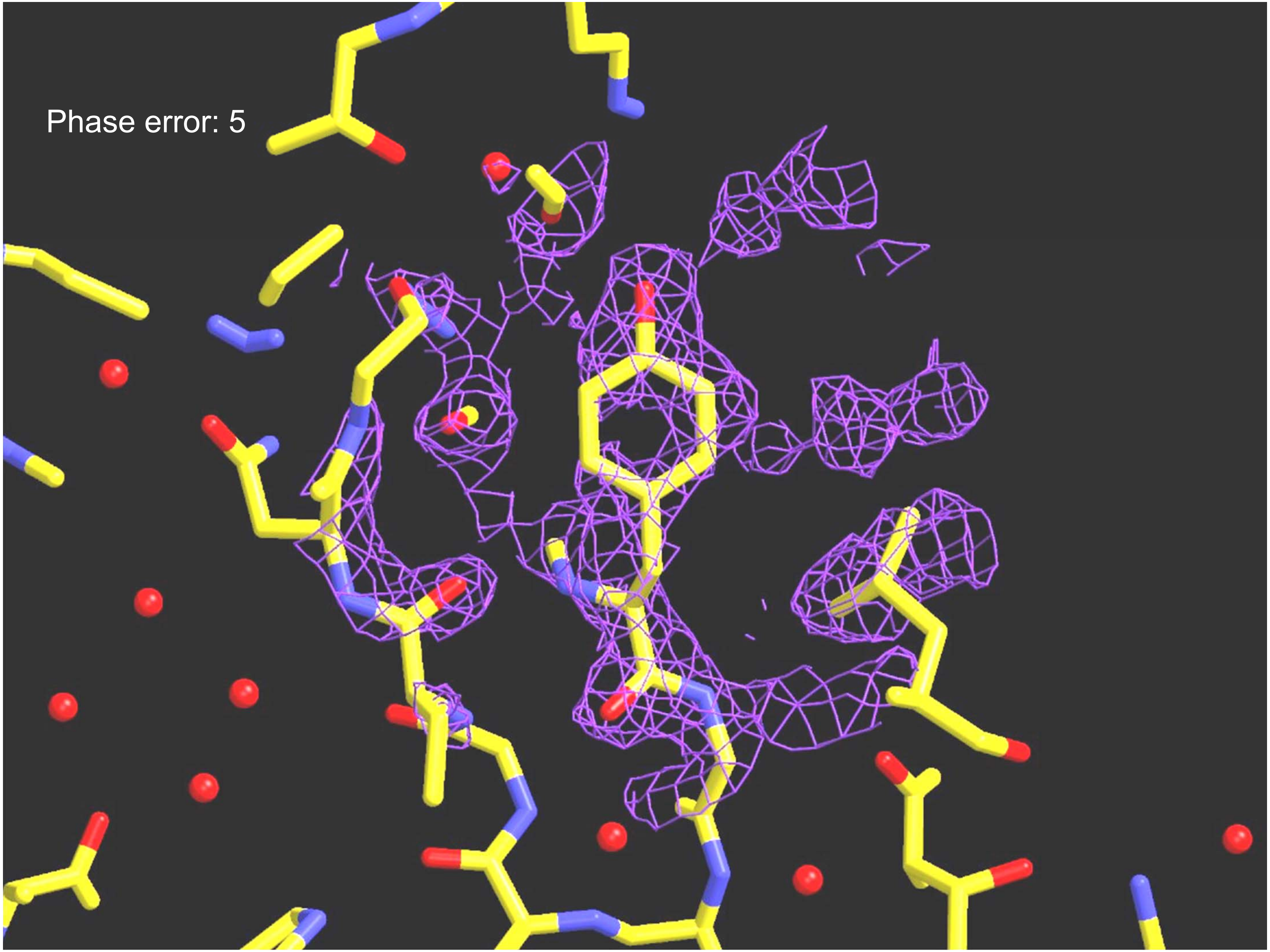
Phase error: 5

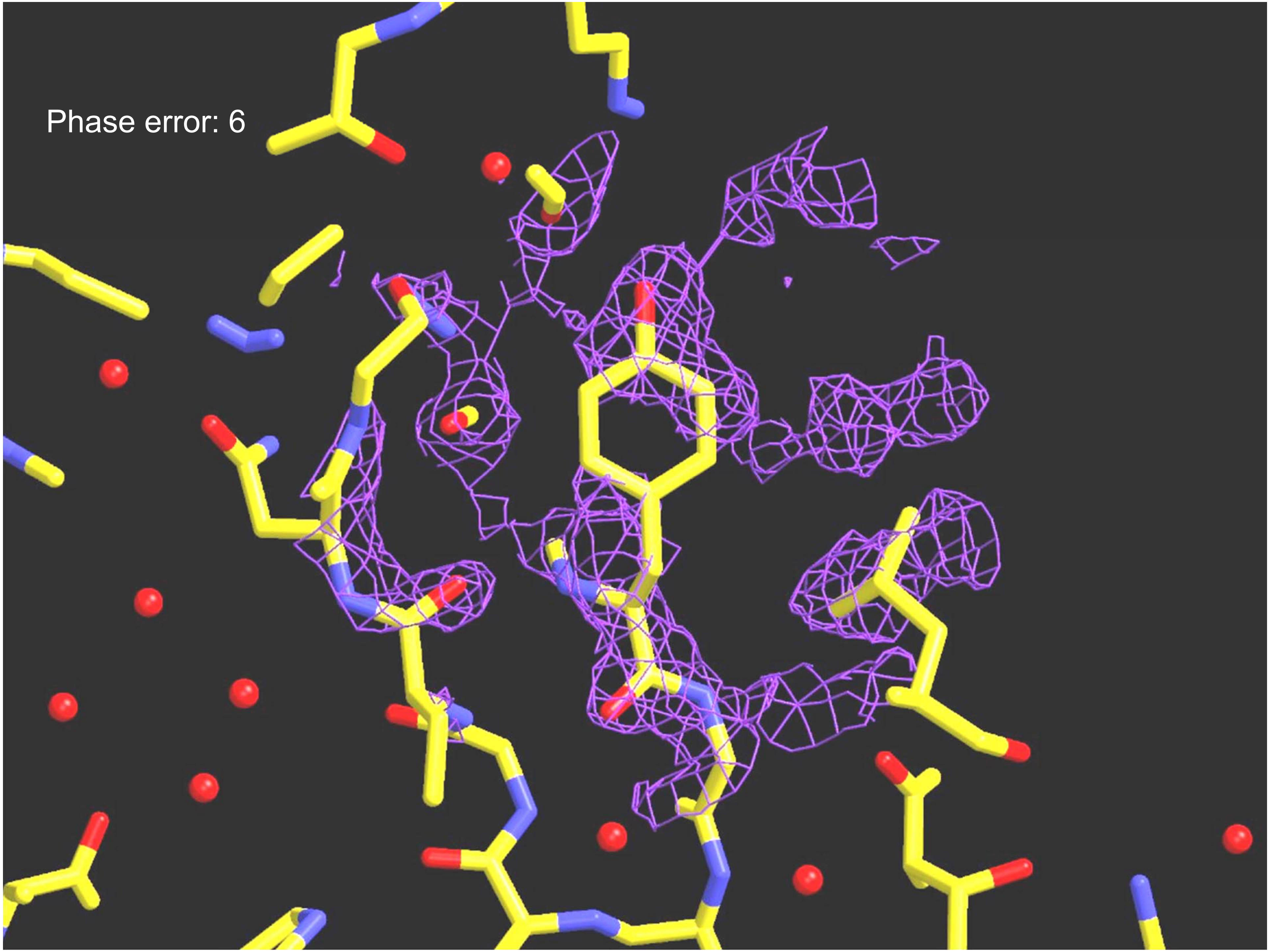
Phase error: 6

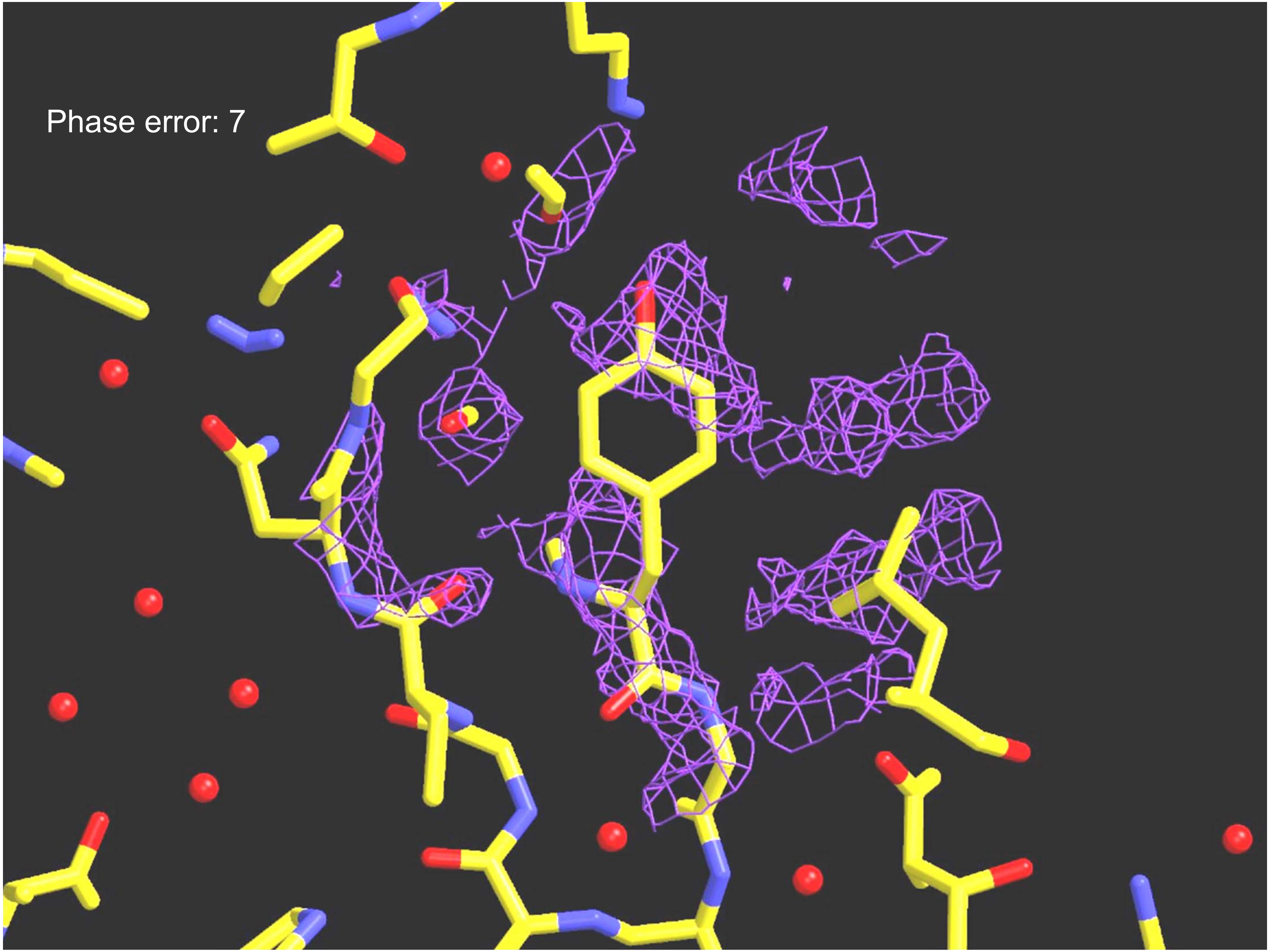
Phase error: 7

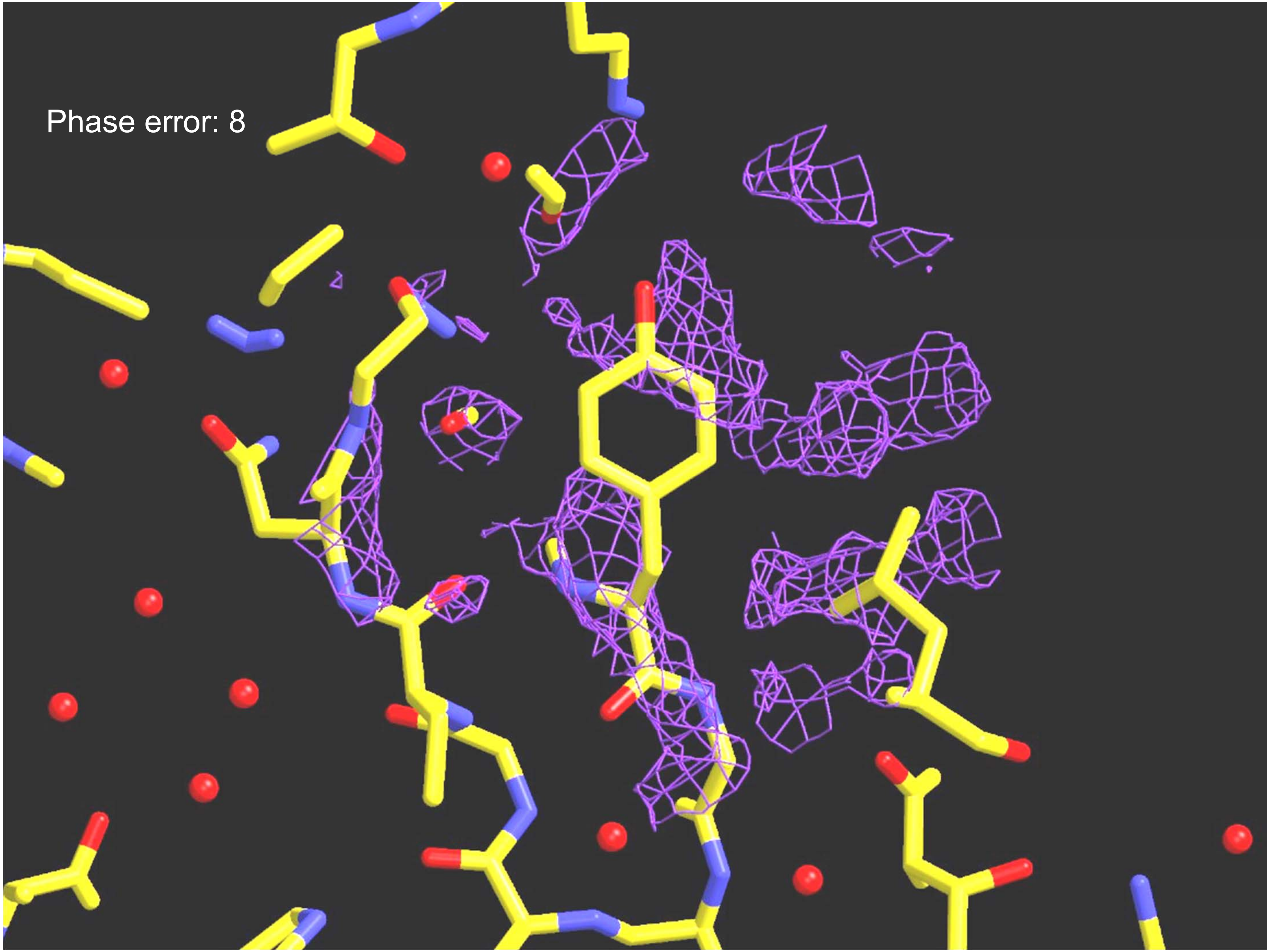
Phase error: 8

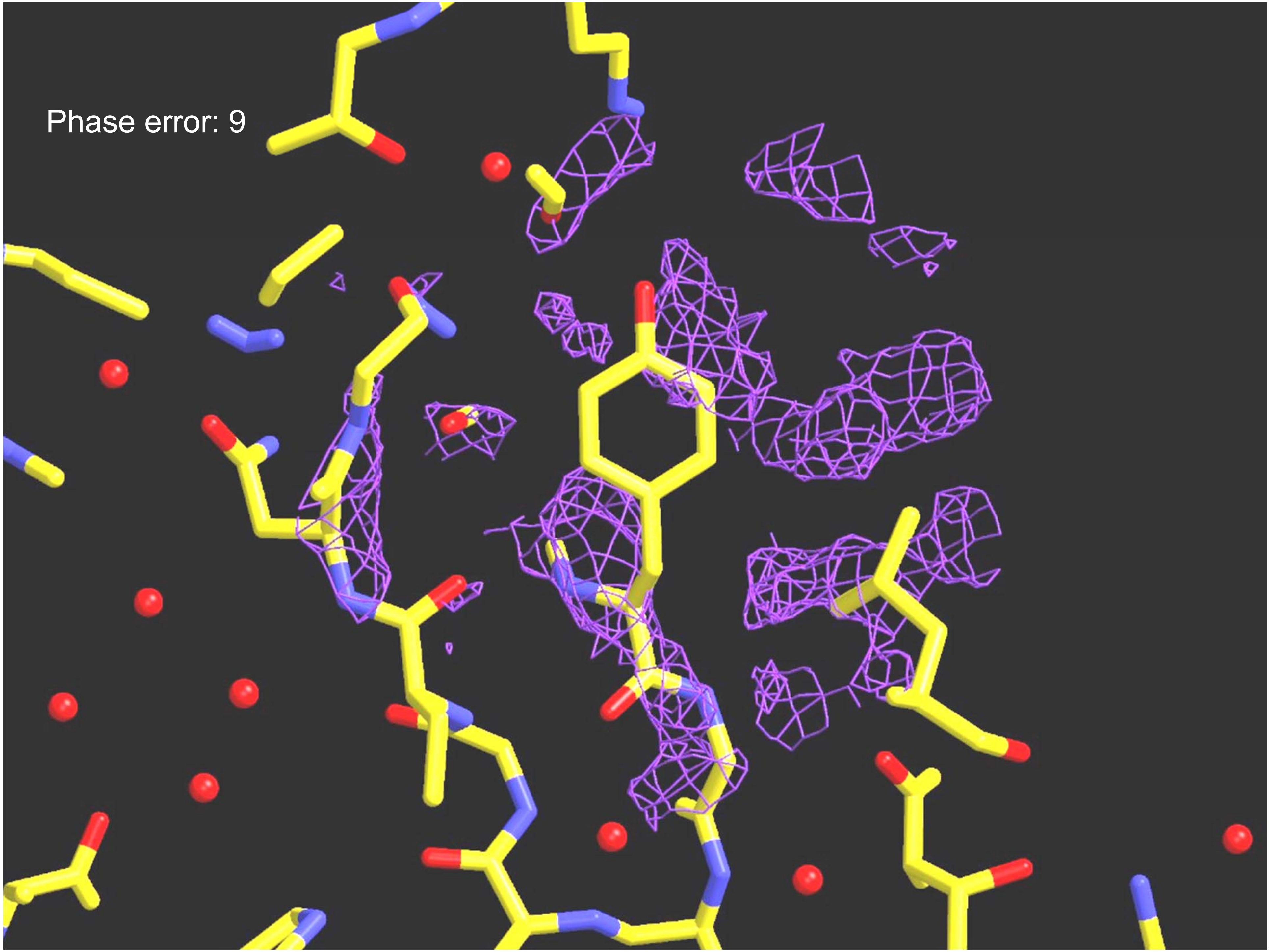
Phase error: 9

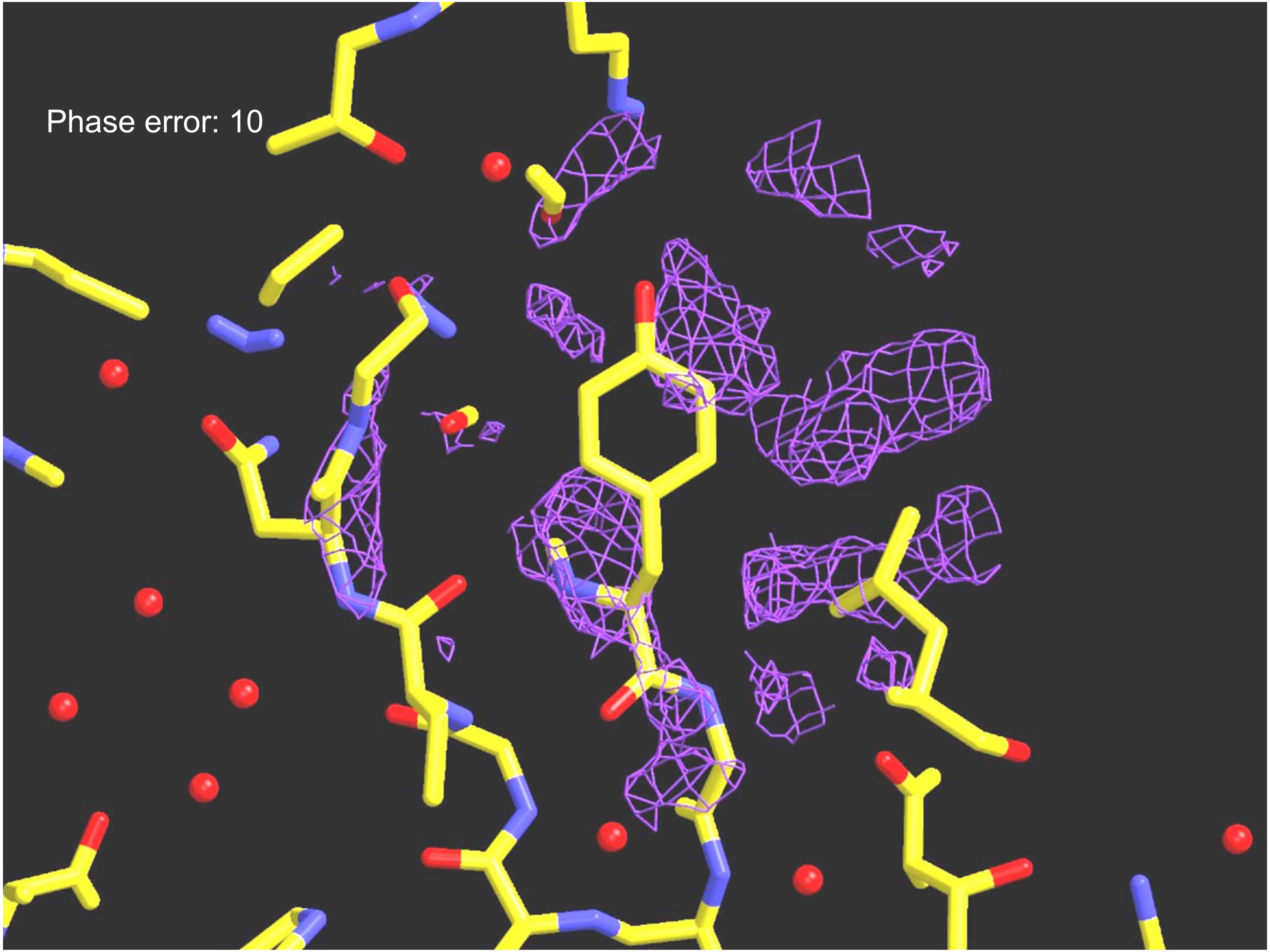
Phase error: 10

Harker Diagram ~ Structure factor and phase

$$\mathbf{F}(\mathbf{h}) = |\mathbf{F}(\mathbf{h})| \exp i\alpha$$
$$= \sum f_j \exp 2\pi i \mathbf{h} \cdot \mathbf{r}_j$$

Complex space

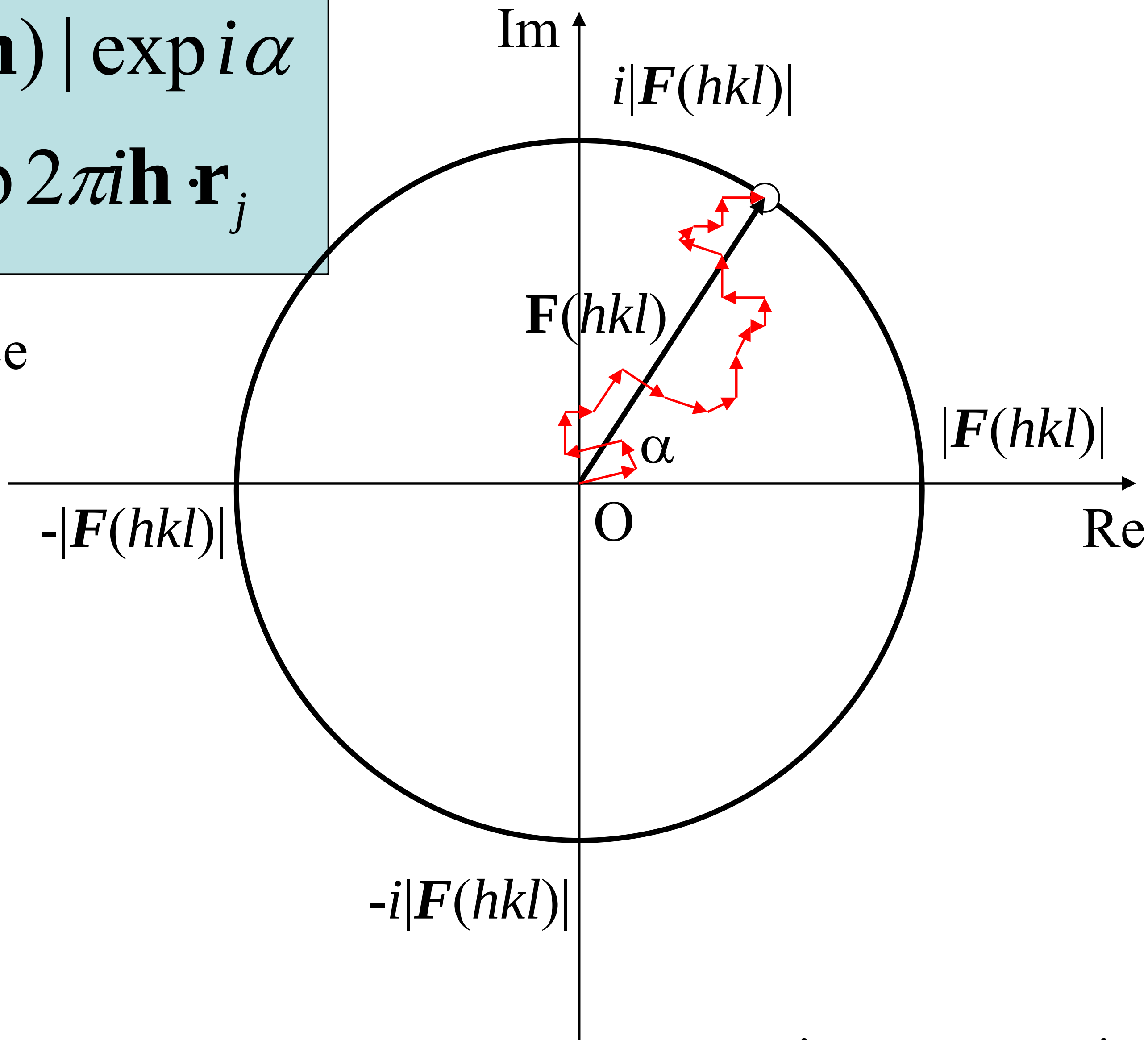

$\exp i\alpha = \cos\alpha + i \sin\alpha$

Isomorphous replacement

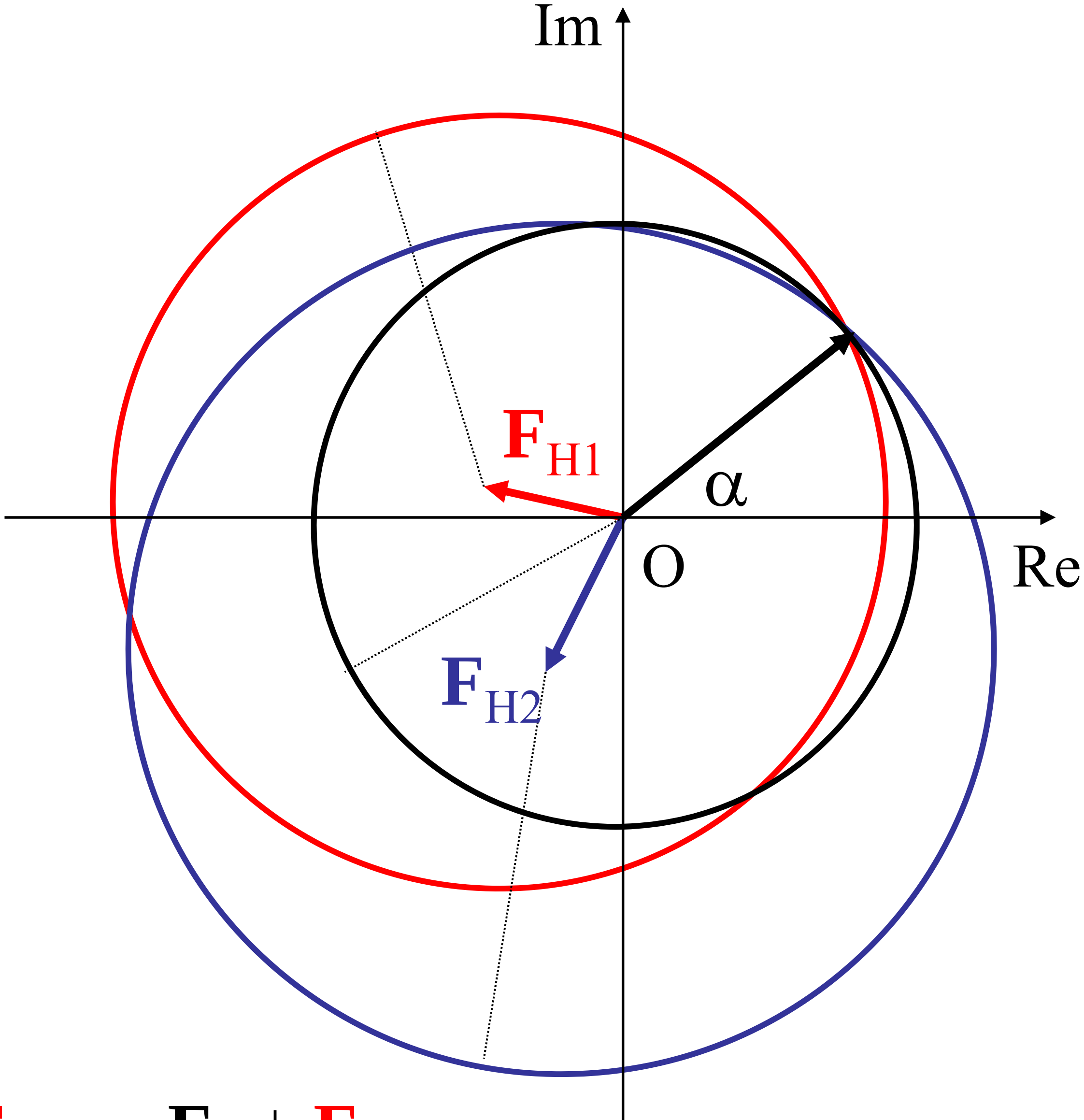

$|\mathbf{F}_P|$: Native

$|\mathbf{F}_{PH1}|$: Derivative 1

$|\mathbf{F}_{PH2}|$: Derivative 2

$$\mathbf{F}_P = |F_P| \exp i\alpha$$

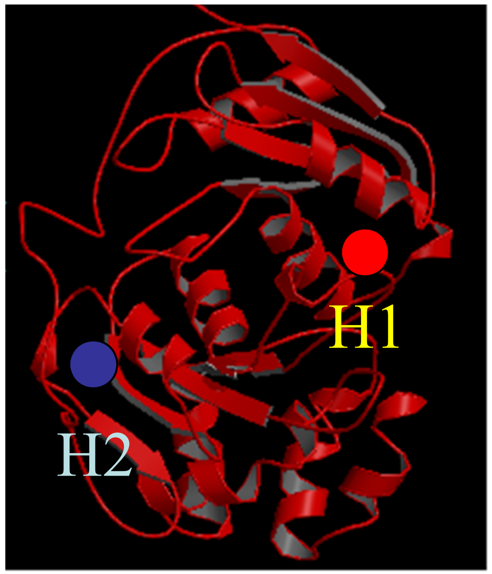

$$\mathbf{F}_{PH1} = \mathbf{F}_P + \mathbf{F}_{H1}$$

Patterson function

Directly calculated from intensity without phase.
The function shows self correlation of electron density.

$$P(\mathbf{u}) = \int_{cell} \rho(\mathbf{r})\rho(\mathbf{r}+\mathbf{u})\mathrm{d}^3\mathbf{r} = \frac{1}{V}\sum_{\mathbf{h}} |F(\mathbf{h})|^2 \exp(-2\pi i \mathbf{h}\cdot\mathbf{u}).$$

Interatomic vector $\mathbf{u} = (u\ v\ w)$

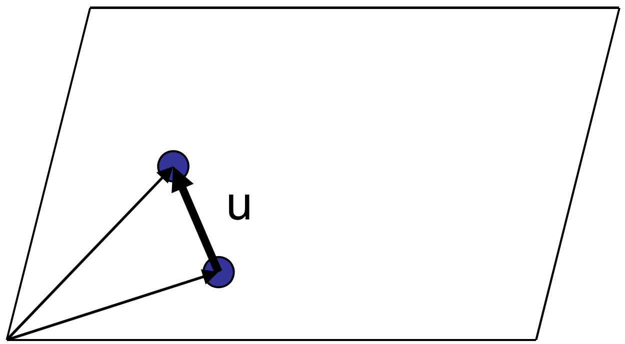

Real space

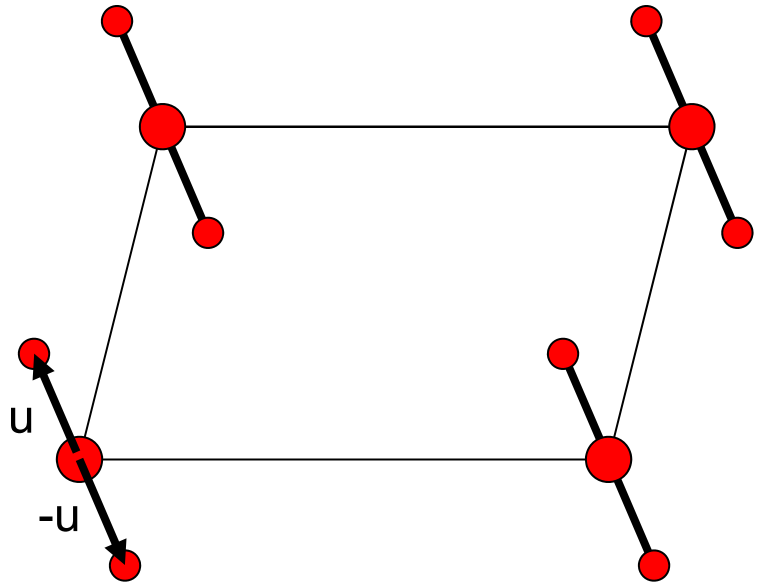

Patterson space

In case of few atoms in cell, their coordinates are determined from Patterson function.

Characteristics of Patterson function

1. Even function: $P(\mathbf{u}) = P(-\mathbf{u})$

2. Screw axis in real space > Rotation axis

3. Harker line / Harker section

$P2_1$: (x, y, z), $(-x, y+1/2, -z)$

$(u, v, w) = (-2x, 1/2, -2z)$

4. Correspond to mathematical convolution

$$f(t) * g(t) = \int_0^t f(t-\tau)g(\tau)d\tau$$

$f(t)*f(t)$: Self correlation
$f(t)*g(t)$: Cross corr.

Rough approximation of F_H from data

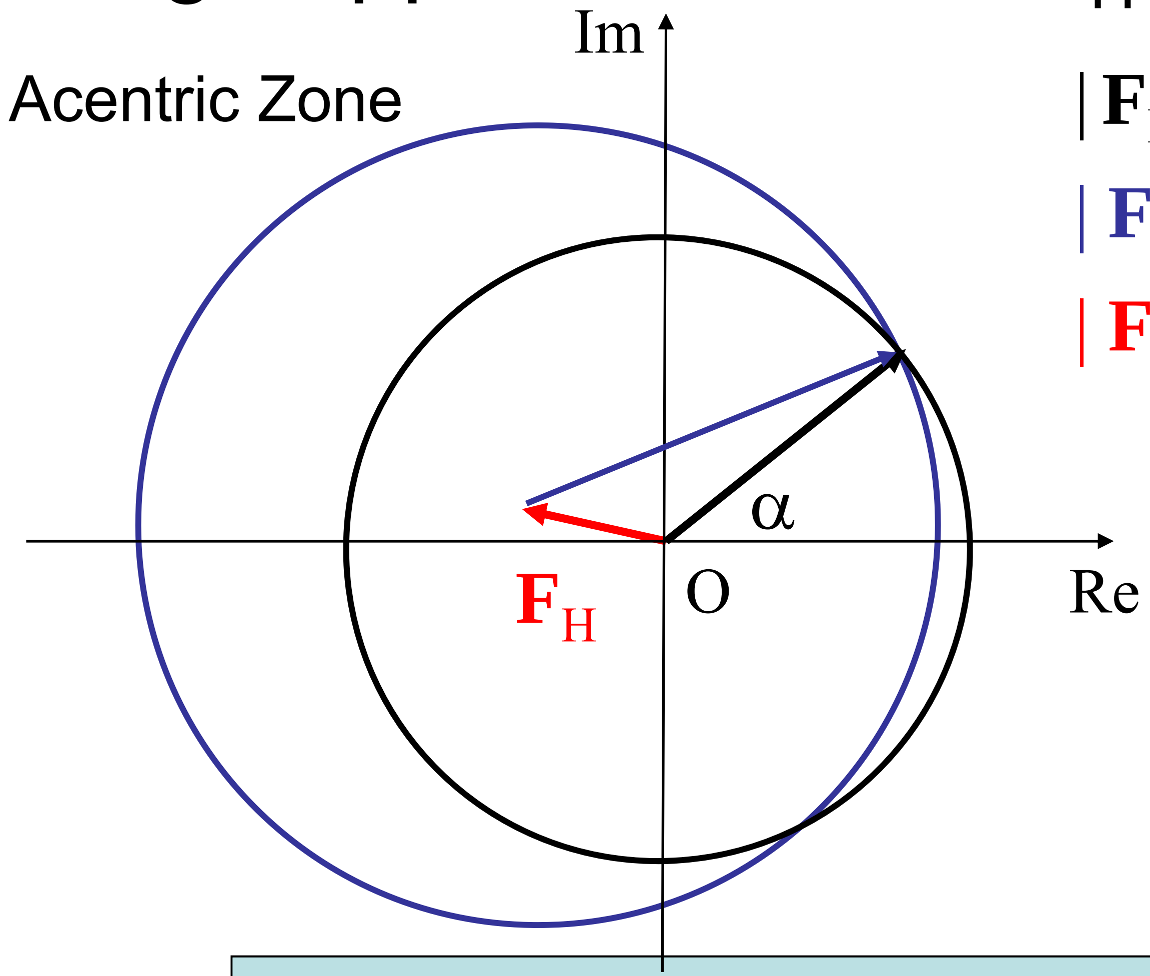

$|\mathbf{F}_P|$, α_P: Native

$|\mathbf{F}_{PH}|$, α_{PH} : Derivative

$|\mathbf{F}_H|$, α_H : Heavy atom

$$\mathbf{F}_P = |F_P| \exp i\alpha$$

$$\Delta F = |F_{PH} - F_P| = \left| F_H \cos(\alpha_{PH} - \alpha_P) - 2F_P \sin^2\left\{\frac{\alpha_P - \alpha_{PH}}{2}\right\}\right|$$

$$\sim |F_H \cos(\alpha_{PH} - \alpha_P)|$$

Harker Section

$P2_12_12_1$ 1: x, y, z, 2: $\frac{1}{2}-x, -y, \frac{1}{2}+z$,
3: $\frac{1}{2}+x, \frac{1}{2}-y, -z$, 4: $-x, \frac{1}{2}+y, \frac{1}{2}-z$

Patterson Peaks $p(u,v,w)$

2-1: $\frac{1}{2}-2x, -2y, \frac{1}{2}$	2-1: $\frac{1}{2}-2x, 2y, \frac{1}{2}$
3-1: $\frac{1}{2}, \frac{1}{2}-2y, -2z$	3-1: $\frac{1}{2}, \frac{1}{2}-2y, 2z$
4-1: $-2x, \frac{1}{2}, \frac{1}{2}-2z$	4-1: $2x, \frac{1}{2}, \frac{1}{2}-2z$
3-2: $2x, \frac{1}{2}, -2z-\frac{1}{2}$	3-2: $2x, \frac{1}{2}, \frac{1}{2}+2z$
2-4: $\frac{1}{2}, -\frac{1}{2}-2y, 2z$	2-4: $\frac{1}{2}, \frac{1}{2}+2y, 2z$
4-3: $-\frac{1}{2}-2x, -2y, \frac{1}{2}$	4-3: $\frac{1}{2}+2x, 2y, \frac{1}{2}$

Relationship among Harker peaks

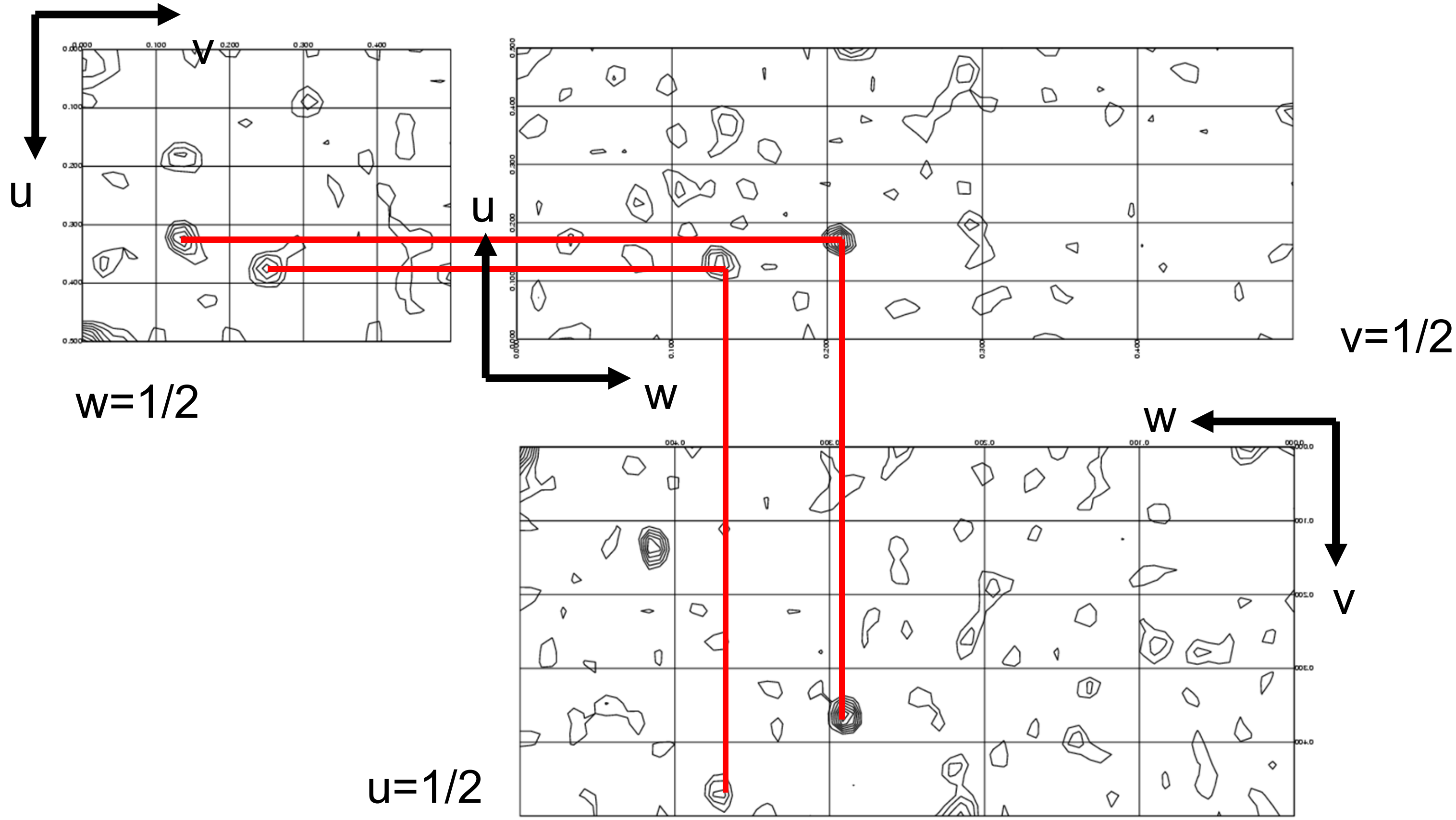

1: (x, y, z) — Patterson space (u, v, w)

2: $(\frac{1}{2}-x, -y, \frac{1}{2}+z)$ — 3-1 $(\frac{1}{2}, \frac{1}{2}-2y, -2z)$, 2-4 $(\frac{1}{2}, -\frac{1}{2}-2y, 2z)$

3: $(\frac{1}{2}+x, \frac{1}{2}-y, -z)$ — 4-1 $(-2x, \frac{1}{2}, \frac{1}{2}-2z)$, 3-2 $(2x, \frac{1}{2}, -\frac{1}{2}-2z)$

4: $(-x, \frac{1}{2}+y, \frac{1}{2}-z)$ — 2-1 $(\frac{1}{2}-2x, -2y, \frac{1}{2})$, 4-3 $(-\frac{1}{2}-2x, 2y, \frac{1}{2})$

Anomalous Phasing

Anomalous Effect: Wavelength dependent absorption ~ XANES

Anomalous term of zinc ($Z_e = 32$)

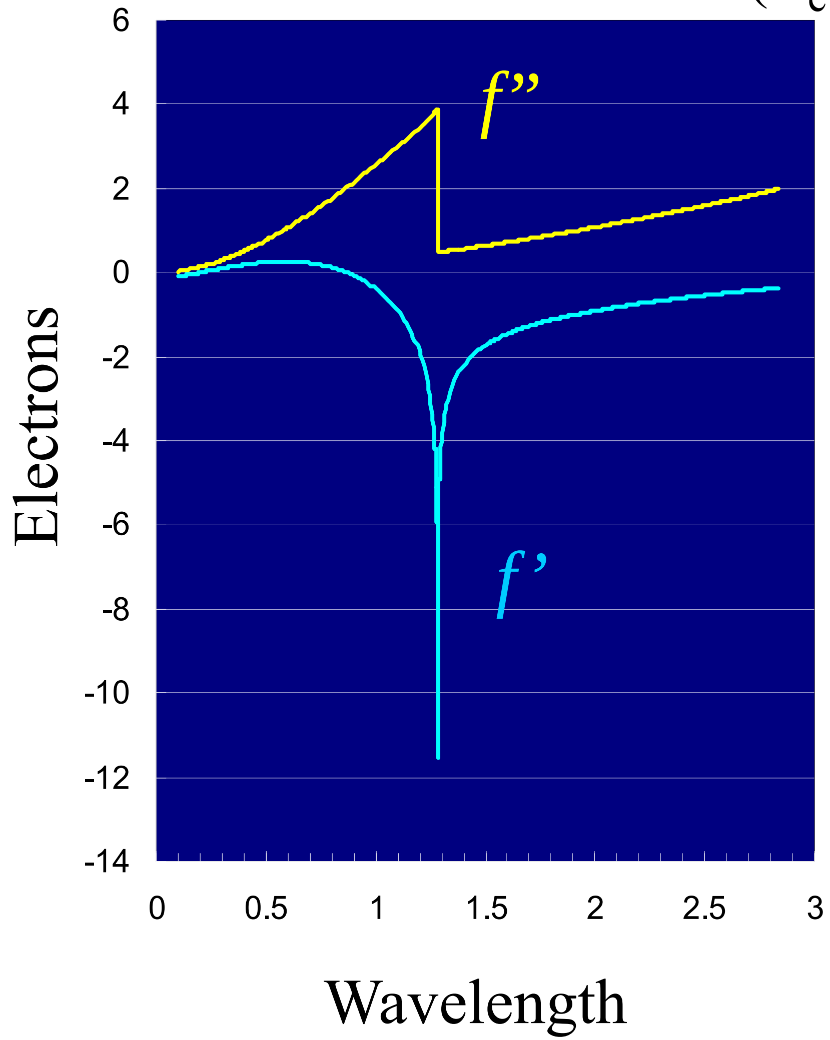

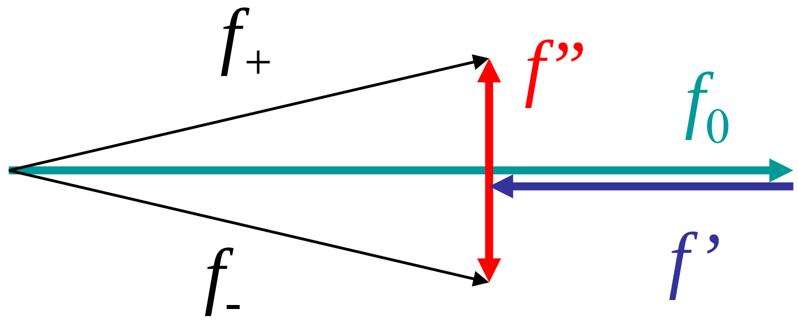

$$f_{\pm} = f_0 + f' \pm i f''$$

Smaller than usual heavy atom effects

↓

Need high quality data

2 Wavelength MAD

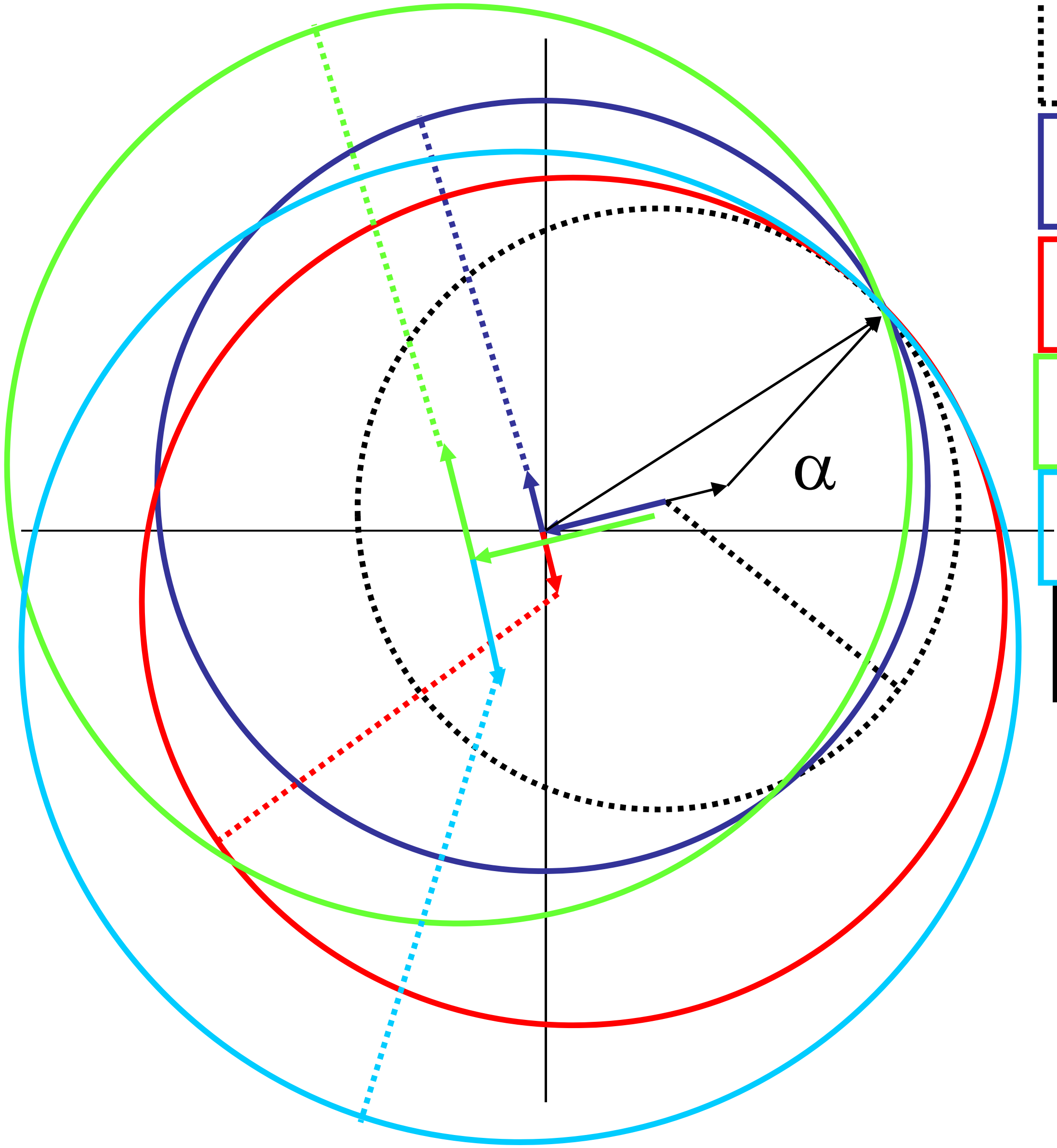

$|F|$: Native

$|F_{\lambda 1}(\mathbf{h+})|$: Anomalous

$|F_{\lambda 1}(\mathbf{h-})|$: Anomalous

$|F_{\lambda 2}(\mathbf{h+})|$: Anomalous

$|F_{\lambda 2}(\mathbf{h-})|$: Anomalous

$\mathbf{F}_P = |F_P| \exp i\alpha$

Single phase solution
can be determined.

Recent trend of isomorphous phasing

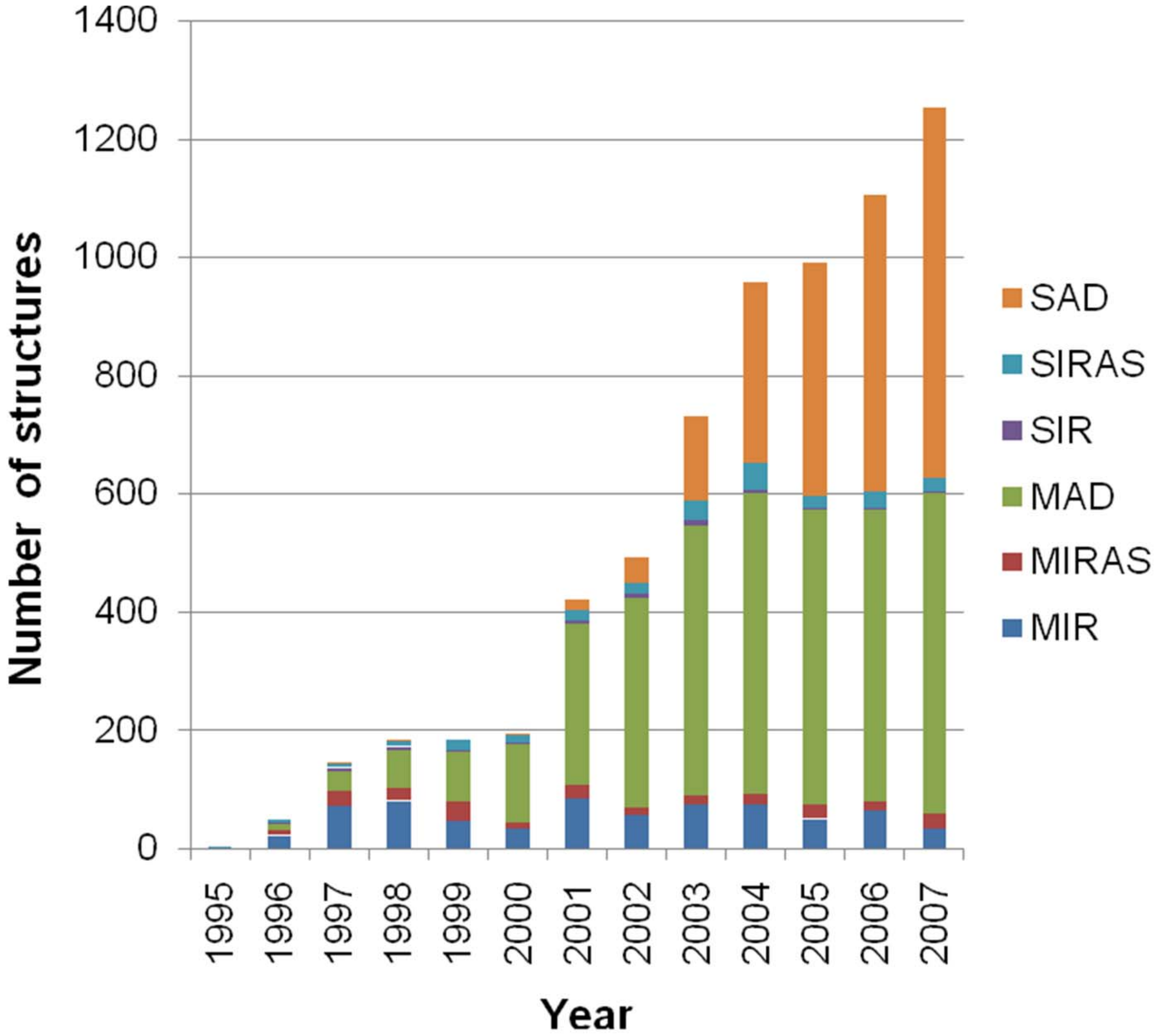

SAD

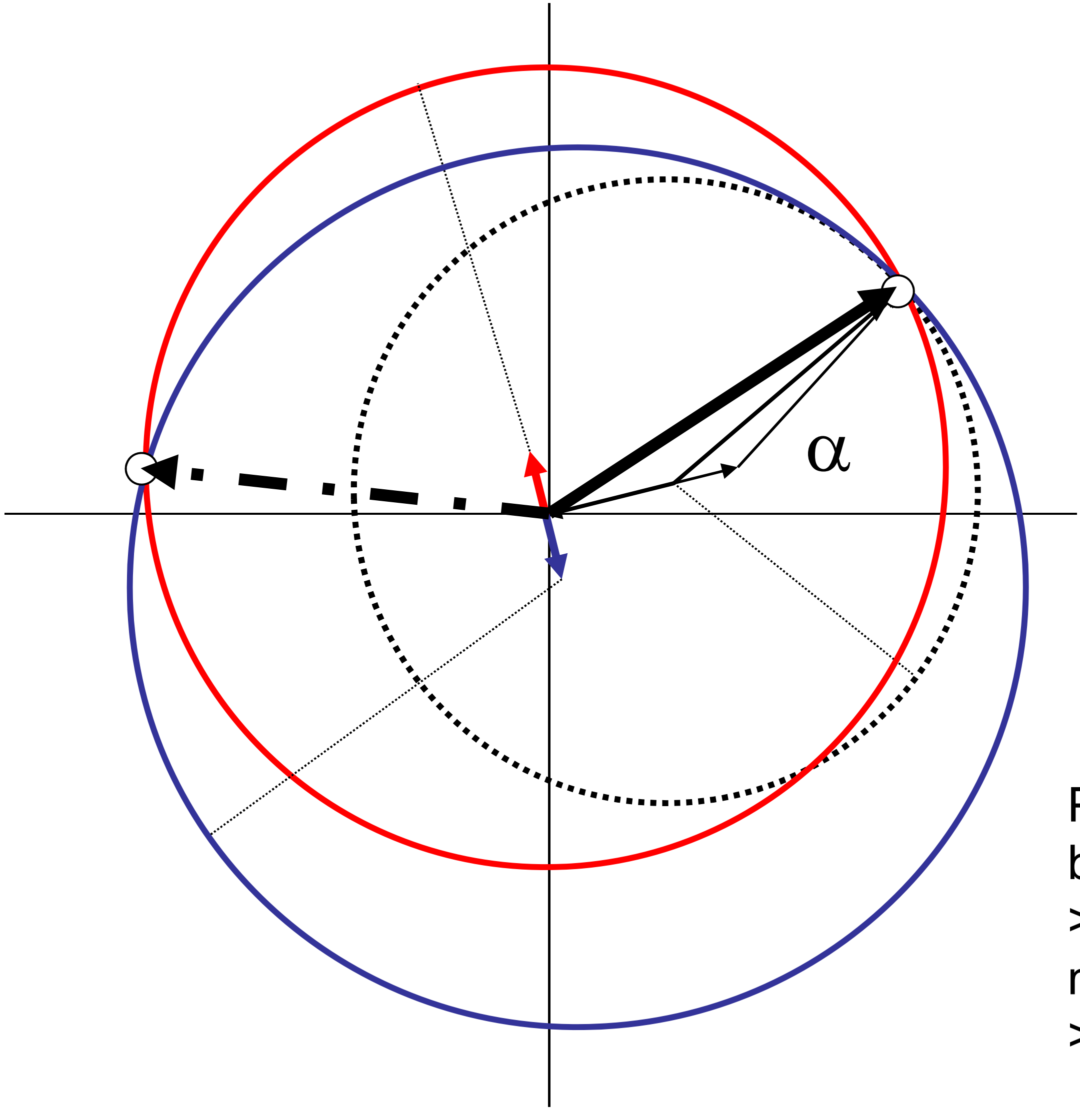

$|F|$: Native

$|F_\lambda(\mathbf{h+})|$: Anomalous

$|F_\lambda(\mathbf{h-})|$: Anomalous

Phase probability function shows bimodal.
>> Phase improvement by density modification
>> High precision data collection

Radiation damage and MAD data set

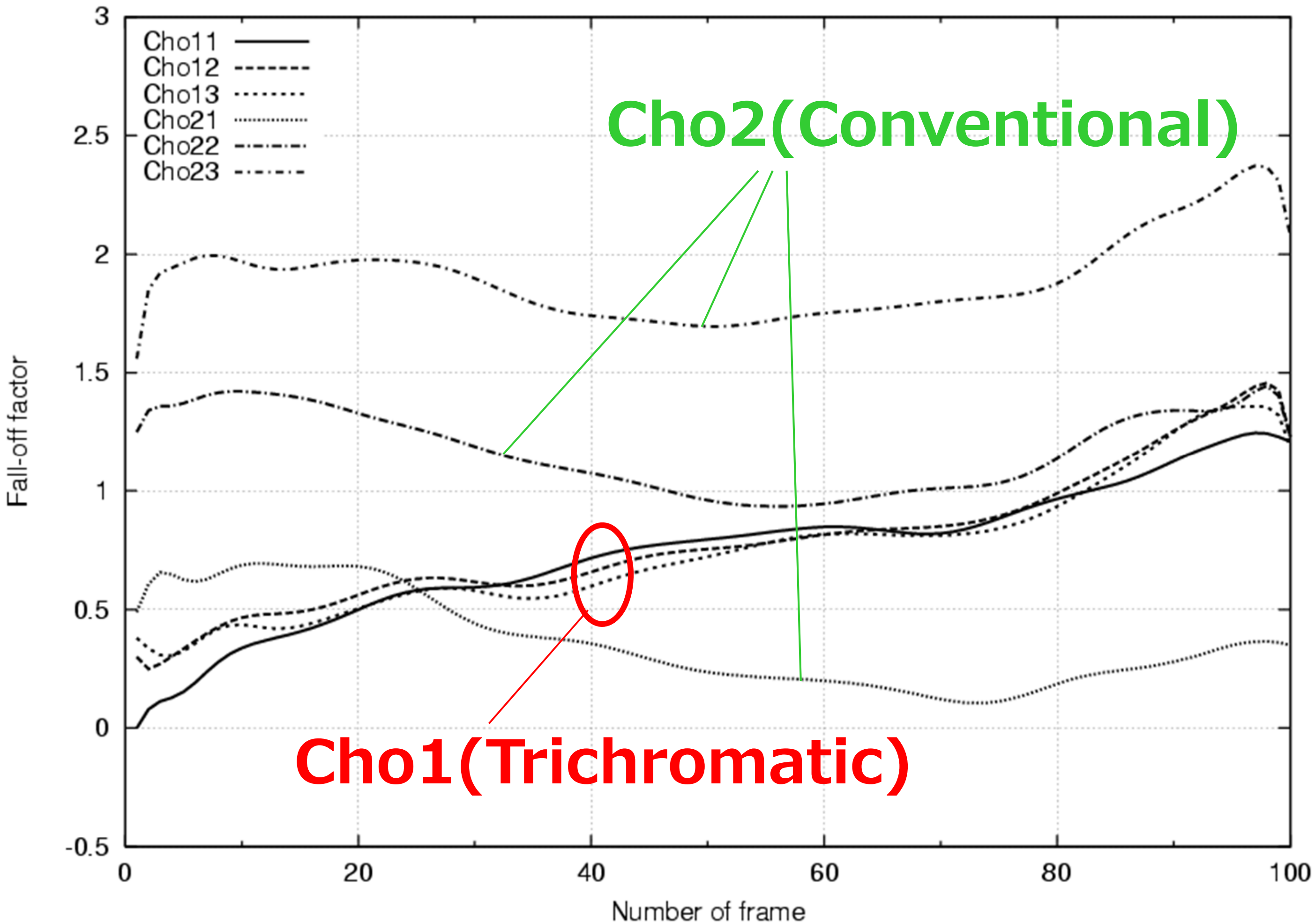

Radiation damage and MAD data set

Effect of data taking way

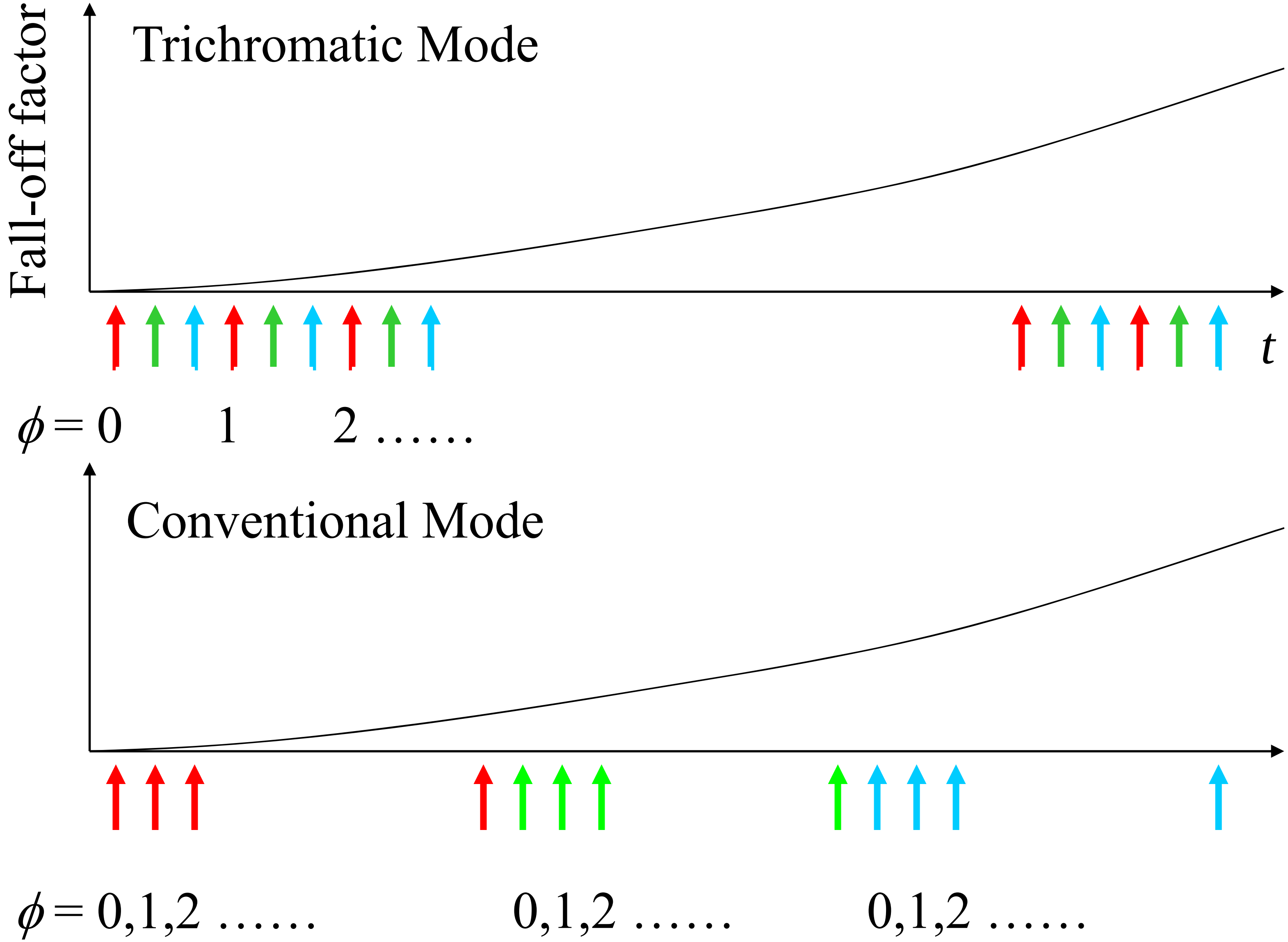

Radiation damage and MAD data set

Comparison with dispersive Patterson maps

Cho1 (Trichromatic) Cho2 (Conventional)

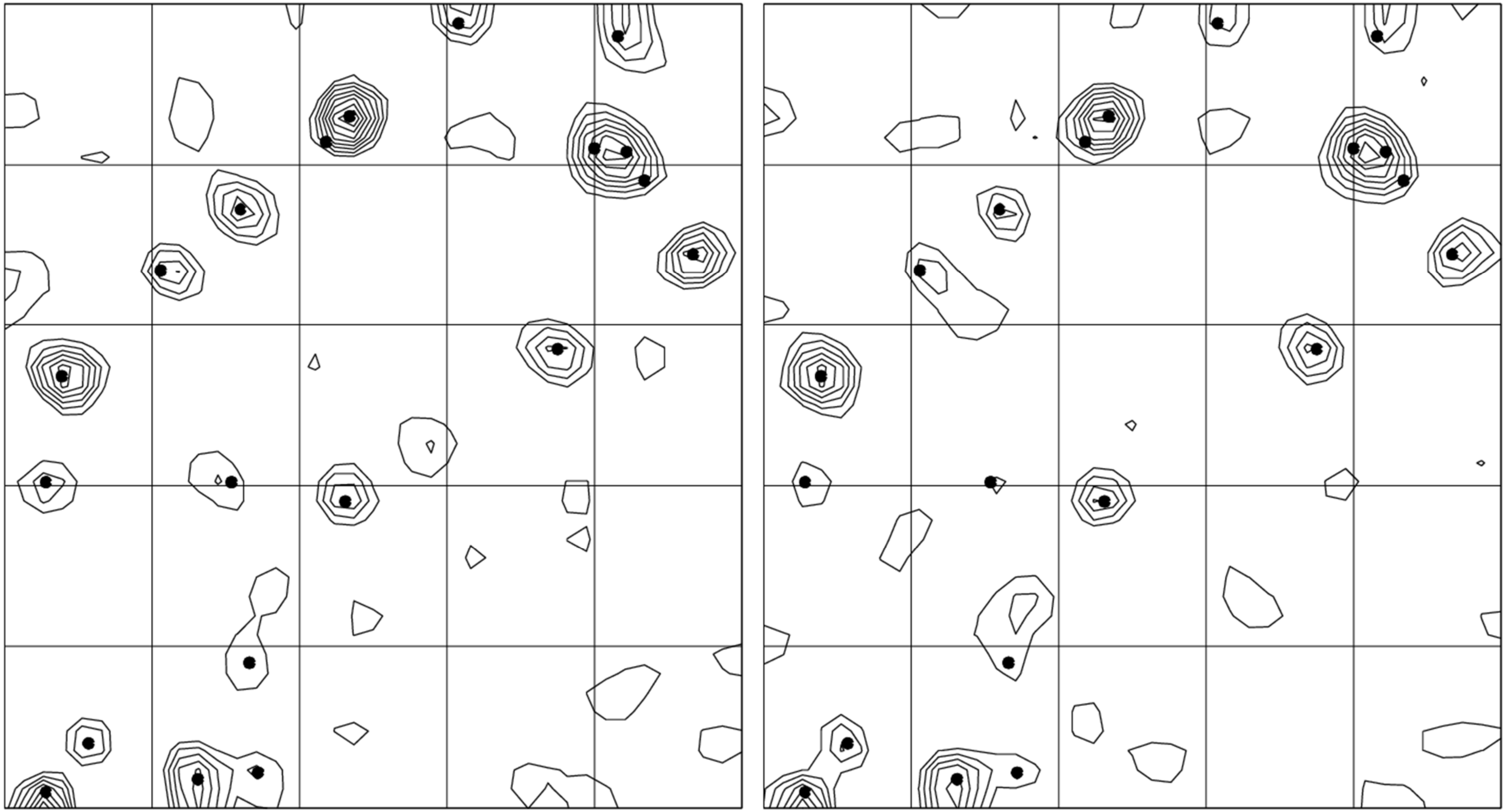

Harker section (w = ½)

Radiation damage and MAD data set

Phasing Statistics (20 – 1.7 Å)

Data	Cho1			Cho2		
	Remote	Peak	Edge	Remote	Peak	Edge
R_{Cullis} (iso)#		0.82 / 0.84	0.83 / 0.88		0.78 / 0.83	0.76 / 0.86
R_{Cullis} (ano)	0.94	0.91	0.99	0.94	0.91	0.99
Lack of closure (iso)#		8.9 / 14.0	8.1 / 12.5		11.4 / 14.7	10.3 / 16.8
Lack of closure (ano)	8.98	16.56	7.32	8.11	15.91	6.37
Figure of merit	0.6057			0.6167		
Phasing power#		1.22 / 0.81	1.19 / 0.82		1.40 / 0.90	1.38 / 0.89
<$\|\Delta\phi\|$>*	44.2	(33.9)		47.8	(39.4)	

#: Acentric and centric values before and after slash.
*: Phase difference against phases calculated from refined model
Parenthesis show the values within the range of 10-2.5 Å.

Radiation damage and MAD data set

Phase difference against true phase

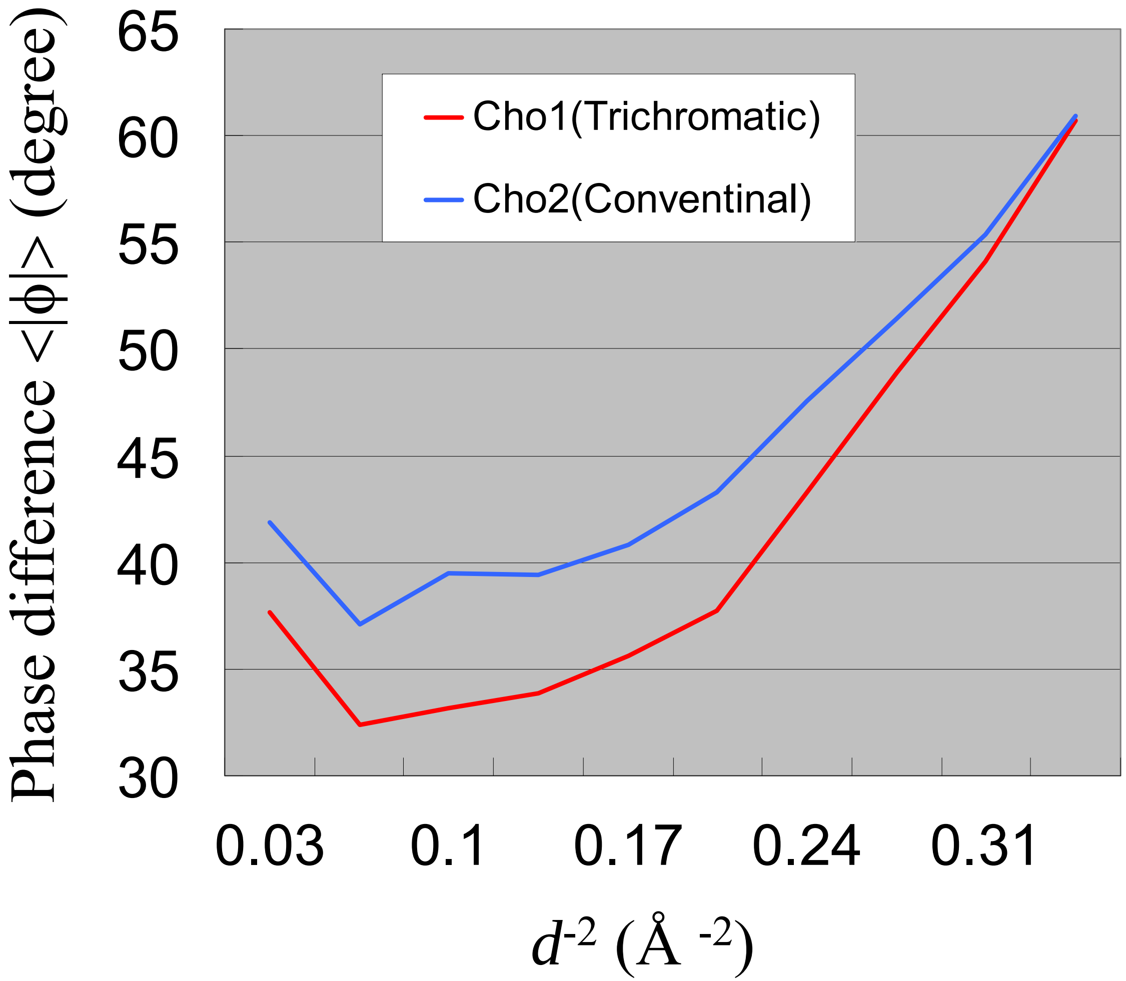

Radiation damage and MAD data set

Quality of electron density map

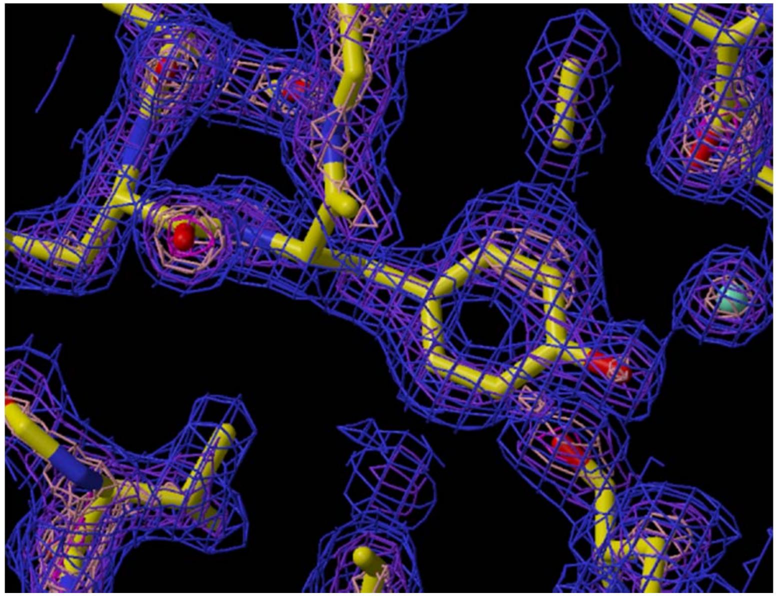

Cho1 (Trichromatic)

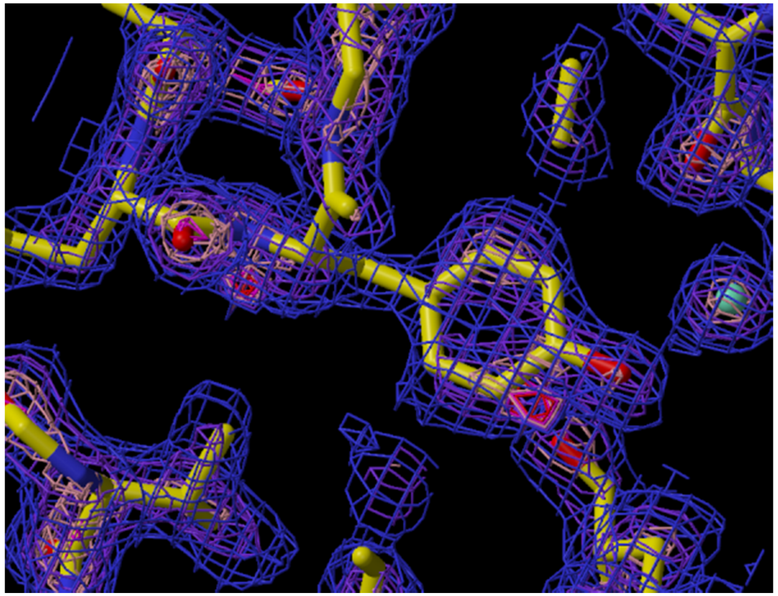

Cho2 (Conventional)

Tyr 165 (Chitosanase A-chain)
1.7 Å MAD phase (without any phase modification)

Molecular replacement

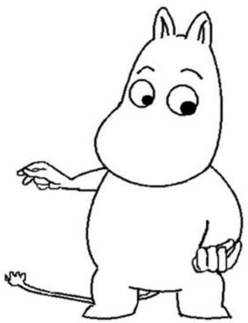

Known determined structure

Unknown
but probably similar
structure

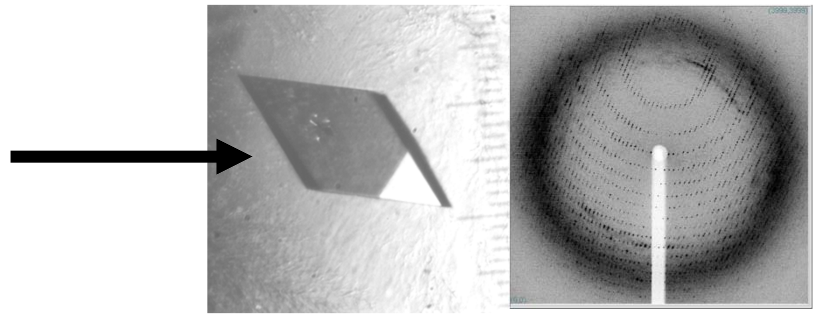

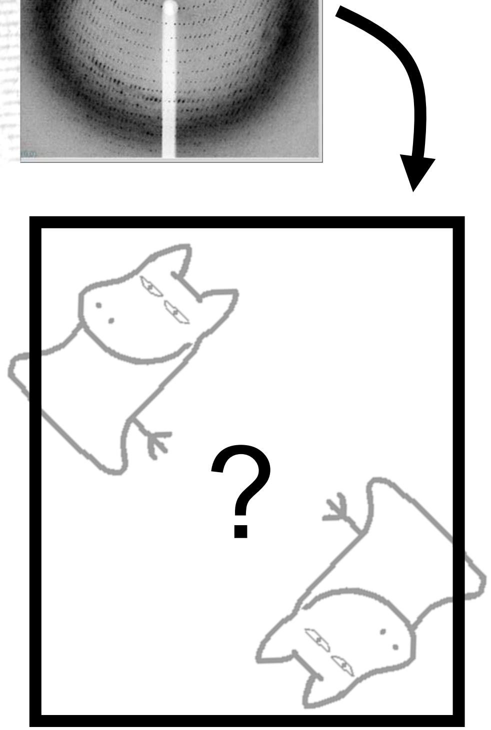

To solve unknown structure, a known structure is used as a approximation.

The known structure will be selected by sequence similarity. Highest sequence similarity might gives highest structural similarity.

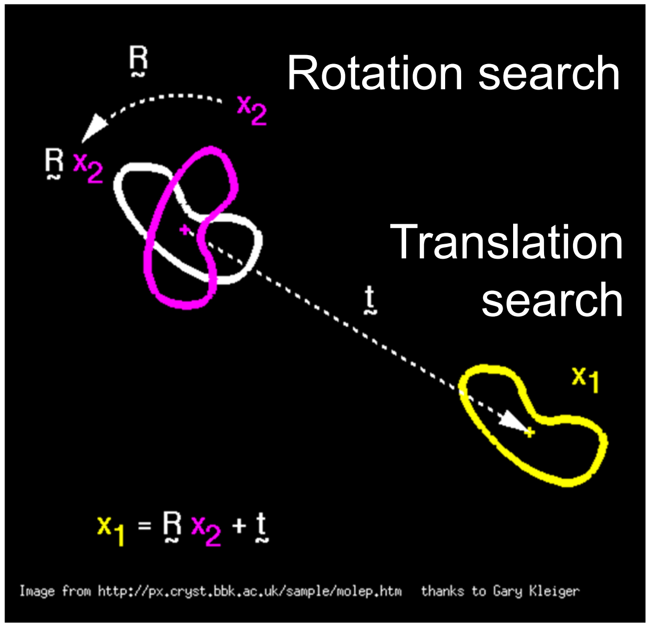

How to pack the molecules into the cell ?
> 6-D search

Patterson function

Intramolecular・Intermolecular vectors

Real space

$$\rho(\mathbf{r}) = \int_S \boldsymbol{F}(\mathbf{S}) \exp[-2\pi i\, \mathbf{S} \cdot \mathbf{r}]\, d\mathbf{S}$$

$$P(\mathbf{u}) = \int_S |\boldsymbol{F}(\mathbf{S})|^2 \exp[-2\pi i\, \mathbf{S} \cdot \mathbf{u}]\, d\mathbf{S}$$

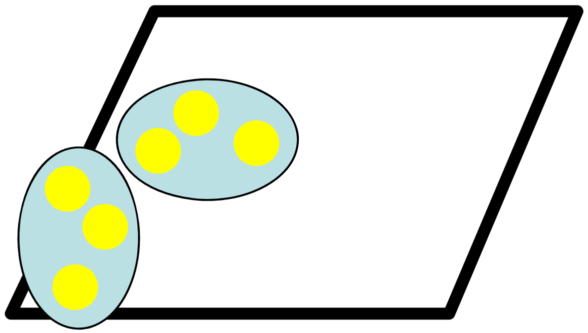

Patterson space

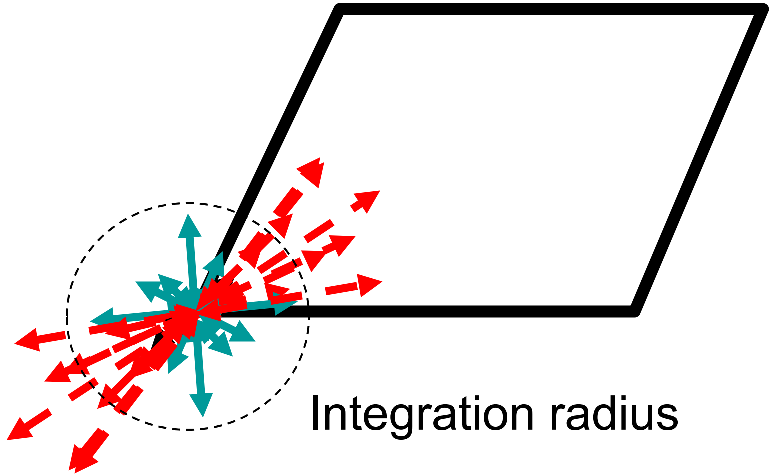

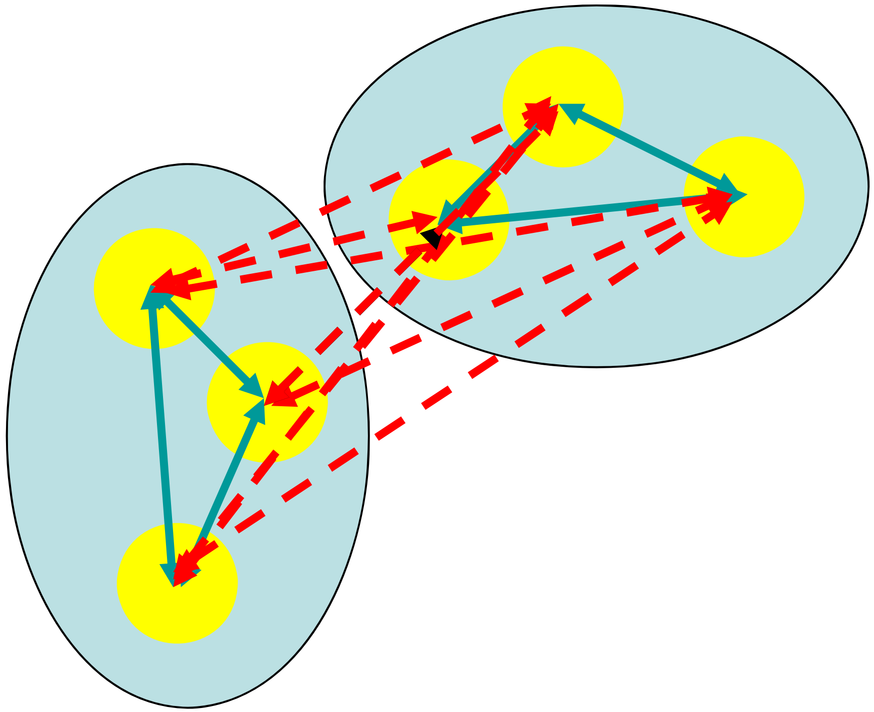

Euler angles, α β γ

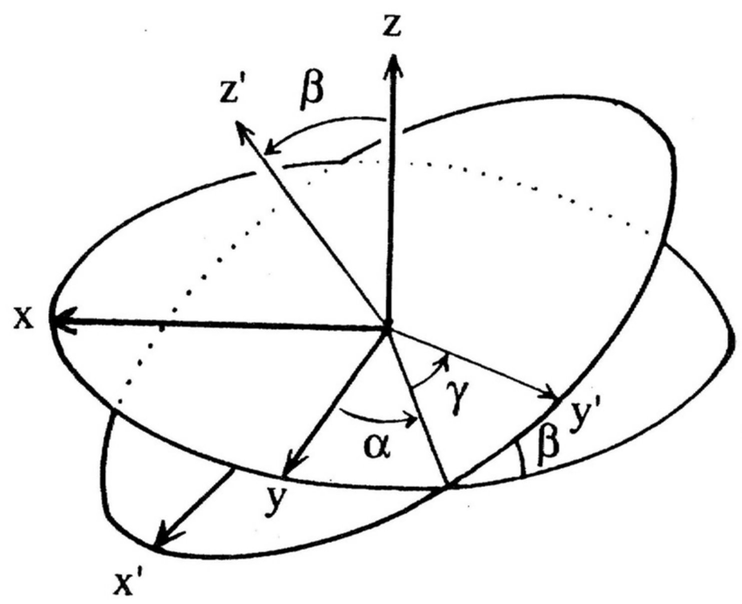

Rotation axis: z'' x' z

$$\begin{pmatrix} \cos\gamma & -\sin\gamma & 0 \\ \sin\gamma & \cos\gamma & 0 \\ 0 & 0 & 1 \end{pmatrix} \begin{pmatrix} 1 & 0 & 0 \\ 0 & \cos\beta & -\sin\beta \\ 0 & \sin\beta & \cos\beta \end{pmatrix} \begin{pmatrix} \cos\alpha & -\sin\alpha & 0 \\ \sin\alpha & \cos\alpha & 0 \\ 0 & 0 & 1 \end{pmatrix}$$

Order in 3 step rotation: 3 2 1

Polar angles, φψκ

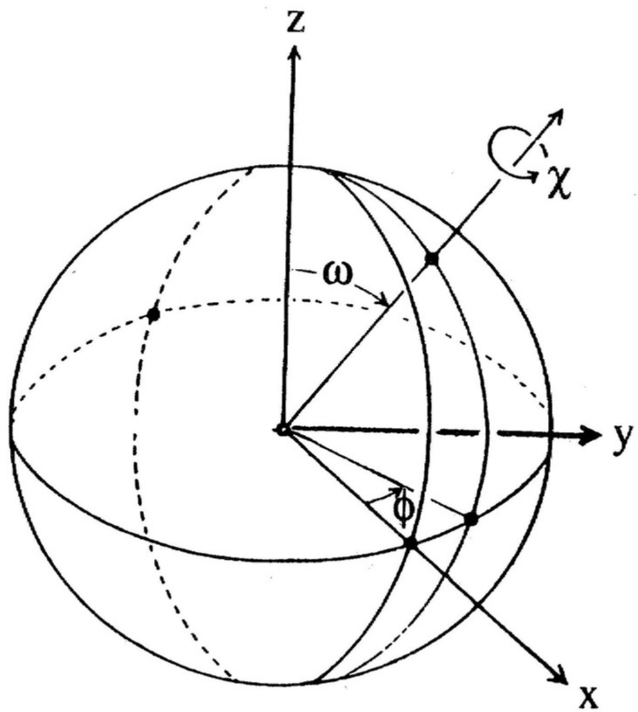

z''''	y'''	z''	-y'	-z

$$\begin{pmatrix} \cos\phi & -\sin\phi & 0 \\ \sin\phi & \cos\phi & 0 \\ 0 & 0 & 1 \end{pmatrix} \begin{pmatrix} \cos\varphi & 0 & -\sin\varphi \\ 0 & 1 & 0 \\ \sin\varphi & 0 & \cos\varphi \end{pmatrix} \begin{pmatrix} \cos\kappa & -\sin\kappa & 0 \\ \sin\kappa & \cos\kappa & 0 \\ 0 & 0 & 1 \end{pmatrix} \begin{pmatrix} \cos\varphi & 0 & \sin\varphi \\ 0 & 1 & 0 \\ -\sin\varphi & 0 & \cos\varphi \end{pmatrix} \begin{pmatrix} \cos\phi & \sin\phi & 0 \\ -\sin\phi & \cos\phi & 0 \\ 0 & 0 & 1 \end{pmatrix}$$

5	4	3	2	1

Real rotation ~ κ

An example of rotation function

α	β	γ	x	y	z	Correlation Coefficient	R-factor
30.37	54.61	351.97	0.000	0.000	0.000	16.0	48.9
59.63	125.39	171.97	0.000	0.000	0.000	16.0	48.9
27.57	41.41	20.51	0.000	0.000	0.000	9.2	51.1
62.43	138.59	200.51	0.000	0.000	0.000	9.2	51.1
17.43	98.67	334.32	0.000	0.000	0.000	7.2	51.7
72.57	81.33	154.32	0.000	0.000	0.000	7.2	51.7
41.73	139.11	197.95	0.000	0.000	0.000	7.7	52.1
48.27	40.89	17.95	0.000	0.000	0.000	7.7	52.1
81.84	98.18	226.67	0.000	0.000	0.000	8.2	51.6
8.16	81.82	46.67	0.000	0.000	0.000	8.2	51.6

Modeling & refinement of structure

Modeling: Construct molecular model to fit obtained electron density using interactive molecular graphics software or automated modeling software.

Refinement: Optimization of observed and calculated F data by shifting atomic coordinates.

R-factor: Crystallographic Reliability-factor

$$R1=\Sigma\ ||Fo|-|Fc(\mathbf{r})||/\Sigma\ |Fo|$$

$$wR2=(\Sigma\ w(|Fo|^2-|Fc(\mathbf{r})|^2)^2/\Sigma\ w(|Fo|^2)^2)^{1/2}$$

Cross validation of R-factor (R_{free})

Refinement of structural model

1) Unrestraint refinement

Only using R-factor refinement

in case of ultra-high resolutions (0.8 A or higher)

2) Restraint refinement

Coupled with molecular mechanics

Model validity is also guaranteed by low energy

~ structural stability

Target function

$$E = E_{\mathrm{chem}} + w_{\mathrm{xray}} E_{\mathrm{xray}}$$

$$E_{\mathrm{xray}} = \sum_{\mathbf{h}} \left| F_{\mathrm{O}}(\mathbf{h}) - kF_{\mathrm{C}}(\mathbf{h}) \right|^2$$

Basics of molecular mechanics (MM)

Energy calculation of atomic bonds and interactions by classical mechanics.

bond length
bond angle
dihedral/torsion
improper dihedral
van der Waals
electrostatic

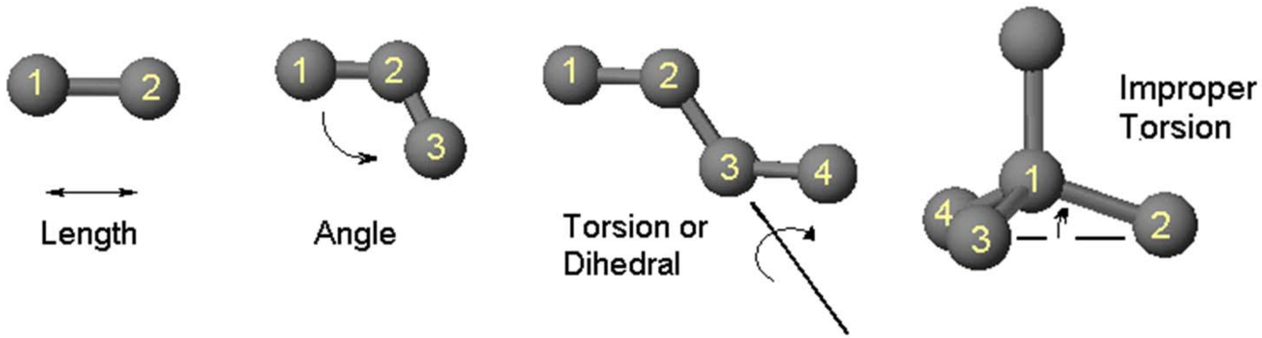

$$E_{chem} = E_{bond} + E_{angle} + E_{dihe} + E_{impr} + E_{vdW} + E_{elec}$$

e.x. Water

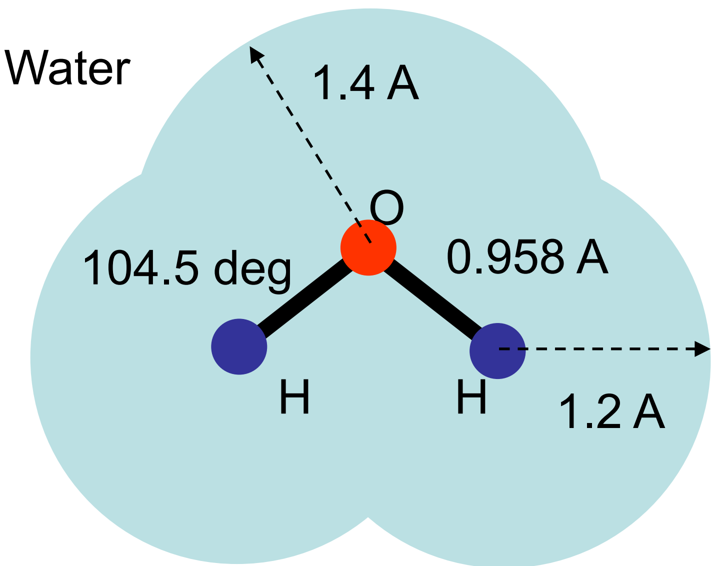

$$E_{bond} = k_{bond}\,(r - r_{ide})^2$$
$$E_{angle} = k_{angle}\,(\theta - \theta_{ide})^2$$

Force Field

TIPS3P Parameter		
Bond O-H	450.0	0.9572
Bond H-H	0.0	1.5139
Angle H-O-H	55.0	104.52

3: Recent advances in PX beamlines

MX Beamlines at SPring-8

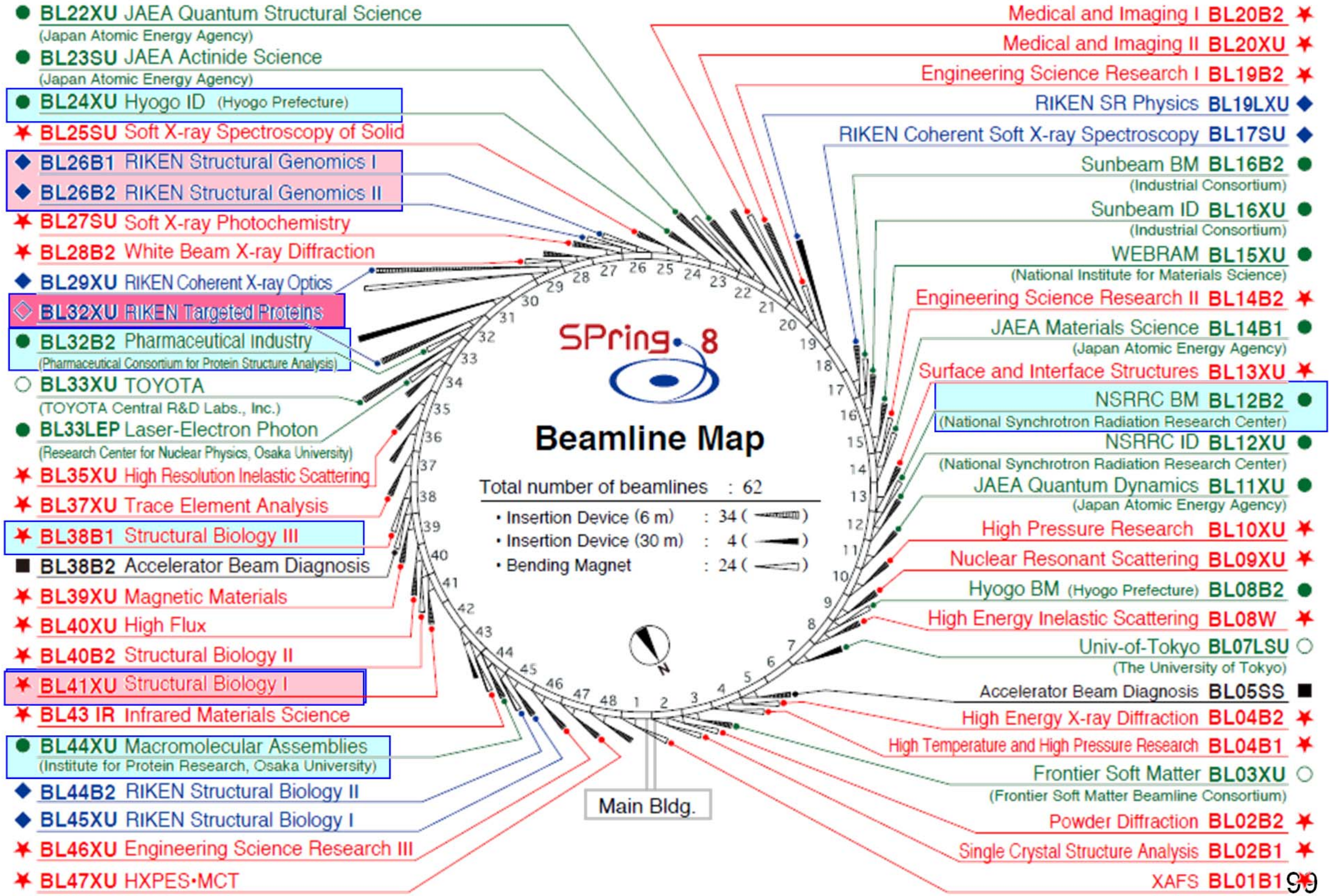

- 9 of 53 beamlines are dedicated to MX

Beamlines and User Accessibility

1. Public Beamlines (BL41XU, BL38B1; JASRI)
   Academic use + Proprietary use (incl. Mail-in service)

2. Contract Beamline (BL44XU; Osaka Univ.)
   Academic use

   Contract Beamline (BL24XU; Hyogo Pref.)
   Academic use + Partially opened to proprietary use

3. RIKEN Beamlines (BL26B1&B2, BL32XU; RIKEN)
   RIKEN's academic research + Partially opened to public use (20%)

4. Pharmaceutical Industrial Beamline (BL32B2; PcProt)
   Fully operated for propietary use
   by the members of
   Japan Pharmaceutical Manufacturers Association (JPMA)

Synchrotron MX

Brilliant synchrotron radiation facilitates MX research

1. For cutting edge research

   High precision data collection

   for Micro-crystal & Large unit-cell samples

2. For structural genomics approach

   Automated and rapid data collection

   for High throughput screening

SPring-8 MX beamline complex

Micro Focus (BL32XU)

- Micro Focus Optics for Micro-Crystal
  < 10 μm
- Sample Handling for Micro-Crystal

SPring-8

High-speed Network

Large Molecular Complex (BL44XU)

- Parallel Beam for Large Unit Cell
  > 500 Å

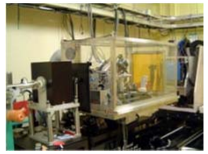

P2 station for Virus

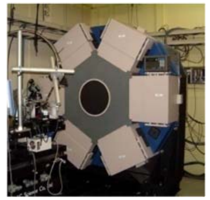

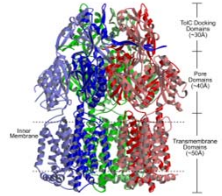

Remote Access

High Throughput (BL26B1/2, BL32B2, BL38B1)

- Stable bending magnet beam
- Beamline automation
- Mail-in Data Collection

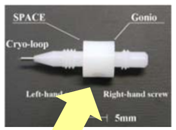

Data Server

- Large Data Storage
- On-line Analysis
- Data base

High-resolution Analysis (BL41XU)

- High Precision Data collection
- Sub-atomic resolution

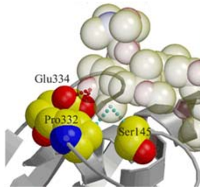

Substrate Complex

Visualization of H-atom

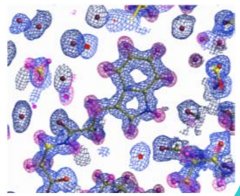

Get more structures and details

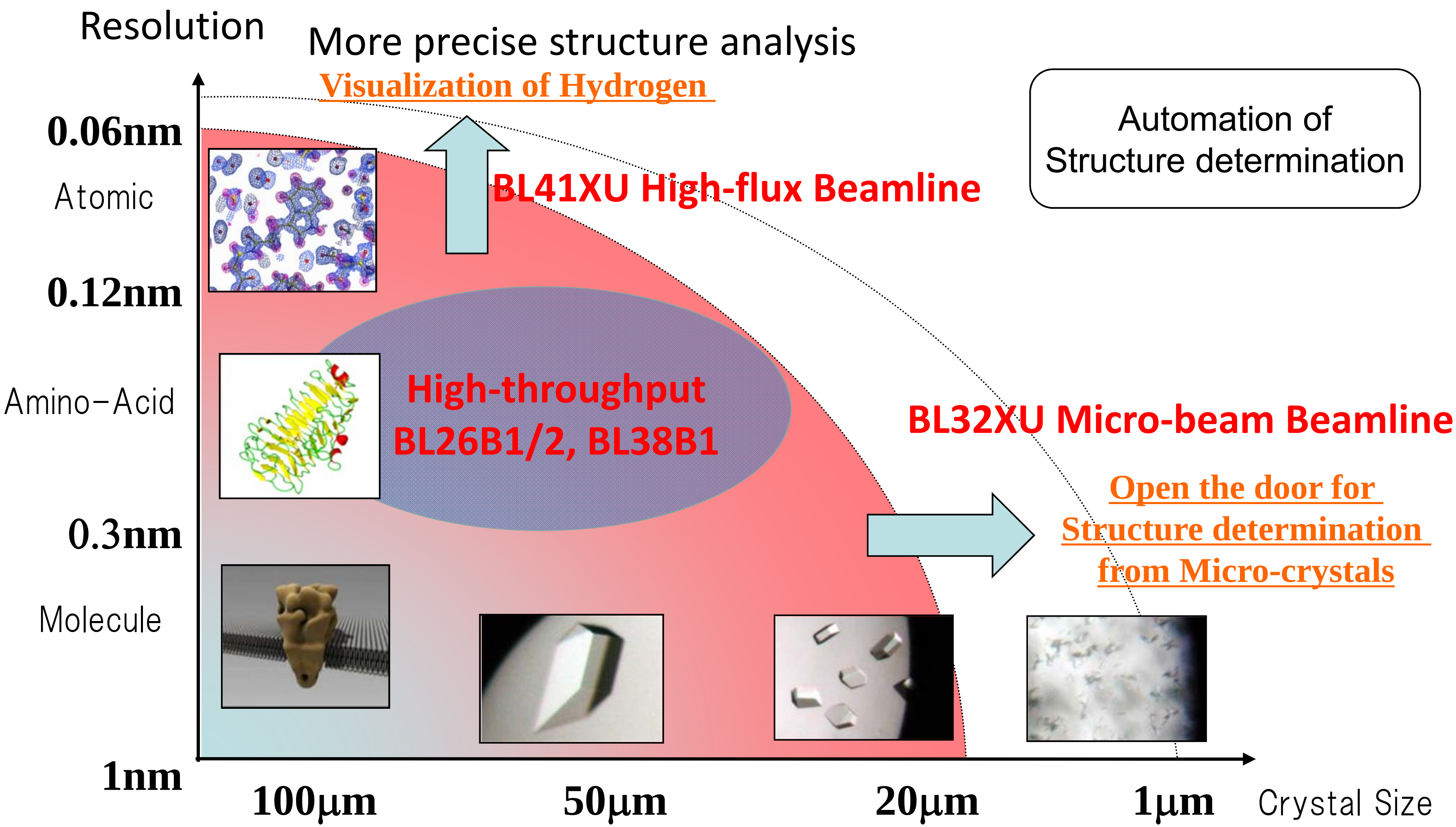

RIKEN Targeted Proteins beamline BL32XU for Targeted Proteins Research Program (TPRP)

- What is TPRP ?
  - Grant: A national project promoted by MEXT, Japan
  - Aims: To reveal the structure and function of proteins that have great importance in both academic research and industrial application.
  - Research Themes:
    Targeted Proteins Research:
    Fundamental Biology / Medicine & Pharmacology / Food & Environment
    Technology Development:
    Protein Production / Structural Analysis / Chemical Regulation / Information Platform
- Beamline Construction
  - Kunio Hirata, Masaki Yamamoto et al. (RIKEN)

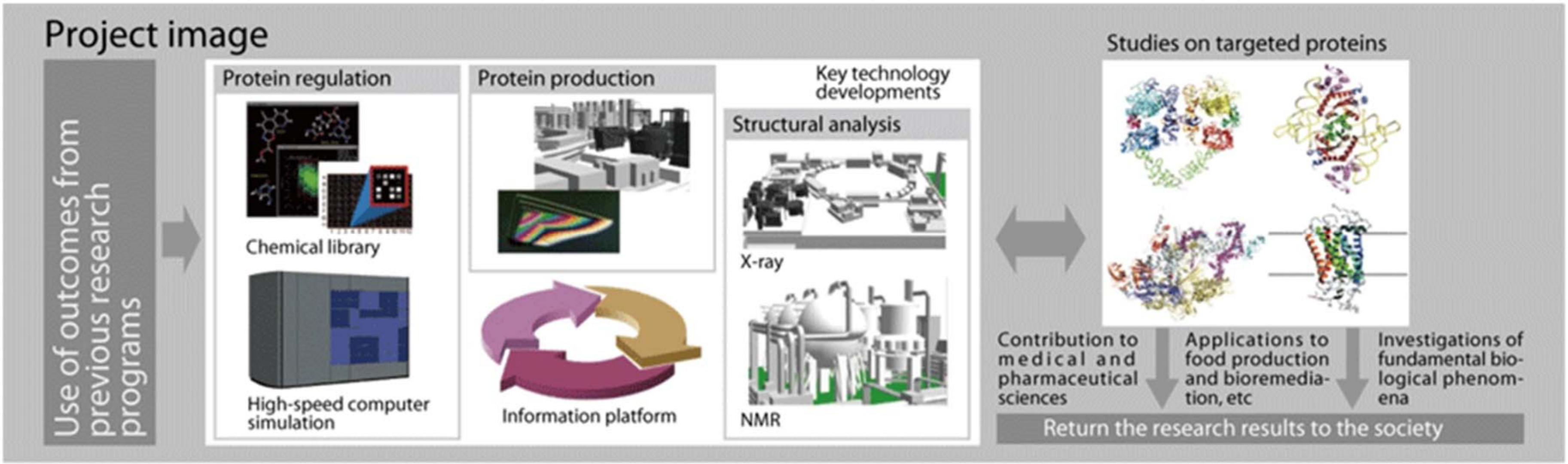

Development of micro-beam beamline

X-ray crystallography of proteins related to human disease and aging.

Micro-beam optimized for Micro-crystal

Standard
>50μm

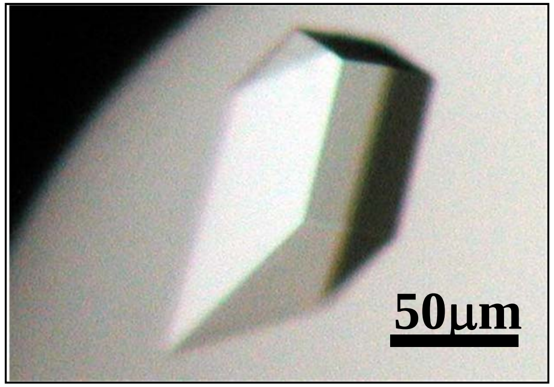

Current Limit
20~30μm

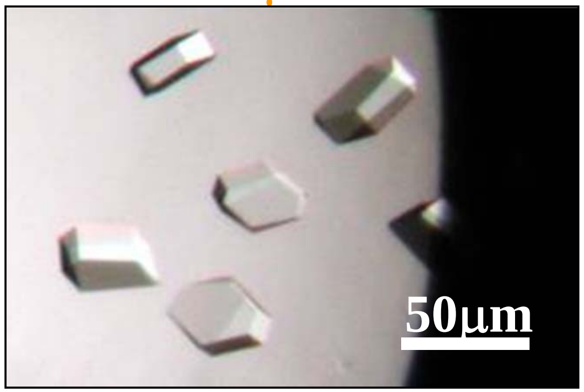

Micro-crystal
<10μm

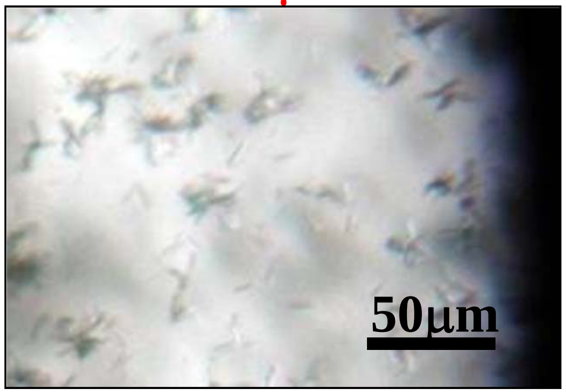

Target Crystals

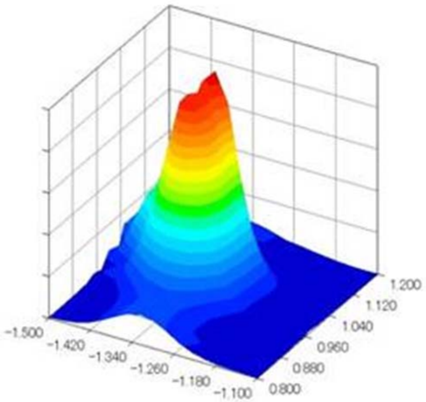

Beam profile of SPring-8 BL41XU

	Current	Target Beam Size	
• Beam Size	30✕30	1✕1	μm^2
• Flux density	10^9	$>10^{10}$	photons/sec./μm^2

R&D target for Micro-crystallography

Micro-crystal
- **Small size crystal（<10mm）**
- **Weak signal（10^6copies）**

Maximize signal-to-noise ratio
- **Generate micro-beam**
- **Optimize experimental equipments**

Generate Micro-beam
- **Stabilize micro-beam**
- **Optimize beam size**

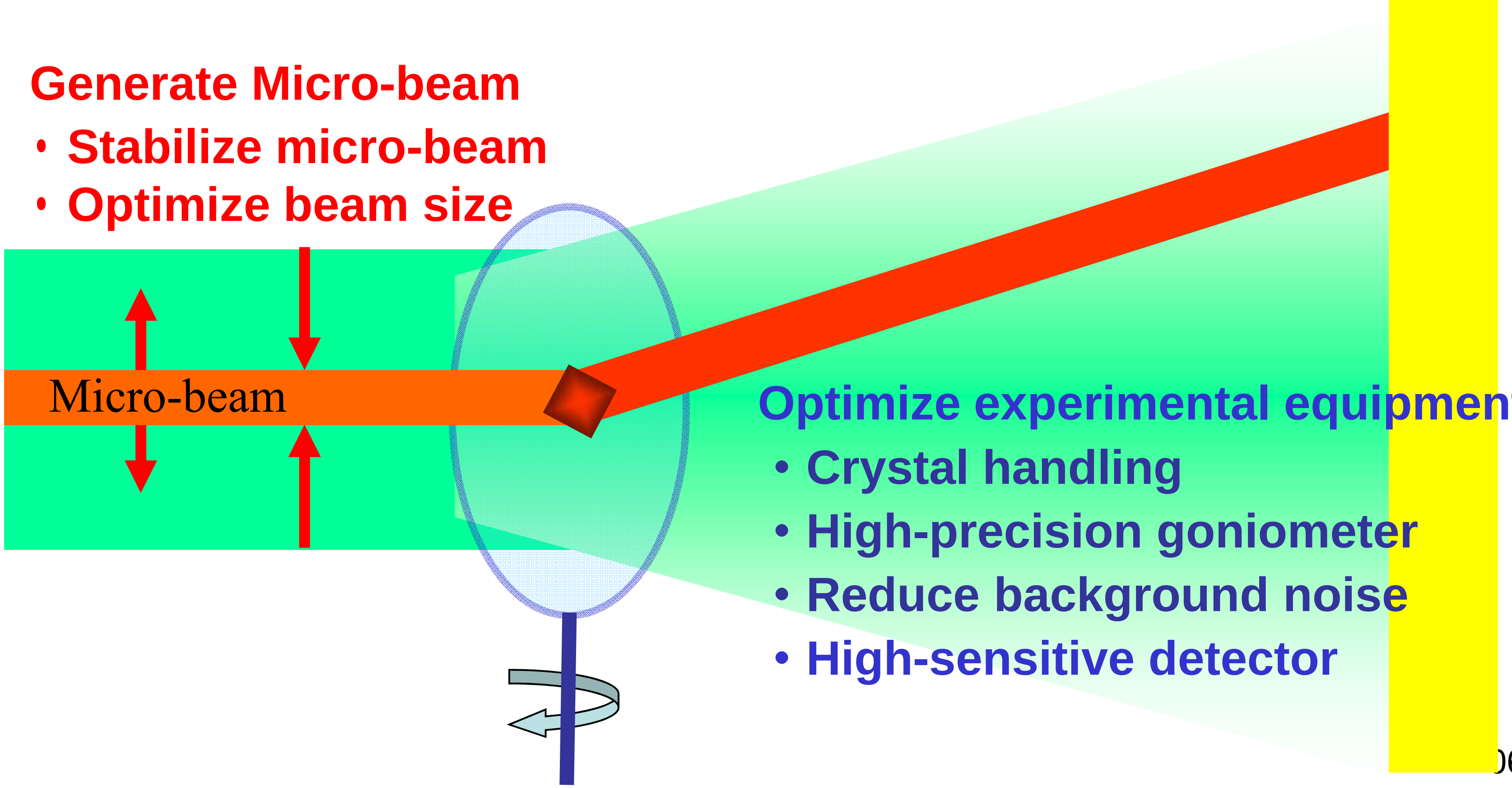

Optimize experimental equipments
- **Crystal handling**
- **High-precision goniometer**
- **Reduce background noise**
- **High-sensitive detector**

Design concept of BL32XU

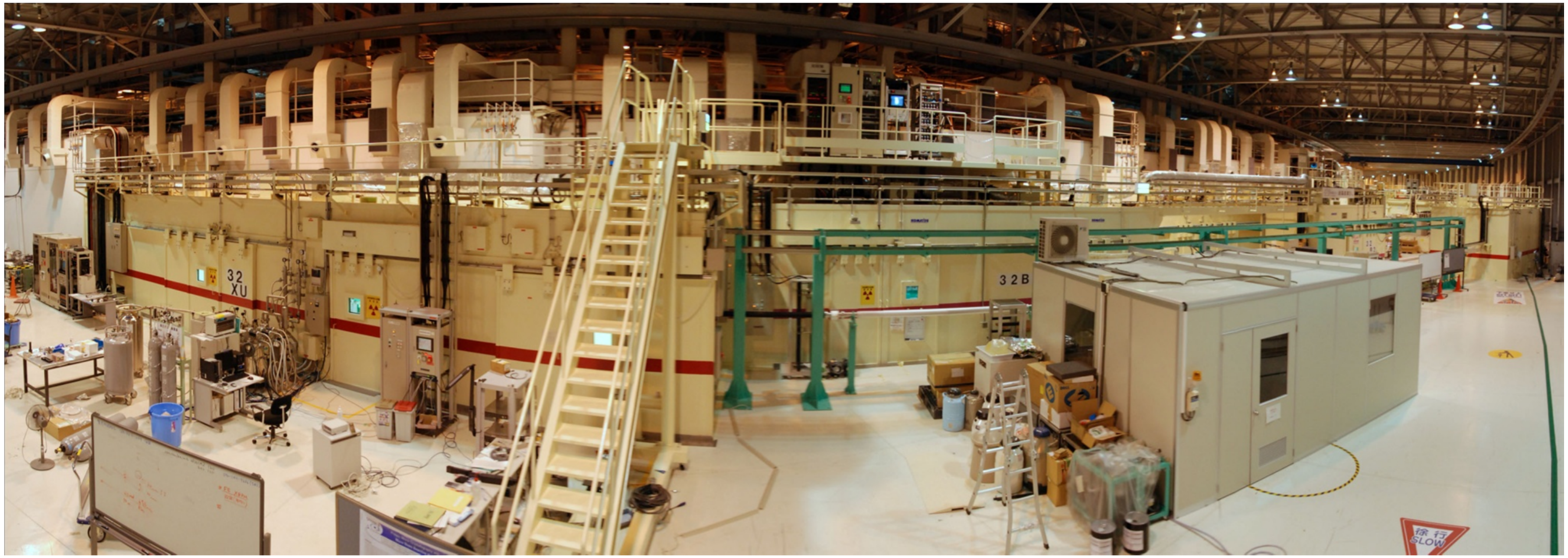

1. Brilliant source
2. Simple components
3. <u>Focusing X-rays with large magnification factor</u>
4. Changeable beam size at sample position

Beamline components


Hybrid in-vacuum undulator

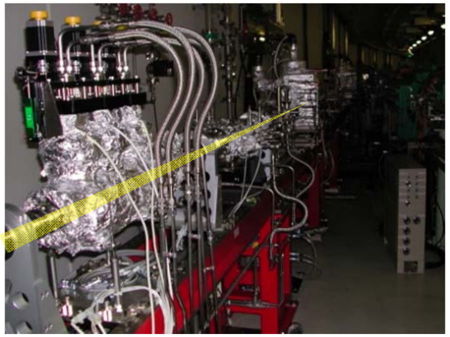
Front end


High precision double crystal monochromator

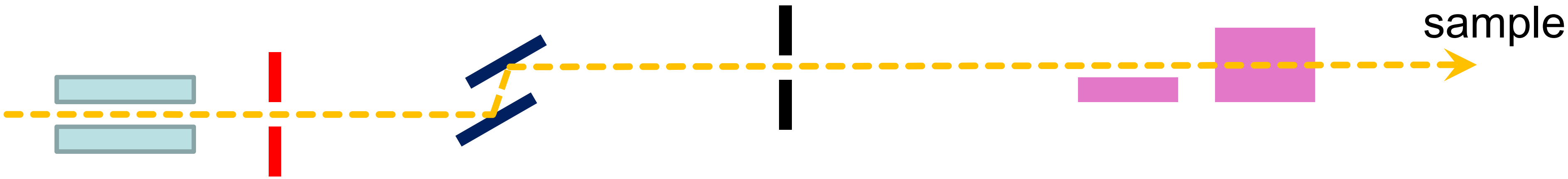

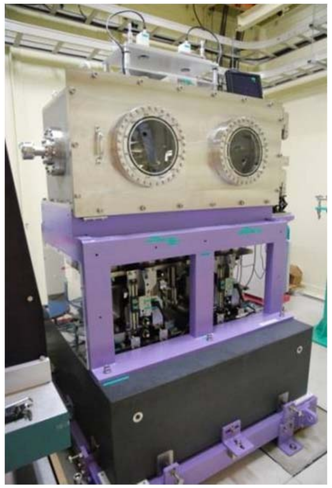
K-B focusing mirrors


Co-axial sample camera


High precision goniometer


High efficient CCD detector

EEM-mirrors for 1 um focusing

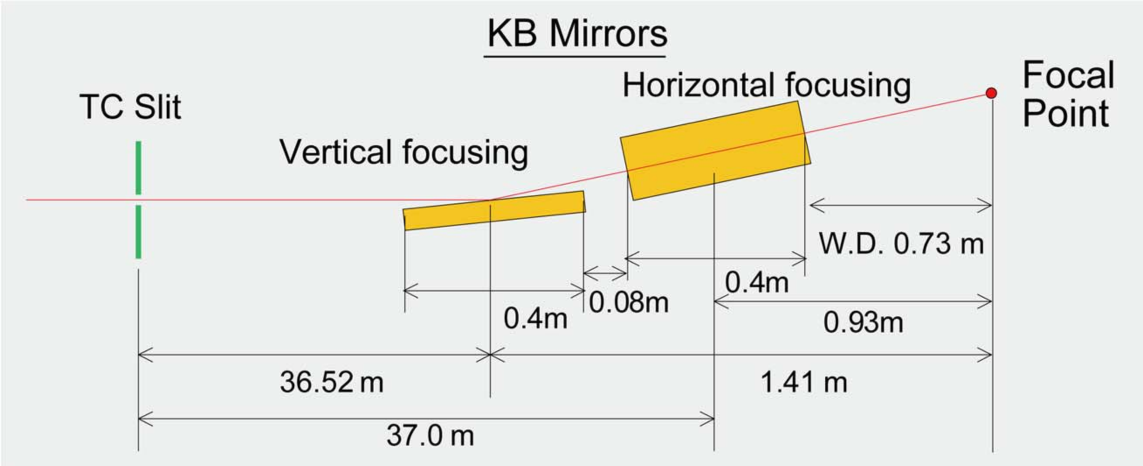

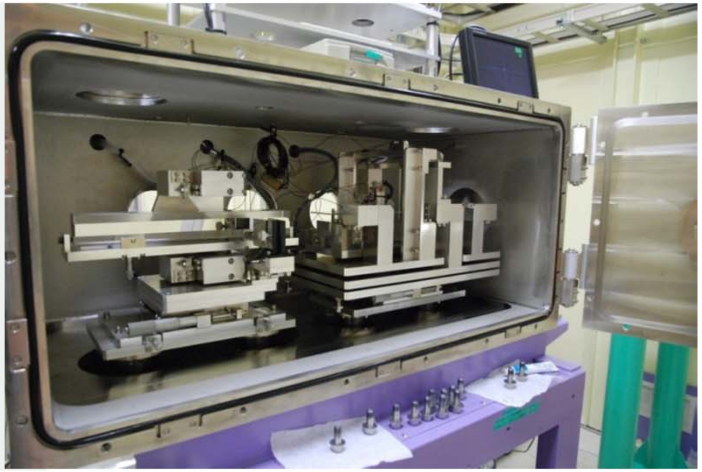

Designed mirror surface shape

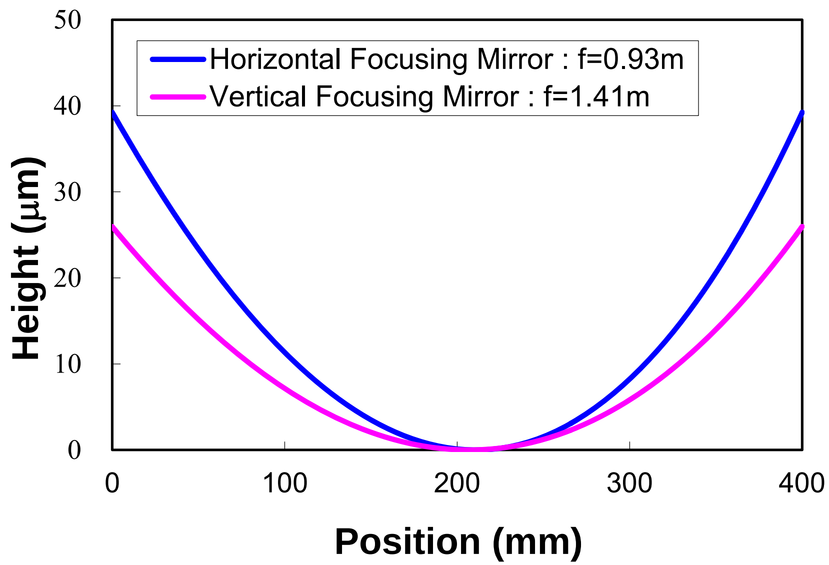

Kirkpatrick-Baez Mirror

Mirror shape :	Elliptical
Mirror length :	400 mm
Energy range :	8-20 keV
Mirror material :	SiO_2
Mirror surface :	Pt-coated
Glancing angle :	3.5mrad

Design of focusing optics

- Virtual light source is TC-Slit (located at 36m upstream of 1st mirror)
- Pt-coated elliptical mirrors with K-B (Kirkpatrick-Baez) configuration
- Magnification factors: 26 in vertical, 40 in horizontal
- Beam divergence at sample position < 2 mrad
- Available X-ray energy range: 8 - 20 keV, especially high-flux at 12.4 -13.8keV

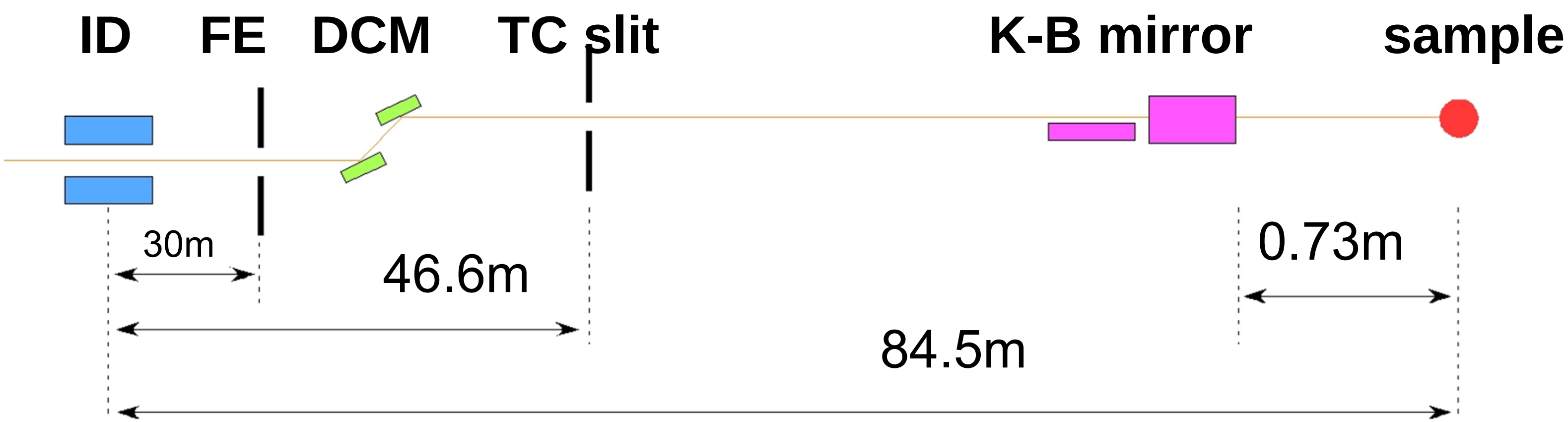

Beam size @ sample	1(H) x 1(V) μm^2	20(H) x 19(V) μm^2
TC slit size	40(H) x 26(V) μm^2	800(H) x 500(V) μm^2
Photon flux@12.4 keV	**6 x 10^{10} photons/s**	2 x 10^{13} photons/s

Glancing angle is designed at 3.5mrad

Achieved beam size（2009/11/27）

Horizontal beam profile

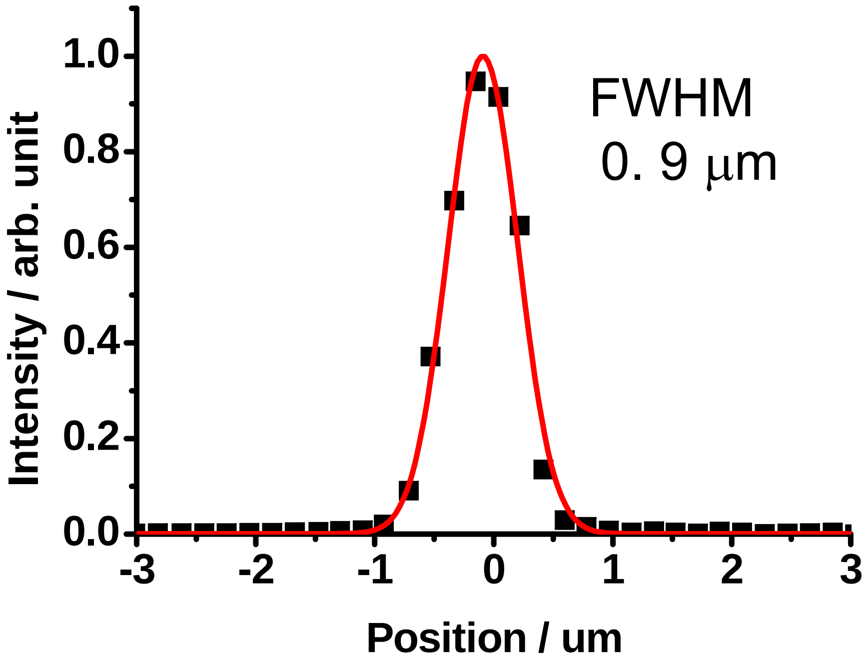

Vertical beam profile

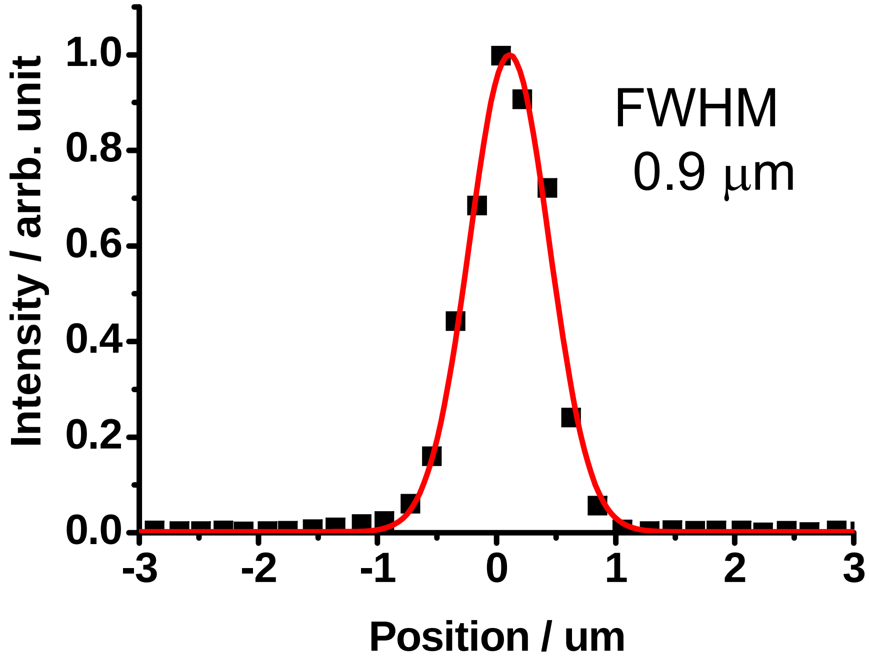

Focused photon flux : 6.2×10^{10} photons/sec

The smallest & highest flux density in the world

Micro-crystal diffractometer

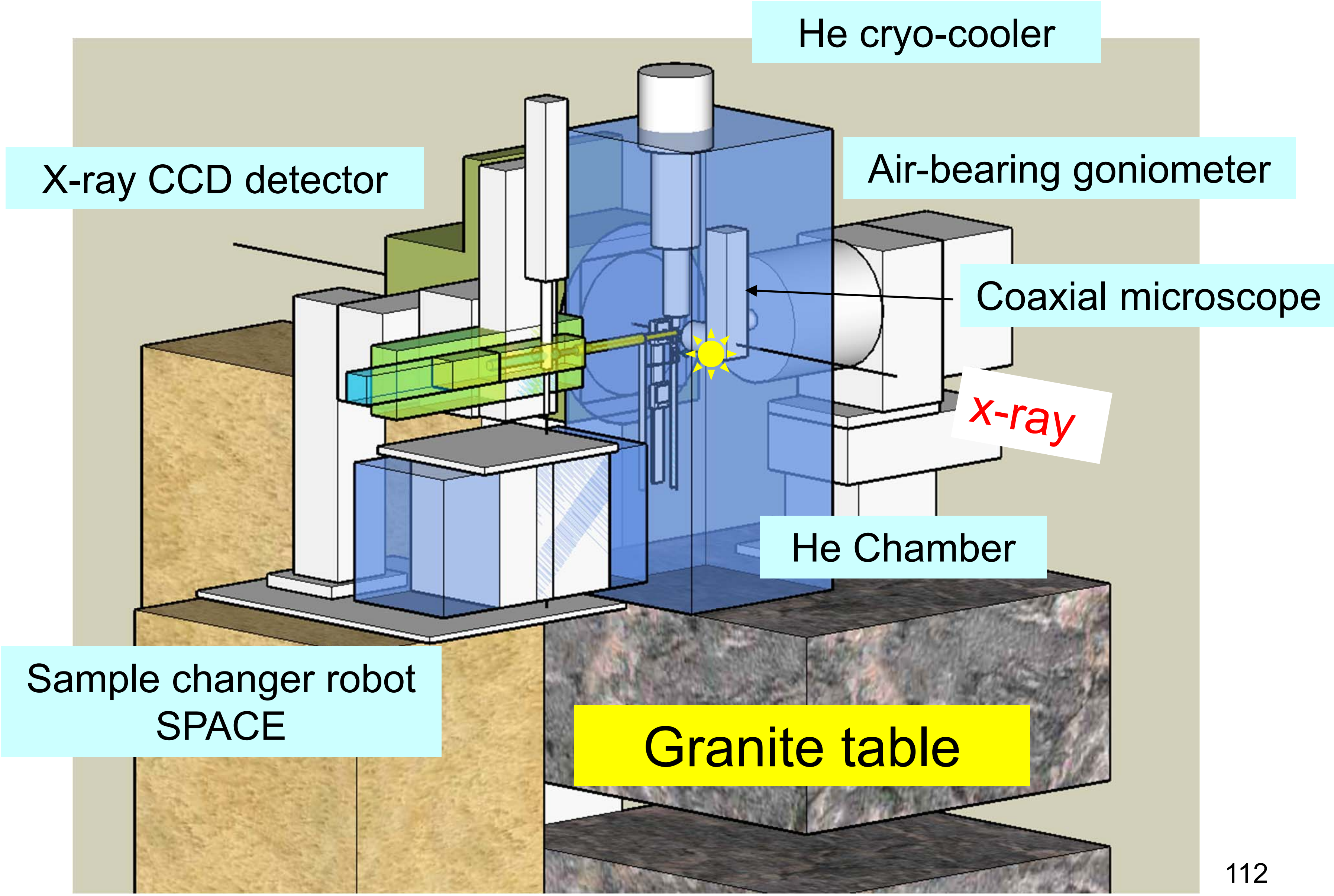

Air-bearing goniometer

- High-precision spindle axis with air-bearing unit
- Hi-speed rotation useful for fast centering, inverse beam geometry etc.

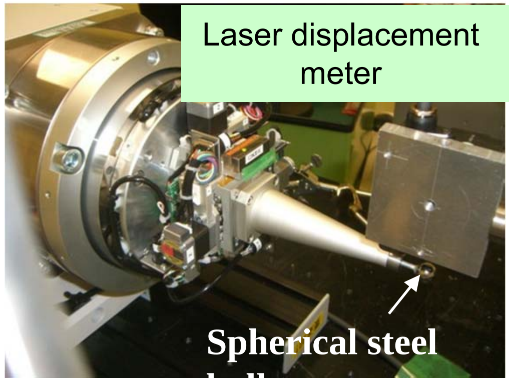

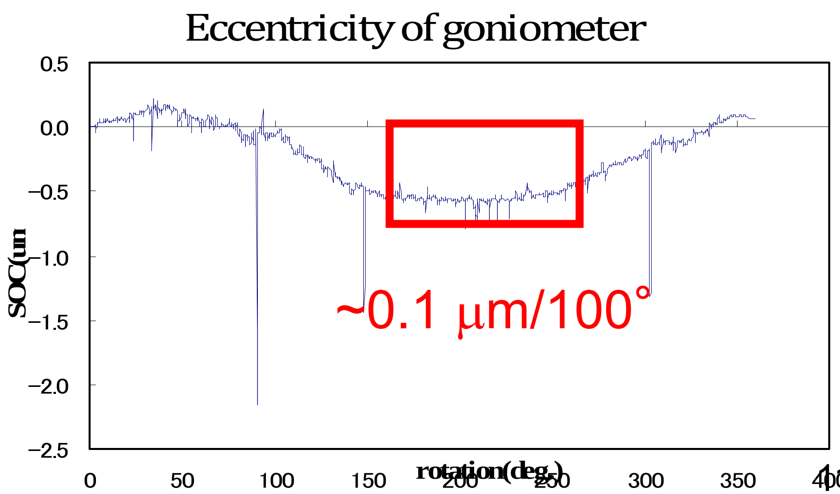

Eccentricity < 0.7μm/360°

（KOHZU PRECISION Co., LTD.）

Tentative diffractometer setting

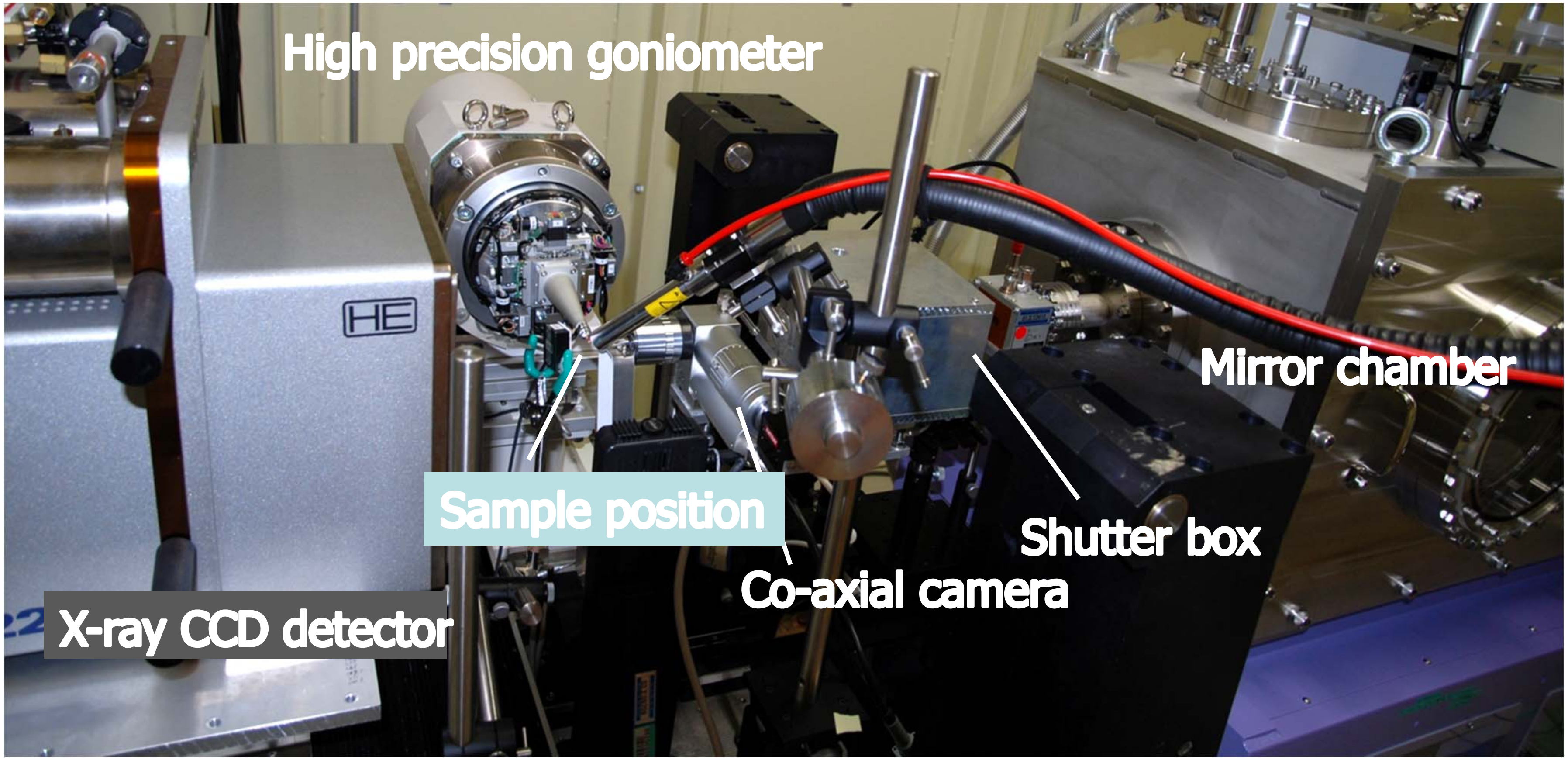

Focusing mirror -> Ion chamber -> Shutter -> Co-axial sample camera -> Collimator -> Back light -> Beam stopper

The first crystal onto the 1μm beam

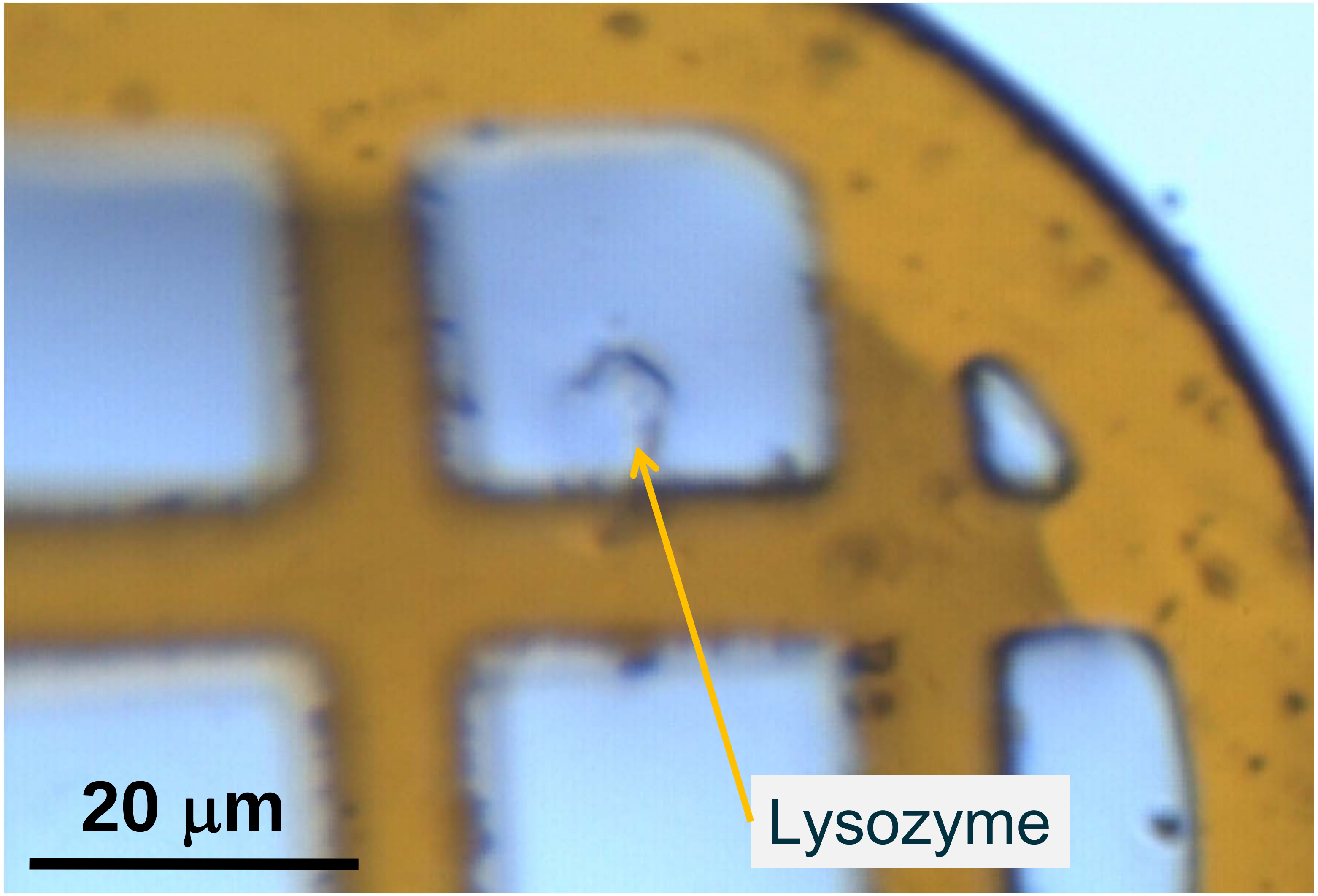

The first diffraction image (09/12/04)

Crystal	Lysozyme 5um crystal
Beam property	1mm square, 2.6 x 10^{10} photons/sec.
Exposure time	1 sec.
Resolution limit	2.0 Å

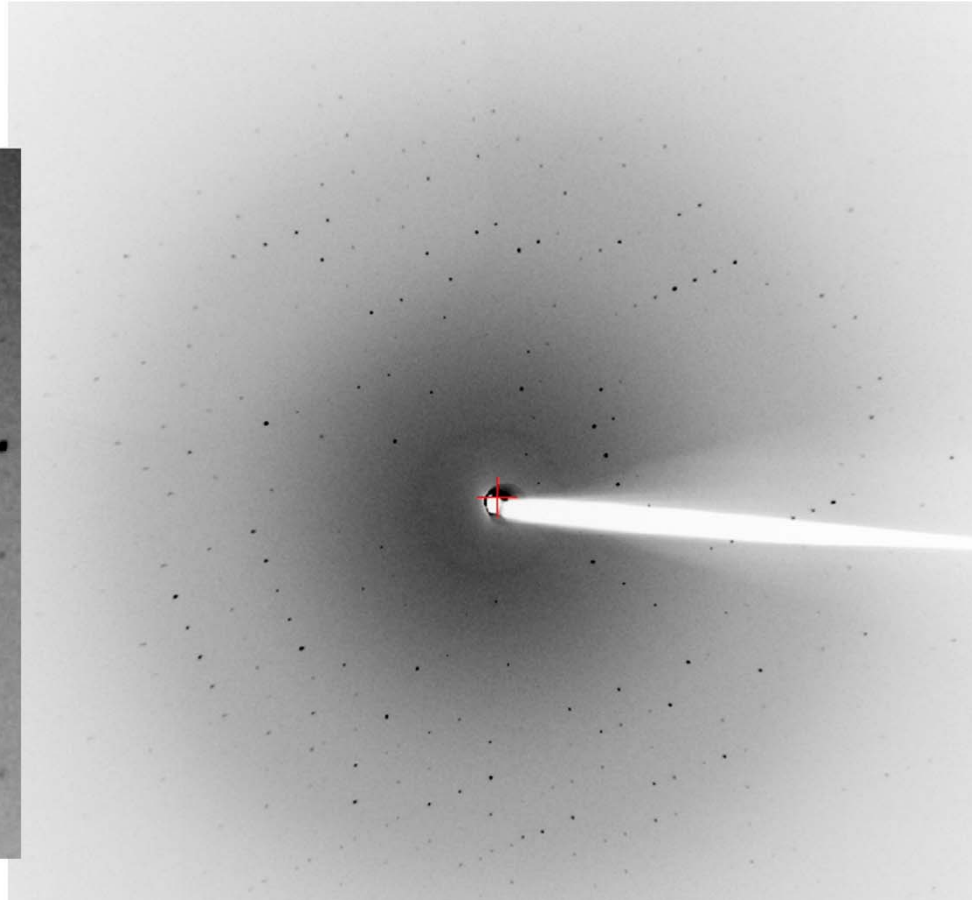

Larger beam divergence did not badly affect diffraction profiles

Data collection limit by crystal size

Acta Cryst. (2008), D64, 158-166

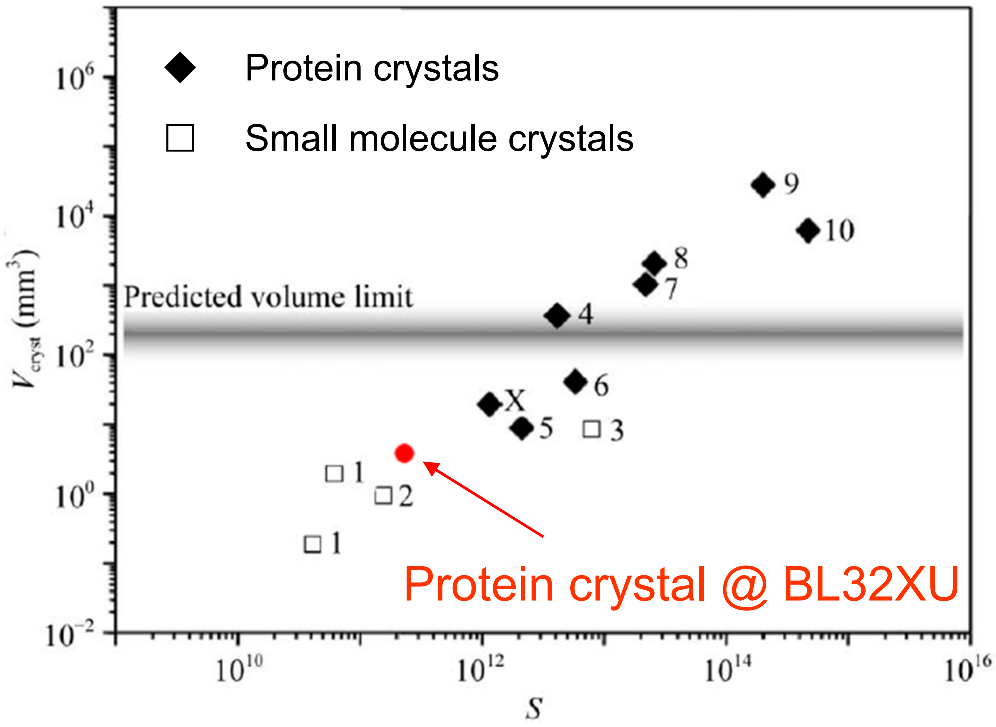

Formula of diffraction power

$$S = (F_{000} / V_{cell})^2 \times \lambda^3 \times V_{cryst}$$

We collect a 2 Å resolution data from 2 um lysozyme crystal.

BL32XU open the new field of Protein micro-crystallography